

**"MATERIAL CHARACTERISATION AND ELECTRO-OPTICAL  
STUDIES OF A FERROELECTRIC LIQUID CRYSTAL"**

**A THESIS SUBMITTED BY**

**P. RAMAKRISHNAN**

**IN PARTIAL FULFILMENT OF THE REQUIREMENTS FOR THE DEGREE OF**

**DOCTOR OF PHILOSOPHY**

**DEPARTMENT OF ELECTRONICS  
FACULTY OF TECHNOLOGY  
COCHIN UNIVERSITY OF SCIENCE AND TECHNOLOGY  
COCHIN - 682 022, INDIA**

**FEBRUARY 1993**

DECLARATION

I hereby declare that the work presented in this thesis entitled " Material characterisation and eletro-optical studies of a ferroelectric liquid crystal " is based on the original work done by me under the supervision of Dr. K.G.Balakrishnan in the Department of Electronics, Cochin University of Science and Technology and that no part thereof has been presented for the award of any other degree.

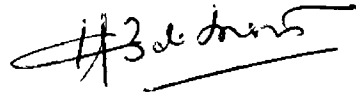
Cochin 682 022  
February 08,1993.



Ramakrishnan. P.

CERTIFICATE

This is to certify that the thesis entitled "Material characterisation and electro-optical studies of a ferroelectric liquid crystal" is a report of the original work carried out by Mr.P.Ramakrishnan under my supervision and guidance in the Department of Electronics, Cochin University of Science and Technology and that no part thereof has been presented for the award of any other degree.



Dr.K.G.Balakrishnan  
Professor  
Department of Electronics  
Cochin University of Science  
and Technology

Cochin 682 022  
February 08, 1993

## ACKNOWLEDGEMENT

This thesis is the outcome of the education, guidance and inspiration I received from my guide Dr. K.G. Balakrishnan, Professor of Electronics, Faculty of Technology, Cochin University of Science and Technology. I wish to express my deep gratitude to him for his invaluable help in steering the course of this study.

I am extremely grateful to Dr. K.G. Nair, Professor and Head of the Department of Electronics for the interest he has shown in this work from time to time.

My special thanks are due to my colleague Mr. James Kurian ( Lecturer, Dept. of Electronics ) for his whole hearted co-operation, encouragement and help throughout this endeavour. I am thankful to Dr. Babu. P. Anto, Dr. K.A. Jose, Dr. N.K. Narayanan and Dr. K.K. Narayanan for thieir help and encouragement during the course of this work. I thank all the members of the Faculty, Laboratory and non-teaching staff for their kind hearted co-operation.

I thank Prof. K. Yoshino of Osaka University, Japan, and Prof. J. Shahidhara Prasad, University of Mysore, for their suggestions and help during the course of this work.

I am indebted to the University Grants Commission for generously awarding me a teacher fellowship under the Faculty Improvement Programme, and the Principal, Government College, Madappally and the Government of Kerala for granting deputation.

## CONTENTS

	Page
Chapter 1. INTRODUCTION	1
1.1 Background	2
1.2 Motivation	7
1.3 Outline of the work and results	10
 Chapter 2. REVIEW OF PREVIOUS WORK	 14
2.1 Introduction	15
2.2 Synthesis	16
2.3 Review of evaluation of material constants	18
2.3.1 Spontaneous polarisation	18
2.3.1.1 Measurement of spontaneous polarisation	19
2.3.1.1.1 Electrical reversal of spont: polarisation	20
2.3.2 Rotational viscosity	23
2.3.2.1 Measurement of rotational viscosity	24
2.3.3 Dielectric constant	27
2.3.3.1 Measurement of dielectric constant	28
2.3.4 Tilt angle	32
2.4 Electro-optic switching studies	35
2.5 FLC light valves and modulaors	39
 Chapter 3. MATERIAL CONSTANTS	 44
3.1 Introduction	45
3.2 The FLC materials and their phases	46
3.3 Cell preparation -- Alignment methods	48
3.4 Experimental arrangements	53
3.5 Temperature controller	54
3.6 Spontaneous polarisation	57
3.6.1 Methodology	58
3.6.2 Results and discussion	60
3.6.2.1 Rectangular waves -- Time separation	60
3.6.2.2 Triangular waves -- Shape separation	68
3.7 Rotational viscosity	72
3.7.1 Square wave experiments	73
3.7.2 Triangular wave experiments	75
3.8 Dielectric constant	75
3.8.1 Experimental Determination	78
3.8.2 Results and discussion	80
3.9 Tilt angle	85
 Chapter 4 STUDIES ON ELECTRO-OPTIC SWITCHING	 88
4.1 Introduction	89
4.2 Experimental setup	93
4.3 Method, results and discussion	96
4.3.1 Nature of response	96
4.3.2 Grey scale	98

4.3.3	Bistability	101
4.3.4	Switching -- Dependence on field parameters	104
4.3.5	Decay of Switched state	106
4.3.6	Multiple pulses	108
4.3.7	Rotational viscosity	109
4.4	Conclusions	111
Chapter 5 ELECTRO-OPTIC MODULATION STUDIES		113
5.1	Introduction	114
5.2	Experimental setup, methodology and results	115
5.3	Discussion	124
5.4	Conclusions	130
Chapter 6 CONCLUSION		132
REFERENCES		139
LIST OF PUBLICATIONS		144

CHAPTER.1. INTRODUCTION.

1.1. BACKGROUND.

1.2. MOTIVATION.

1.3. OUTLINE OF THE WORK AND RESULTS.

## INTRODUCTION

### 1.1. BACKGROUND

Liquid crystals represent a special state of matter, assigned a place between highly ordered solid state and completely disordered isotropic liquid state. Usually this phase is associated with the melting of long molecular crystals. On heating, instead of changing directly to liquid phase, these molecules form an intermediate phase. In this mesophase the orientational order of the molecules is retained while they lose the translational order. As a result the material can flow freely, though along certain selected directions, while retaining the anisotropy of almost all its physical properties, similar to crystalline solids. These types of phases are termed Liquid crystalline phases. Subsequent heating of these mesophases leads to breakup of their residual ordering and the material becomes an isotropic liquid.

Though these thermotropic liquid crystals have been discovered a century ago [1 & 2], it is the potential applications of these materials in electro-optic devices that brought about the renewed interest in them. Further



their applications as light modulators, image converters, choppers and temperature sensors render these materials technologically important.

Displays have become a field of tremendous importance during the last few decades as they provide the best means for interface between man and machine through man's most versatile and sophisticated sense- the vision. Out of the two major types of displays, the electro-optic displays are becoming more popular than mechanical displays. Electro-optic displays allow direct indication and reading of symbols, letters and numbers and can display more information in less space compared to analog meters and devices.

A large number of displays such as vacuum fluorescent, incandescent lamps, nixie tubes, light emitting diodes, electroluminiscence and liquid crystals are presently available. Of all these displays liquid crystal display has emerged as the most promising display during the last decade, capturing 30% of the market for displays (excluding cathode ray tubes). Though there are a number of operating modes, the basic working principle of all liquid crystal displays remains the same, namely the control of light from selected pixels or small areas of the display. Since liquid crystals retain the flow properties and are anisotropic,

their molecules can be arranged in a specified direction by means of an electric or magnetic field of relatively lower strength. This orientation of the director in an applied field is the basis of all electro-optic effects in liquid crystals. Thus liquid crystal displays are passive electro-optic displays which modulate the light passing through it i.e. they do not generate light. On application of a voltage on desired segments these areas become visibly different from the rest of the background giving rise to numeric, alpha numeric, dot matrix etc. characters. The extremely low power consumption (microwatt per square centimeter), low voltage operation, readability in glaring sunlight, compactness and flexibility of size are some of the distinct features which make liquid crystals displays preferable over other types of displays. Another important advantage is its capability to interface directly with integrated circuits. Liquid crystal displays are truly flat panel and do not emit any harmful radiation as in the case of cathode ray tubes.

The first generation of liquid crystal displays operate on a mechanism termed dynamic scattering mode (DSM), which requires a liquid crystal material of negative dielectric anisotropy. In the absence of an electric field a thin layer of liquid crystal looks transparent. When a field

is applied, due to the flow of ions these materials exhibit a marked turbulence that turn them from transparent to white. Thus the reflection of light in the medium can be electronically controlled. Dynamic scattering mode operates only at low frquencies (1kHz) and consumes more power (milliwatt per square.cm).

Another important mode of operation is the twisted nematic liquid crystal display which is based on a field effect. In such a device, normally light polarisation is twisted through 90 degrees in the liquid crystal. When an electric field is applied the twisting structure is neutralised and light cannot be transmitted (in the crossed polariser set up ). In recent years this device has dominated the electronic watch display.

With the increased use of fiber-optic communication systems, during the last decade greater attention is being paid to fibre-optic devices like sensors, modulators, couplers and switches involving novel concepts. Liquid crystals can serve as external passive modulators, as even weak signals can bring about a change in molecular orientation of the liquid crystal that results in a change in the refractive index along a given direction of the material. When light is passed through such a liquid crystal medium, the output intensity varies according to

variations in the applied electric field (signal). Such intensity modulation of light has been obtained using nematic liquid crystals by many research groups.

Another important area of application of liquid crystals is in light valves or spatial light modulators. They convert an input image written in a certain wavelength, intensity and coherence conditions to an output image in which some or all of these parameters are varied. They find application in image amplifiers, wavelength converters and incoherent to coherent image converters. A series of silicon-photoconductor based liquid crystal light valves have been developed by Hughes Research Laboratories in recent years [3].

The most significant advances in the liquid crystal devices are in material synthesis and device fabrication. A variety of high purity liquid crystal materials have been developed with reasonable operating ranges and high response to fields. Alignment techniques like oblique evaporation of silicon monoxide, Polymer coating and rubbing, application of a low frequency ac, coating with a silane etc. have been developed for obtaining the desired molecular orientations in various cell configurations.

In large screen and high resolution displays the

switching speeds of the material should be very high. The drawbacks arising from the comparatively low switching speeds of liquid crystal are overcome either by using a charge storing device such as varactor diodes, solid ferroelectrics along with the liquid crystal or by employing multiplexed addressing schemes.

## 1.2. MOTIVATION

Though much progress has been achieved in the production of liquid crystal displays, the electro-optic performance of these displays, mostly using nematic liquid crystals presents some fundamental limitations.

One of the main drawbacks is the low switching time. The main driving force in these displays is the interaction of the applied electric field with the dielectric anisotropy of the material. The rise time of these displays depend also on the electrical conductivity, elastic moduli and viscosity of the material and is usually of the order of milliseconds. ( 20 ms to 10 ms). Such a low response becomes a serious drawback at increased multiplexing rates. Moreover it is very difficult to obtain memory states as well as sharp threshold voltages for electro-optic effects in these nematic materials.

In matrix addressed displays usually a capacitance

is connected along with nematic liquid crystal cell to the drain of the switching transistor to overcome this slow response. This capacitor stores the signal charges and discharges it to the liquid crystal in due course. This reduces the scanning time required for each frame, thus improving the effective response of the display, matching it with the requirements of some of the consumer products like television.

Instead of capacitors, solid ferroelectric materials are also used along with the liquid crystal to store the signal charges [4]. Here voltage levels are stored as polarisation states in the ferroelectric. This method also provides the sharp threshold voltage necessary for switching. Even here the integration process of the matrix junction is tedious and calls for much involved techniques.

All these difficulties can be solved to a large extent if a ferroelectric liquid crystal (FLC) is used as the display element. Ferroelectric liquid crystals have a spontaneous polarisation moment which can be used as a memory state. Further this polarisation can be reversed by applying an electric field. Also the response time of the device can be brought down to sub-microseconds range, since an additional driving force is derived from the field-

polarisation interactions.

Ferroelectric liquid crystal displays (FLCD) in different configurations like Surface Stabilised ferroelectric liquid crystal, ac stabilised ferroelectric liquid crystal, Transient Scattering Mode and those using electroclinic effect (Soft Mode ferroelectric liquid crystal) have been demonstrated by various groups of researchers, after the discovery of ferroelectricity in liquid crystal by Meyer [5].

The main motivation of this thesis is to investigate the possibilities of establishing well defined optical levels in an ferroelectric liquid crystal corresponding to the parameters of the applied electric field. To this end the electro-optic switching properties of the ferroelectric liquid crystal 4'-[ Octyl benzoyloxy ]-4-[2- Octyloxy ]-biphenyl (OBOB) are studied and measurements of the risetimes, decaytimes as well as transmission levels for specified values of the voltage and pulse width of electrical pulses are carried out. Further it is intended to study the potential use of ferroelectric liquid crystals as optical modulators. Such a device can find application as transmitters in optical fiber communication and as spatial light modulators in image converters. A special technique is developed, where the modulating signal is applied to an

ferroelectric liquid crystal cell, biased with a dc voltage to obtain intensity modulation. The variation of modulation depth with frequency is also studied. A qualitative explanation of this modulation is also attempted on the basis of partial unwinding of the helical structure of the ferroelectric liquid crystal under an applied electric field.

### 1.3. OUTLINE OF THE WORK AND RESULTS

The thesis is presented in six chapters. Chapter.2 reviews the recent developments in liquid crystal displays, mainly in ferroelectric liquid crystal displays and is meant to establish necessary background for the following chapters. Various techniques used to evaluate the material constants of ferroelectric liquid crystal like spontaneous polarisation, rotational viscosity, tilt and dielectric constant have been reviewed briefly.

The main ferroelectric liquid crystal display configurations, their electro-optic effects and experimental results as regards to rise time, decay time, grey scale capability etc. have been surveyed in this chapter.

The application potential of a material depends primarily on a thorough knowledge of its material constants. In chapter.3, the material constants of the ferroelectric



liquid crystal, OBOB are studied. The liquid crystal cell is made of two conducting transparent glass plates ( $\text{SnO}_2$  coated). Thickness of liquid crystal material is controlled by Mylar spacers (20 microns) and thin films of silicon monoxide coated on the glass plates (2 microns). Homogenous alignment is achieved by coating the glass surface with polyvinyl alcohol (PVA), rubbing and using a low frequency electric field. Oblique evaporation of silicon monoxide also is used for this purpose.

The temperature of the specimen is controlled to an accuracy of  $\pm 1^\circ\text{C}$  by a microprocessor based temperature controller and by keeping the specimen in vacuum.

The phase transition temperatures are studied using differential scanning calorimetry (DSC) and optical polarising microscope. OBOB shows chiral smectic phase in the temperature range of  $62^\circ\text{C}$  to  $74^\circ\text{C}$ .

The spontaneous polarisation of OBOB is evaluated by square wave method [6] and triangular wave method [7]. Spontaneous polarisation varies from 28 nC/square cm to 3nC/square cm with increase in temperature of the  $\text{SmC}^*$  phase. Rotational viscosity, another important parameter for display application is also measured by square wave and triangular wave methods at various temperatures.

Chapter.4 presents the detailed investigation of electro-optic switching behaviours of OBOB for pulses of varying pulse widths and voltages. The experimental arrangement uses a Helium-Neon laser as the optical source and photodiode as the detector along with a memory scope.

The ferroelectric liquid crystal shows a sharp threshold in its voltage/ pulse width transmission characteristics. At higher temperatures of SmC\* phase (74° C) bistable switching is observed for pulses of voltage higher than the threshold. At lower temperatures (66° C) and for small pulsewidths (below 10 ms) intermediate optical transmission levels are observed for the sample. These levels are found to depend both on height and width of the applied pulses. Another important result is that a pulse of height just lower than the threshold voltage can reset the switched state back to the opaque state.

In chapter.5 the electro-optic effects of ferroelectric liquid crystals for low voltage continuous signals of varying frequency are investigated. At first a pure sine wave is applied to the specimen. It is found that the electro-optic output does not follow the variations in the input. But on biasing the ferroelectric liquid crystal with a constant dc voltage (less than  $E_c$ , the critical

unwinding voltage) and then applying a sine wave signal along with the dc, the output variations followed exactly the input signal.

The experiments are repeated for a sweeping sine wave and it is found that the depth of modulation decreases with increase in frequency of the modulating signal. Finally speech signals are applied to the ferroelectric liquid crystal with proper dc biasing. Corresponding optical output recorded in the oscilloscope shows that the output is a replica of the input though there is a reduction in amplitude at higher frequencies. The above results are explained on the basis of partial unwinding of the deformed helical structure of the ferroelectric liquid crystal under the resultant action of dielectric and ferroelectric forces.

Experiments are also conducted for comparatively thin samples (1 to 2 microns) of OBOB. In this case alignment of molecules is obtained by oblique evaporation of silicon monoxide. Thin films of SiO coated in vacuum serve as spacers also. At these thicknesses modulating properties similar to those of thicker samples are obtained, but at lower voltages.

Chapter.6 concludes this work and suggests a few directions for future research.

## CHAPTER. 2 REVIEW OF PREVIOUS WORK

- 2.1. Introduction.
- 2.2. Synthesis
- 2.3. Review of evaluation of material constants.
  - 2.3.1. Spontaneous polarisation.(Ps).
    - 2.3.1.1. Measurement of spontaneous polarisation.
      - 2.3.1.1.1. Electrical reversal of spontaneous polarisation.
  - 2.3.2. Rotational viscosity.
    - 2.3.2.1. Measurement of rotational viscosity.
  - 2.3.3. Dielectric constant.
    - 2.3.3.1. Measurement of dielectric constant.
  - 2.3.4. Tilt angle.
- 2.4. Electro-optic switching studies.
- 2.5. FLC light valves and modulators.

## REVIEW OF PREVIOUS WORK

### 2.1. INTRODUCTION.

This chapter gives a summary of major works related to the characterisation and electro-optical switching studies of ferroelectric liquid crystals. The discovery of ferroelectricity in tilted smectic phase by Meyer in 1975 [5] confirmed that as in solids, molecules can have spontaneous polarisation in the liquid crystalline phases also. This has stimulated many studies from both fundamental and practical points of view. The ultimate aim of all these efforts is the realisation of a ferroelectric liquid crystal display which can meet the stringent requirements such as quick response, good grey scale capability and contrast so that their performance is comparable to that of cathode ray tubes.

The main steps involved in the fabrication of such a ferroelectric liquid crystal device are

1. Synthesis of a ferroelectric liquid crystal compound that shows ferroelectricity at room temperature and has comparatively high value of spontaneous polarisation, low rotational viscosity. The identification of phases is also done at this stage .

2. Evaluation of material constants such as spontaneous polarisation, dielectric constant, rotational viscosity and tilt angle as well as designing a suitable cell geometry and developing an aligning technique to orient the molecules in the desired configuration forms the next step.

3. A detailed study of the dynamic electro-optic characteristics of the material such as rise time, decay time, bistability and grey scale capability under varying signal conditions are also carried out in this stage.

4. Finally an addressing technique which depends on the particular application and the material properties will be arrived at.

In the last seventeen years many results have been published in each of the above categories by a number of workers. Some of these important contributions, which are relevant to the present work, are reviewed in this chapter.

## 2.2. SYNTHESIS.

Display operation requires a chemically and photochemically stable ferroelectric liquid crystal with wide temperature range around room temperature. For individual compounds the range of ferroelectric liquid crystal phase is small and most of them are at higher temperatures. This problem was solved by making eutectic

mixtures of different compounds [8,9 & 10]. The dependence of material constants of these mixtures on the magnitude and direction of the spontaneous polarisation ( $P_s$ ) and pitch values were studied by Goodby and Leslie [11].

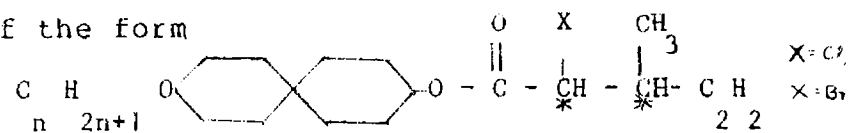
From Meyers arguments of occurrence of ferroelectricity in liquid crystals itself, it is understood that the extent of hindrance to the molecular rotation along its long axis is a measure of the magnitude of spontaneous polarisation. Based on this fact Uemoto et al. [12] synthesised a series of DOBAMBC type ferroelectric liquid crystal with higher number of carbon atoms ( $n$ ) in the alkoxy chain. They observed that for molecules with  $n < 5$ , value of spontaneous polarisation is very small. For  $n > 6$ , spontaneous polarisation was found to increase with the number  $n$  of carbon atoms, as the molecular rotation is reduced very much for these compounds.

Sakurai et al.[13] obtained high spontaneous polarisation values by using secondary alcohols as the chiral source of DOBAMBC type ferroelectric liquid crystal instead of primary active alcohols.

The increase in the value of spontaneous polarisation of these compounds is mainly due to the proximity of the chiral centre to the dipole.

Yoshino et al. [14] synthesised a series of

compounds of the form



The magnitude of spontaneous polarisation is 250 nC/sq.cm ie 20 orders of magnitude higher than that of DOBAMBC.

Recently R.J.Twieg et al. [15] synthesised a series of new ferroelectric liquid crystals characterised by the presence of a thioester core and an alkoxy carbonyl tail derived from a chiral 2-alkanol. Some of them shows spontaneous polarisation values of 220 nC/sq.cm at near room temperatures.

New ferroelectric smectic thiadaxosle derivatives synthesised by Tschieske et al. [16] gave spontaneous polarisation values of 350 nC/sq.cm. Due to the high value of spontaneous polarisation these ferroelectric liquid crystals can find application in high speed displays.

### 2.3. REVIEW OF EVALUATION OF MATERIAL CONSTANTS.

#### 2.3.1. Spontaneous Polarisation.

The potential application of ferroelectric liquid crystal materials in any device depends on the strength of spontaneous polarisation because an external field applied to such a material can couple with this polarisation. This interaction provides an additional driving force for the



molecular orientation other than the forces due to dielectric anisotropy.

#### 2.3.1.1. Measurement of Spontaneous Polarisation.

The first estimate of magnitude of spontaneous polarisation was obtained from the measurement of the dc field ( $E_c$ ) necessary to unwind the helical structure [5].  $E_c$  is given by the equilibrium between the electrical energy and the elastic energy.

$$E_c = \frac{\pi^2 K \theta^2 q^2}{16 P_s}$$

where  $q$  is the helical wave vector. The value of  $K$ , an elastic constant is not known accurately. Hysteresis of unwinding and ionic screening of applied field causes errors in actual experiments.

To obtain a direct measurement of spontaneous polarisation, the sample is prepared in the planar configuration. On reversing the dipoles, which are perpendicular to the electrodes in this case, by some external fields and observing the current profile, then the integral of the induced current is  $2PA$  ( $A$  is the area of the specimen).

But difficulties arise from the large conductive and capacitive currents evolving along with the current due to spontaneous polarisation reversal. The total current  $I$  on the upper electrode can be written as

$$I = A \frac{dp}{dt} + \frac{A}{d} \frac{d(\epsilon U)}{dt} + I_{\text{ionic}} = I_p + I_c + I_i$$

t is the time,  $\epsilon$  is the permittivity of the compound and U is the applied voltage.

The different electrical methods employed to evaluate spontaneous polarisation either compensate the capacitative current or separate the spontaneous polarisation current from the other components in time or shape. The shear and pyroelectric methods keep  $U=0$  so that  $I_i=0$  and  $I_c=0$ .

Yu et al. [17] and Blinov et al. [18] used pyroelectrical method for evaluating spontaneous polarisation. The sample is subjected to small periodic temperature jumps by means of laser pulses.

$$\text{Then } \int I dt = -A \frac{dp}{dt} \int dt$$

Where I is the current during one pulse.

This method avoids errors due to the induced polarisation and ionic currents. But for good results a perfect alignment is required and it is very difficult to determine the temperature dependence of spontaneous polarisation.

#### 2.3.1.1.1. Electrical reversal of spontaneous polarisation.

In these methods, an alternating voltage (pulse or

continuous wave) is applied to the specimen to reverse the spontaneous polarisation. It was first introduced by Martinot-Lagarde [19]. He applied a square wave voltage to the specimen in SmC\* state and the integral of the bump due to spontaneous polarisation reversal was calculated. The square wave produces a quick reversal of dipoles and hence a good time separation between the different current components. But due to the non-linearity of the ionic current it is very difficult to fix a base line as a reference for the measurement of the spontaneous polarisation current. Hence the values obtained are not matching with theoretical and other experimental values.

This ambiguity in fixing a base line was later solved mainly by two methods.

Miyasato et al. [7] showed that the non-linear behaviour of the background current can be avoided by using a triangular wave instead of a square wave. In this case the rate of variation of the applied voltage is low. Hence the bump due to the polarisation reversal appears on a straight base line. So the background current due to capacitative and ionic contributions can be directly subtracted to obtain the current due to polarisation reversal. Further it is easy to obtain a good high voltage triangular wave than a square one.

Sometimes, depending upon the alignment method and thickness, two or three bumps [20] are obtained due to the spontaneous polarisation reversal itself. In this case the integral of these bumps gives the spontaneous polarisation.

Skarp et al. [6] solved the problem of separation of the background current in a more rigorous method. They first considered a model of the ferroelectric liquid crystals placed between two electrodes. In the absence of spontaneous polarisation, it can be regarded as a capacitor (C) in parallel to a resistor (R<sub>p</sub>). (Fig.2.1).

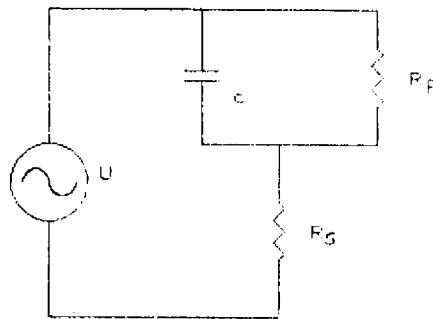


Fig. 2.1 Equivalent circuit of a FLC between two electrodes in the absence of P<sub>s</sub>

Hence when a square wave voltage U is applied the background current should obey the equation

$$C R_s \frac{dI}{dt} + (R_s + R_p) I / R_p = U / R_p + C \frac{dU}{dt}$$

This equation is solved numerically to obtain the value of I at any instant for a given U. It is then subtracted from the measured value to get the current due to polarisation reversal, which is then integrated to get the charge Q on the electrodes.

Then  $Q = 2PA$

Ferroelectric liquid crystals synthesised recently have a very high value of spontaneous polarisation (350 nC/sq.cm). The methods to measure the spontaneous polarisation in these compounds have to take into account their high ionic conductivity and permittivity. This is achieved in differential measurements or by using rectangular or triangular voltages to separate the current components by their time behaviour.

### 2.3.2. Rotational Viscosity.

The application prospects of liquid crystals in any device relies on the possibility to induce structural changes by an externally applied electric field. The dynamical behaviour of the related switching process may often be described by introducing a suitable viscosity term in the equation of motion.

In nematic liquid crystals the viscous forces are estimated using the Leslie-Erickson model [21]. In ferroelectric liquid crystals we have to introduce two rotational viscosities denoted by  $\gamma_\phi$  &  $\gamma_\theta$  [22]. At very high fields, magnitude of the tilt angle  $\theta$  can be changed appreciably. Hence to account for the viscosity at high fields (softmode effect) the coefficient  $\gamma_\theta$  is introduced. But for moderate fields the motion of the director is along

a cone of angle  $\theta$  (Goldstone mode). Hence only the direction of  $\theta$  varies. Hence it is the rotational viscosity  $\gamma_{\phi}$  which influences the ferroelectric switching process involving comparatively lower electric fields. Therefore the determination of  $\gamma_{\phi}$  is of prime interest in response time studies related to dynamical switching in ferroelectric liquid crystals.

#### 2.3.2.1. Measurement of Rotational viscosity

Measurement of rotational viscosity for nematics have been carried out for a long time using several methods. Some of these methods were applied to smectic C\* also. But many new methods, which take advantage of the ferroelectricity have additionally been developed in recent years.

Pieransky et al. [23] evaluated rotational viscosity by studies of dynamic conoscopic picture and by disturbing the helix in the SmC\* phase by an alternating shear or Poiseuille flow and measuring the current. The complicated experimental setups and inconsistent results render these methods obsolete.

One of the most convenient ways for evaluating rotational viscosity is to measure the optical response time in thin samples [24 & 25] on an applied voltage step. The

time measured from 10 to 90 % of the transmission between crossed polarisers is related to rotational viscosity by the equation:

$$\gamma_{\phi} = 1 / 1.8 \cdot T_{10-90} \cdot P_s \cdot E$$

The switching model holds good for the region of the electric field high enough so as to neglect the elastic effects. Though the method is simple, it requires a separate setup for the measurement of spontaneous polarisation. Further the extraction of rotational viscosity from the measurements is influenced by several factors such as wavelength dependence of the light transmission and dielectric anisotropy.

The polarisation reversal methods started by M. Lagarde [19] overcomes some of the drawbacks of earlier methods. Originally used to evaluate spontaneous polarisation, it was later found to be a very good method to measure rotational viscosity also [25,26,27]. Now several simplified analytic switching models exist enabling a detailed evaluation of such polarisation reversal experiments.

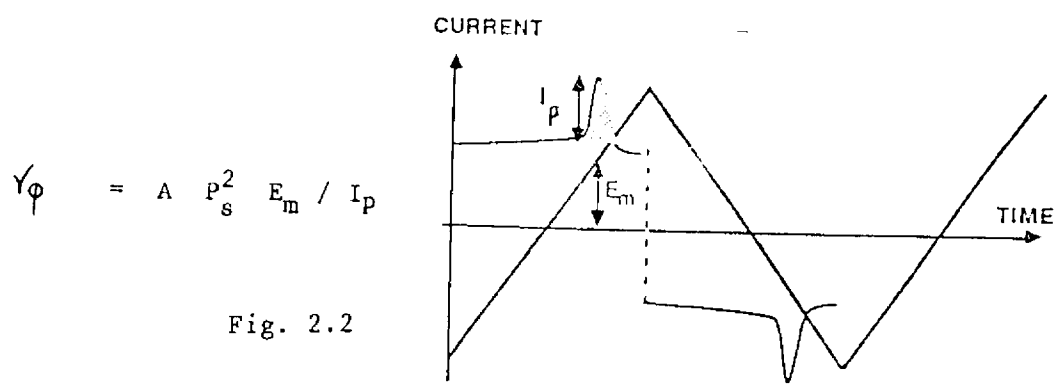
In earlier studies rotational viscosities were calculated from the position of the current peak on the time axis. But this peak position depends on the elastic effects

and hence the evaluation becomes difficult.

Later it was established that the most important parameter of relevance for rotational viscosity measurements is the width of the half height of the current peak. They are related by the equation

$$\gamma_{\phi} = 1 / 1.8 T_w P_s E$$

Geelhar et.al [28] evaluated viscosity by analysing the current response of a triangular voltage to the ferroelectric liquid crystal. The evaluation method is shown in Fig.2.2. In the current peak the maximum height  $I_p$  at the electric field  $E_m$  is noted. Then



where A is the area of electrodes.

But the question remains whether viscosity measured in thin cells corresponds to the bulk viscosity of the system, or it is influenced by boundary effects.

Levstik et al. [29] demonstrated a method by which the rotational viscosity can be determined for bulk samples by measuring the dielectric constant of the system together with polarisation and tilt angle. Their results also showed that the variation of viscosity with temperature obeys



Arrhenius law. The advantage of this method over electro-optic and spontaneous polarisation reversal methods is that the director is excited to small oscillations and the use of bulk samples reduces the boundary effects.

Skarp et al. [25] measured the rotational viscosities of four ferroelectric liquid crystals with varying structure and macroscopic characteristics. They compared the results obtained by ac bridge, electro-optical, triangular and square wave methods. All methods were found to be sensitive to cell preparation, especially on the alignment of smectic layers.

### 2.3.3. DIELECTRIC CONSTANT.

The dielectric response of materials has been of great interest to scientists and technologists for a long time. This is especially true for ferroelectric materials. In the case of liquid crystals the investigation of dielectric behaviour of SmC\* materials near the phase transition from high temperature SmA phase can contribute to the understanding of mechanism of phase transition. Further, the sign of the dielectric anisotropy decides the speed of electro-optic switching and bistability of switched states in an applied electric field.

The complex permittivity of a dielectric material

is expressed as  $\epsilon^*(\omega) = \epsilon'(\omega) - j \frac{\epsilon''}{\omega}$

where  $\omega$  is the angular frequency of the measuring field.

The real part  $\epsilon'$  of the permittivity is the usual dielectric constant while the imaginary part  $\epsilon''$  accounts for dielectric losses.

The dielectric behaviour of chiral smectic C phase and its dependence on temperature and frequency, measuring field strength, pressure, sample thickness and electric bias field has been studied by several groups during the last few years. The main outcome has been the characterisation of the dielectric properties of the Goldstone mode in the C\* phase and the soft mode in the A\* and C\* phases. The first is related to the rotations of the molecules along the smectic cone while the second mode is related to rotations in which the tilt of the molecules get changed.

#### 2.3.3.1. Measurement of dielectric constant.

The dielectric constant of ferroelectric liquid crystals is usually measured either by the capacitance bridge or an impedance analyser or by a lock-in amplifier.

Temperature dependence of dielectric constant of p-decyloxybenzylidene-p-amino-2-methylbutylcinnamate (DOBAMBC) in the planar oriented samples of thickness 250,

100, 50 and 30 microns were studied by Yoshino et al.[30]. For low frequencies (< 1kHz), they obtained a maximum value of dielectric constant at a temperature near the phase transition temperature  $T_c$  from the smectic A to the  $SmC^*$  phase. Frequency dependence of dielectric constant at various thicknesses were also measured at different temperatures. The results showed that at high frequencies (>10 kHz), there is no appreciable change of permittivity in the  $SmC^*$  state.

Sakurai et al. [13] prepared a new series of ferroelectric liquid crystals and the dielectric measurements at low frequencies (30 Hz) showed a sharp increase in value in the  $SmC^*$  state.

Using a mixture of compounds Levstik et al. [29] produced a room temperature ferroelectric liquid crystal with the  $SmC^*$  phase from 15°C to 44°C. For a 130 micron thick planar sample dielectric constant was determined in the smectic A and  $SmC^*$  phase for frequencies from 20 Hz to 8 kHz.

Glogarova et al. [31] measured the temperature dependence of dielectric constant in planar samples of DOBAMBC with simultaneously observing the structure. They repeated the experiments using samples unwound by a dc electric field. At high fields no appreciable change in

dielectric constant was observed on passing from the smectic A to SmC\* phase. Their results also showed that dielectric constant showed a relaxation behaviour at higher frequencies (>200 Hz). Far above this frequency the value of dielectric constant is comparable to the value obtained at high biasing fields and in the smectic A phase.

Applied field dependence of static dielectric constant and also dc bias field dependence of high frequency dielectric constant for 1 MHz to 100 MHz were measured in the helicoidal smectic C phase of DOBAMBC by Maruyama et al. [32] using lock-in amplifier, thermal noise and bridge method. He observed a very low characteristic threshold field in the static dielectric constant measurement by lock-in amplifier. This corresponds to the minimum excitation field of the Goldstone mode. The high frequency dielectric constant was found to be temperature independent above 10 MHz.

The static dielectric constant ( $\epsilon$ ) in the smectic A and SmC\* phase of the ferroelectric liquid crystal 4(3-methyl-2-chlorobutanoyloxy)-4-heptyloxybiphenyl was determined by Bahr et al. [33]. They observed strong pre-transitional effects in the smectic A phase. When the Goldstone mode contribution in the SmC\* phase was quenched

by an applied electric field, a cusp like behaviour of dielectric constant at the C\*- A transition, similar to solid ferroelectrics were observed.

The soft mode behaviour of ferroelectric liquid crystal 4-octyloxy-4-(2-methyl butyloxy) carbonyl phenylester was investigated by Pavel and Glagarova [34]. For this they measured the complex permittivity of the material in the vicinity of smectic A-- SmC\* phase transition with a dc field applied to the specimen to unwind the helix. This helped them to eliminate the contribution to dielectric constant from the Goldstone mode.

They found that at 100 Hz the temperature dependence of the soft mode contribution had the form of the Currie-Weiss law on both smectic A and SmC\* phase. At higher frequencies the maximum of dielectric constant at Tc is lowered and at about 40 kHz a minimum appeared. Similar results were obtained by Legrand et al. [35] for large range of frequencies.

In all the above measurements of dielectric constant in SmC\* phase means the dielectric constant perpendicular to the helix. However for the calculation of dielectric torque, the important information lies in the anisotropy of dielectric constant. ie

$$\Delta\epsilon = \epsilon_{\parallel} - \epsilon_{\perp}$$

where  $\epsilon_{\parallel}$  relates to an electric field applied along the molecular axis and  $\epsilon_{\perp}$ , to the field perpendicular to the axis. In the smectic A and smectic A\* phase the field directions are in accordance with this definition. But in the SmC\* phase, in the homeotropic configuration the measuring field makes an angle  $\theta$  (the tilt angle) with the director. In spite of this the measured dielectric constant was noted as  $\epsilon_{\parallel}$ . Similarly in the planar geometry also, due to the presence of the tilt the measuring field is no longer perpendicular to the director. But the measured dielectric constant was denoted as  $\epsilon_{\perp}$ .

This discrepancy was realised by Hoffmann et al. [36]. By a transform of the tensor from the coordinate frame related to the main axes of molecule to the laboratory frame, they calculated the actual dielectric anisotropy of DOBAMBC samples.

Such measurements of dielectric anisotropy for a series of commercially available ferroelectric liquid crystals were conducted by Gouda et al. [37] for frequencies from kHz to MHz ranges. Their results are useful in calculations of dielectric torque in applied devices.

#### 2.3.4. TILT ANGLE.

The tilt angle  $\theta$  of molecules inside the smectic

layers is the order parameter of smectic phase. It is the order parameter of the SmC\* phase also since the polarisation itself is proportional to the tilt angle. Further the tilt angle represents the tilt of the long axis of any second rank tensor associated with the molecules like the diamagnetic susceptibility, the dielectric constant and optical indices. Hence the measurement of tilt and the investigation of its dependence on the molecular structure, temperature and the composition of mixtures is necessary for selecting and tailoring new ferroelectric materials for electro-optic devices.

Two important methods usually employed for measuring tilt angle are the X-ray method and the optical method. If  $l$  is the length of the molecule of ferroelectric liquid crystal and  $d$  the thickness of the tilted smectic layers, then

$$d = l \cos\theta .$$

In X-ray method [38]  $d$  is derived from the layer periodicity of the sample in the SmC\* phase and  $l$  from that in the smectic A phase close to the smectic A-SmC\* phase transition temperature. The periodicity is obtained from X-ray photographs by measuring the separation between the lines formed by the beams scattered and non scattered by the

smectic layers. Then using the Bragg relation

$$n \lambda = 2d \sin \theta$$

where  $\lambda$  is the wavelength of the X-ray radiation and  $\theta$  the Bragg reflection angle.

Martinot-Lagarde et al. [38] studied the variation of tilt angle with temperature for ferroelectric liquid crystals like DOBAMBC, OOBAMBC, OOBMBCC and TDOBAMBC using the X-ray method and obtained good results.

In optical measurements, the tilt angle of the main axis of optical dielectric tensor gives the angle  $\theta$ . Martinot Lagarde et al. [38] measured this angle after unwinding the helix using an electric field. In the unwound state, all the molecules are tilted across the normal to the layers by the tilt angle  $\theta$ . By reversing the field direction the molecules are tilted by an angle  $-\theta$ . Thus the angle between two extinction positions, under crossed polarisers is  $2\theta$ . Their experiments in planar and homeotropic geometries gave accurate values of tilt angle at different temperatures.

One disadvantage of optical method compared to optical method is the necessity of a strong electric field. But the X-ray method is inadequate when the molecules possess long end chains.



Takezoe et al. [39] measured the tilt angle for different sample thickness of DOBAMBC in which the helix was unwound by glass surfaces. The apparent value of tilt angle increased with decreasing thickness and reached a constant when sample thickness was less than the pitch of the helix. This value is taken as the true value of tilt angle.

#### 2.4. ELECTRO-OPTIC SWITCHING CHARACTERISTICS.

The choice of an ferroelectric liquid crystal material for any particular application depends on its electro-optical switching characteristics like rise time, decay time, grey scale capability and bistability. The geometry (configuration) of the cell is the most important factor that decides these characteristics, other than the material constants. Since ferroelectric liquid crystals have a layered structure, many types of configurations, making use of different mechanisms such as helical unwinding, domain switching and optical birefringence have been studied by many workers.

From an application point of view a broad classification of these configurations is based on the thickness of the material ( $d$ ) compared to its pitch ( $P_0$ ). For thick cells ( $d \gg P_0$ ) the optical effects are explained

on the basis of winding and unwinding of the helix. In this case if the pitch is comparable to the wave length of light used, then strong scattering is the mechanism of optical effect. When pitch is less than wave length, scattering decreases and the incident light sees an apparent refractive index averaged over the helix (Deformed helix FLC ). Since the helix is easily distorted by electric fields, it is possible to modify electrically the average optic axis to obtain electrical contrast.

For thick cells (10 microns to 250 microns) experiments were conducted by Yoshino et al. [40] with an aim to establish bistability in thick cells of DOBAMBC, by utilising the change in light scattering that follows the transition between wound and unwound states of the helix of the ferroelectric liquid crystal. But the unwound, uniformly aligned monodomain structure regained its original helical form on removal of applied field. Moreover the threshold voltage was high and the response was slow.

Another method tried by this group is based on the transient light scattering at the instant of domain switching due to the polarity reversal of the applied field [41]. Here for both polarities of applied voltage, the medium is transparent whereas during the reversal of the

field it is opaque. There is an improvement in response, as both winding and unwinding are controlled by the applied field. But bistability is not achieved in this case also.

In the deformed helix ferroelectric effect suggested by Ostrovski et al. [42] a ferroelectric liquid crystal with a very short pitch is used. When the pitch is shorter than the wave length of the incident beam, they showed that an average optical indicatrix can be considered. Initially the optic axis of the helical structure coincides with the helical axis. The distortion of the helix by an applied field leads to a change of refractive index and hence to a change in optical transmission through the material. A low voltage, high response liquid crystal--photoconductor structure with a spatial resolution of 40 lines per millimeter and reversible memory was developed by Bersenev et al.[43] based on this effect. Recently Funkschilling and Schadt proposed a highly multiplexible deformed helix ferroelectric liquid crystal device [44] with response time in 10 micro seconds region and good grey scale capability. A major drawback of this effect is the unwinding of the helix under slightly higher voltages.

For thin cells ( $d \ll P_0$ ) the helix can be unwound by means of surface forces. Clark & Lagerwall [45] was able

to arrive at such a geometry (SSFLC) in which the UP and DOWN states are stabilised by surface interactions. The change in birefringence due to the transition between these two uniformly aligned states, on reversing the polarity of the applied field, is utilised for getting optical switching. They obtained sub-microsecond switching speeds at very low fields (2 V/micron).

Patel [46] studied the switching behaviour of such SSFLC cells and established bistability and the presence of a dynamic threshold in cells of 1 to 2 microns thickness. He obtained a linear relation between inverse of pulse width and voltage for a particular transmission level.

Patel and Goodby [47] examined the temperature and pulse shape dependence of optical switching in these surface stabilised configurations using simple and complex waveforms.

AC field stabilisation is another method [48] used to stabilise the switched state of an ferroelectric liquid crystal with negative dielectric anisotropy. The ac should alternate the field polarity in a time shorter than liquid crystals response time. Theoretical studies on this effect has been carried out by Schiller et al. [49] and Jiu Zhi et al.[24]. Detailed experimental studies regarding influence

of spontaneous polarisation and  $\gamma_{\phi}$  on this effect have been done by Nagata et al. [50].

A drawback in all these thin cell configurations is the lack of inherent grey scales. This has been solved to an extent by using the technique of multiple frequency addressing and making use of the phenomena of multidomain switching [51].

The soft mode effect, first suggested and studied by Garoff and Meyer [52] utilises the electroclinic response of chiral orthogonal smectic phases. ( A\*, B\* and E\* ) in bookshelf geometry. In addition to a submicrosecond response time and wide continuous dynamic range the devices based on this effect has full grey scale capability [53]. Very small temperature dependence and good linearity of response are further advantages of this effect.

## 2.5. FLC LIGHT VALVES AND MODULATORS.

Modulation essentially consists in imprinting an information on a carrier wave. In image converters, projection displays and transmitters of optical communication systems, light is the carrier. So in optical modulation, phase or intensity of a light beam is to be modified according to the modulating signal.

The modulation can be obtained either by direct

switching of the light source or by using an external modulator. The use of an external modulator has a distinct advantage over direct modulation as it relieves the burden imposed on the light source. By passing a carrier wave through a modulator, a sub carrier that contains information can be generated by applying the signal on the modulator crystals, which can be electro-optic, magneto-optic or acousto-optic.

The electro-optic modulation of light is based on a linear electro-optic effect in crystals whose refractive index is changed upon the application of an electric field. Liquid crystals thus offer a natural choice of such materials as the orientation of the molecules and hence the refractive index can be easily changed by an external electric field. Nematic liquid crystal based optical modulators have been fabricated by many workers. The increased response time and improved bistability of ferroelectric liquid crystals make them more attractive as materials in these devices.

Presently two types of modulating mechanisms are suggested in ferroelectric liquid crystal based modulators. When the thickness of the liquid crystal layer is much higher than the pitch ( $d \gg P_0$ ) and applied field is less than

the critical unwinding field ( $E < E_c$ ) and light beam aperture is greater than the pitch ( $a > P_0$ ), then the light modulation is due to the helix deformation (DHF effect) [42].

On the basis of this effect a low voltage light modulator with switching time of 250 micro seconds was fabricated by Bersenev et al. [43]. Funfschilling and Schadt obtained 10 micro seconds response time by applying high voltage pulses of short duration before the low voltage probe pulse [44].

In a recent paper Panarin et al. studied dependence of switching time of such deformed helix ferroelectric devices on driving voltages and frequencies [54]. A nonlinearity of response characteristics was observed at higher voltages and frequencies.

Using chiral dopants and multicomponent mixtures ferroelectric liquid crystals of very small pitch are available now. This offers good chances for developing modulators using this effect.

When the major concerns are response time and bistability, thin cells are superior to thick ones. Both the SSFLC and SMFLC configurations have been used to construct high frequency low-voltage modulators. In applications like optical processing, photoaddressed

ferroelectric liquid crystal- spatial light modulators (FLC-SLM) are of particular interest as it offers parallel optical addressing with a potentially high frame rate. Armitage et al. obtained write and erase speeds of 100 micro seconds for an imaging test device using ferroelectric liquid crystals [55].

For binary operations SSFLC effect is more suitable due to its good bistability. But for continuous gradations (grey scales) the linear electroclinic effect of SMFLC configuration is superior.

A FLC-SLM using a hydrogenated amorphous silicon as photoconductor was constructed by Yamamoto et al. [56] using SmC\* ferroelectric liquid crystal in a coupled configuration. Response times of 500 micro seconds for 1 micro seconds pulses, a contrast ratio of 200:1 and a resolution of 80 lines per millimeter are achieved in this model.

Mao et al. [57] demonstrated that optically addressed spatial light modulators with SmA\* and SmC\* materials and an amorphous silicon photosensor can be used to perform high speed low power optical phase conjugation. Frequency response of 10 k Hz were achieved by them.

Electro-optic modulators in the polarisation mode



using materials in the SmA\* and SmC\* phase were fabricated by Karppinan et al. [58]. In the SmA\* configuration 3 micro seconds time were attained for 40 volts (peak to peak).

Using a mixture of ferroelectric liquid crystal compounds Anderson et al. [59] obtained a tilt of 11.25 for a SmA\* phase at room temperature and at moderate field strengths. By means of multiple cell technique good grey scale generation and response times of 10 micro seconds were obtained.

To summarise, ferroelectric liquid crystal based electro-optic modulators can be used as choppers, function generators and optical power controllers with better efficiency and speed. Reset pulse techniques in thick cells and electroclinic effects in thin cells can be effectively exploited for improving response times. If SmC\* material with high spontaneous polarisation and low viscosity and SmA\* materials with large tilt are available, high speed requirements of light valves for applications in spatial light modulators in image converters and optical processors can be realised.

## CHAPTER 3. MATERIAL CONSTANTS.

- 3.1. Introduction.
- 3.2. The FLC materials and their phases.
- 3.3. Cell preparation --Alignment methods
- 3.4. Experimental Arrangements.
- 3.5. Temperature Controller.
- 3.6. Spontaneous Polarisation.
  - 3.6.1. Methodology.
  - 3.6.2. Results and Discussion.
    - 3.6.2.1. Rectangular waves--Time separation.
    - 3.6.2.2. Triangular waves--Shape separation.
- 3.7. Rotational Viscosity.
  - 3.7.1. Square wave experiments.
  - 3.7.2. Triangular wave experiments.
- 3.8. Dielectric Constant.
  - 3.8.1. Experimental determination
  - 3.8.2. Results and Discussion.
- 3.9. Tilt Angle

## MATERIAL CONSTANTS

### 3.1. INTRODUCTION.

Measurement of material constants forms an essential part in selecting and tailoring a material for any practical application. In ferroelectric liquid crystals the important material parameters relevant to display applications are:

1. The temperature range of SmC\* phase.
2. Spontaneous polarisation.
3. Rotational viscosity.
4. Angle of tilt.
5. Dielectric constant and
6. The helical pitch.

In practical applications, usually several ferroelectric liquid crystal compounds are mixed to form a most appropriate material. For this it is very important to measure the material constants of individual compounds accurately.

In this chapter, studies carried out to determine some of the above material constants are described. In general the accuracy of measurement of ferroelectric liquid crystal material parameters depends on the quality of alignment of liquid crystal cell. Some of the existing

alignment techniques for ferroelectric liquid crystals are modified and better results are obtained.

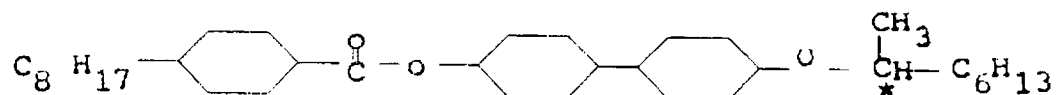
Since the studies are mainly concentrated on the SmC\* state, the transition temperatures corresponding to this state is studied in detail. Texture identification using polarising microscope and differential scanning calorimetry (DSC) are employed for this purpose.

When used as a display element, the response of the ferroelectric liquid crystal to an applied electric field is the most important parameter of interest. Though it depends on the geometry of the ferroelectric liquid crystal cell, a quick response will be obtained for materials having a high value of spontaneous polarisation and a low value of rotational viscosity. The spontaneous polarisation, rotational viscosity, dielectric constant and the tilt angle of a ferroelectric liquid crystal in the SmC\* state are measured and the variation of these properties with temperature by different methods are also studied.

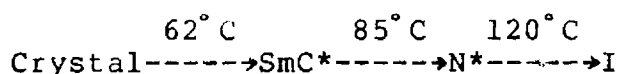
### 3.2. THE FERROELECTRIC LIQUID CRYSTAL MATERIALS AND THEIR PHASES.

The main ferroelectric liquid crystal under investigation is

4-(4-n-octylbenzoyloxy)-4-2-octyloxy biphenyl. [OBOB]



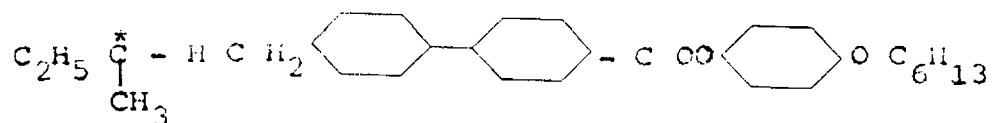
It has a phase transition sequence of



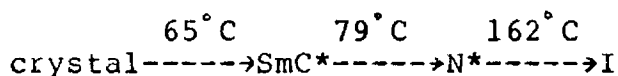
Two commercially available ferroelectric liquid crystals  
CE3 and CE8 from BDH pool, UK are also studied.

CE3 is

4-(n-Hexyloxy phenyl)-4-(2-methyl butyl) biphenyl-  
4-carboxylate.

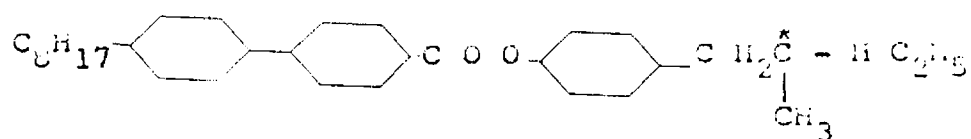


The standard phase transition sequence is

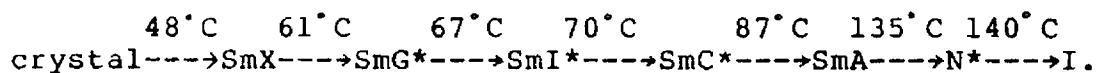


CE8 is

4-(2-methylbutyl) phenyl-4-n-octylbiphenyl-4-carboxylate.



Its transition temperatures are



The transition temperatures of the materials are

determined using differential scanning calorimetry (Fig.3.1) and by observing the textures through a polarising microscope (Fig.3.2). Changes in optical transmission through the sample also is used in some cases to substantiate the results.

The phase transition temperatures, obtained by observing the texture changes, for samples sandwiched between glass plates, are found to be less than that observed in DSC measurements. It may be due to the fact that the cells used in our studies utilised surface anisotropy for alignment which can produce an enhanced effect on these transitions. Also some transition temperatures for CE3 and CE8 are found to be differing from those reported in Ref:11.

The phase transition temperatures for the materials are fixed after a series of observations on textures, optical transmission characteristics and DSC measurements. (Table.3.1)

### 3.3. CELL PREPARATION AND ALIGNMENT METHODS.

Optically plane (of the order of 2 microns) glass plates are used in these experiments. On one side they are coated with  $\text{SnO}_2$  to form a conducting transparent layer. The resistivity of the conducting layer is always

G 535A-

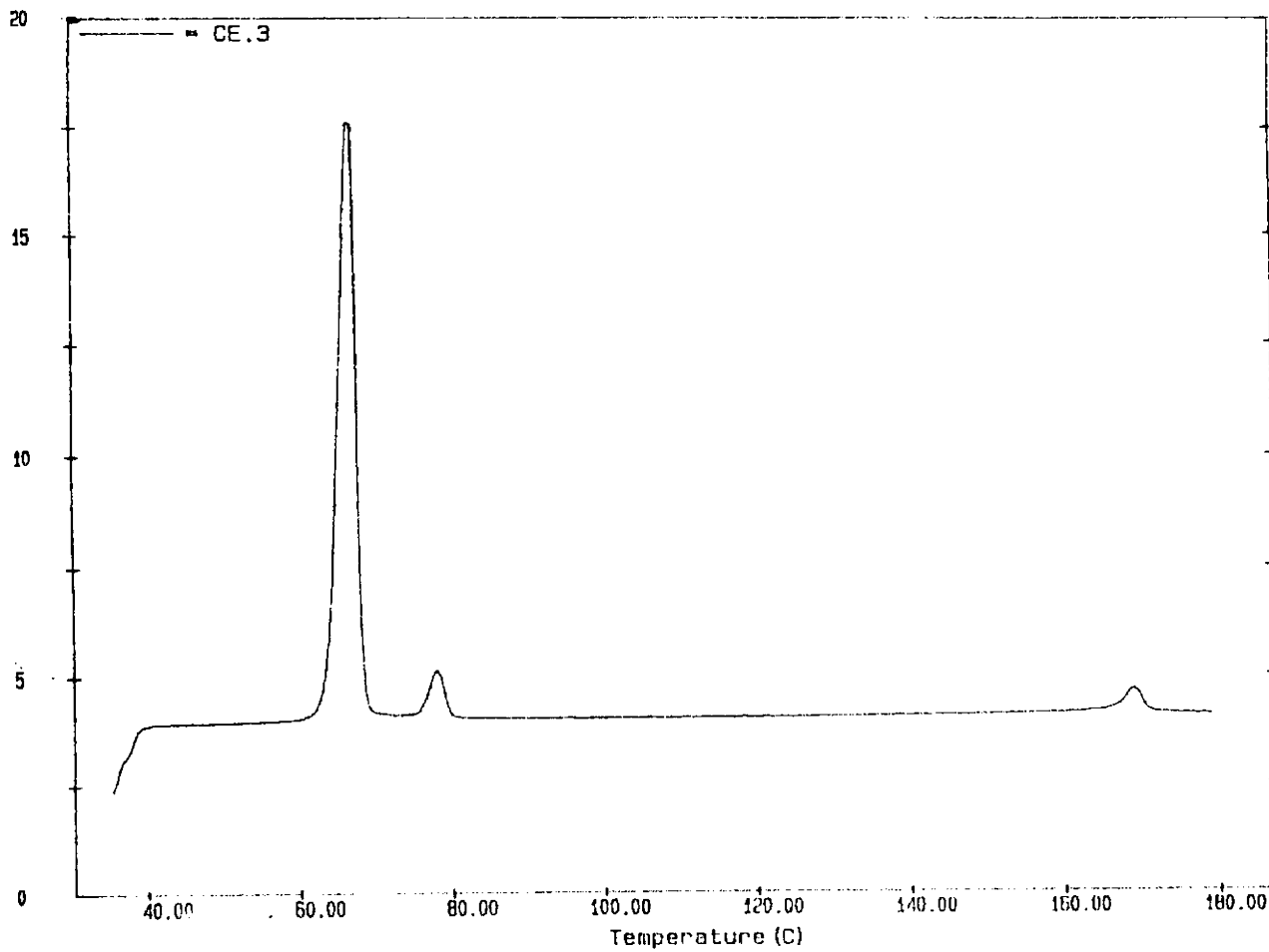
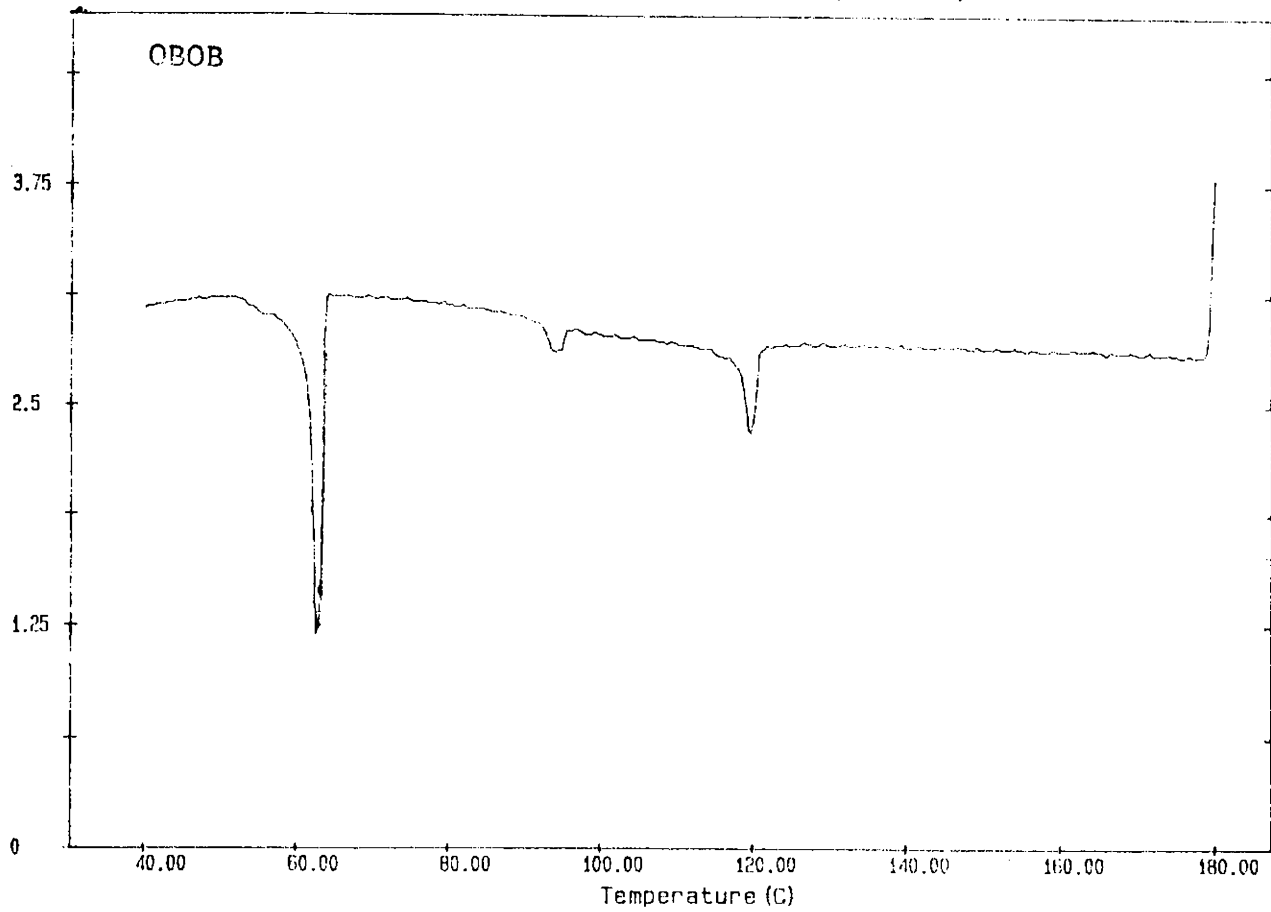
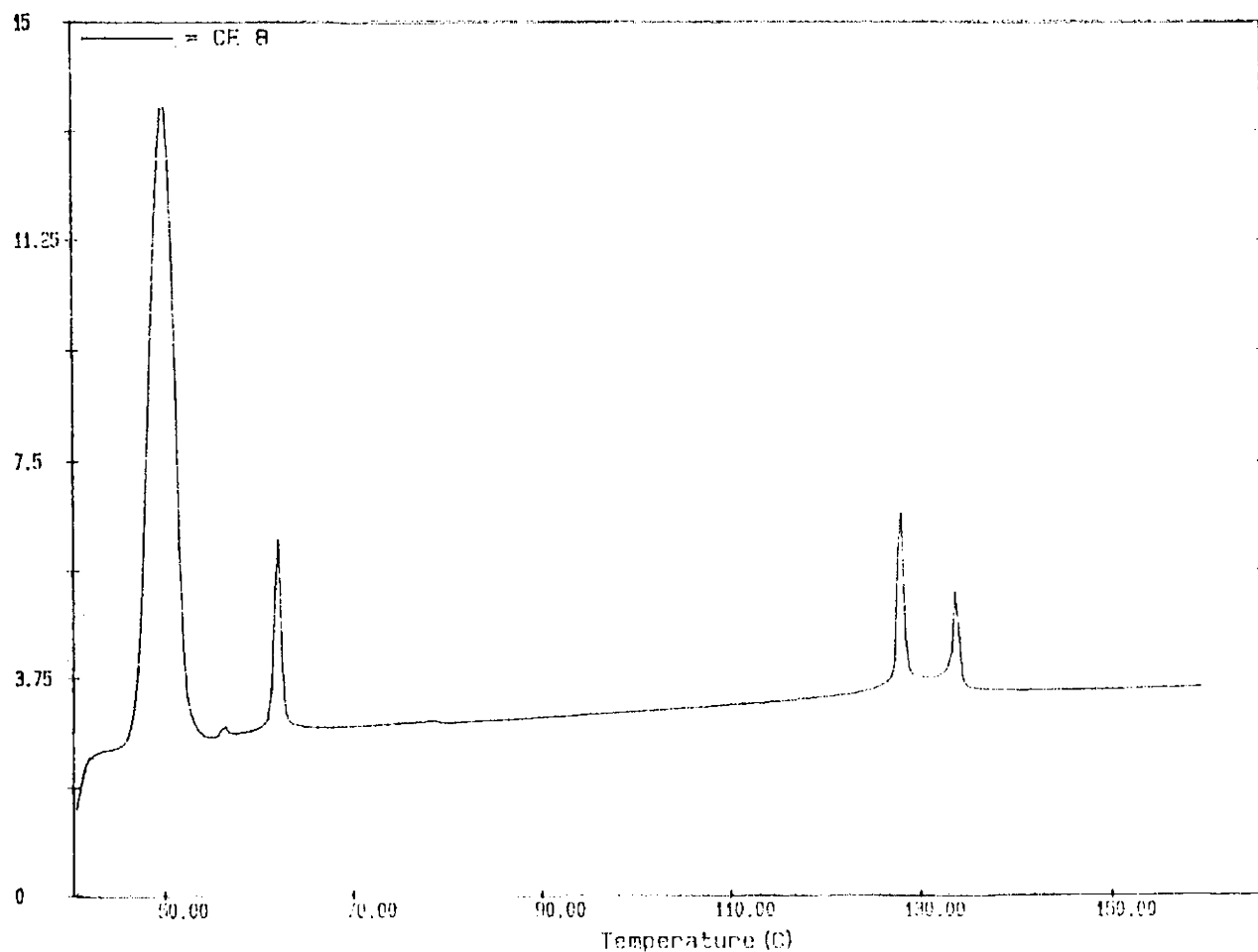


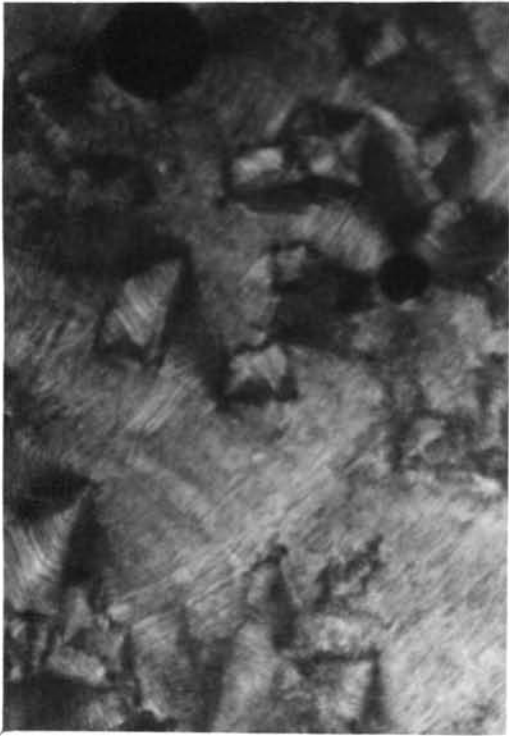
Fig. 3.1 D.S.C charts of (a) OBOB, (b) CE3 and (c) CE8



OBOB	62°C	85°C	120°C			
Crystal	-----SmC*	-----N*	-----I			
CE3	62°C	77°C	162°C			
Crystal	-----SmC*	-----N*	-----I			
CE8	48°C	61°C	68°C	87°C	135°C	140°C
Crystal	-----SmG*	-----SmI*	-----SmC*	-----SmA	-----N*	-----I

Table 3.1 Phase transition temperatures of the materials

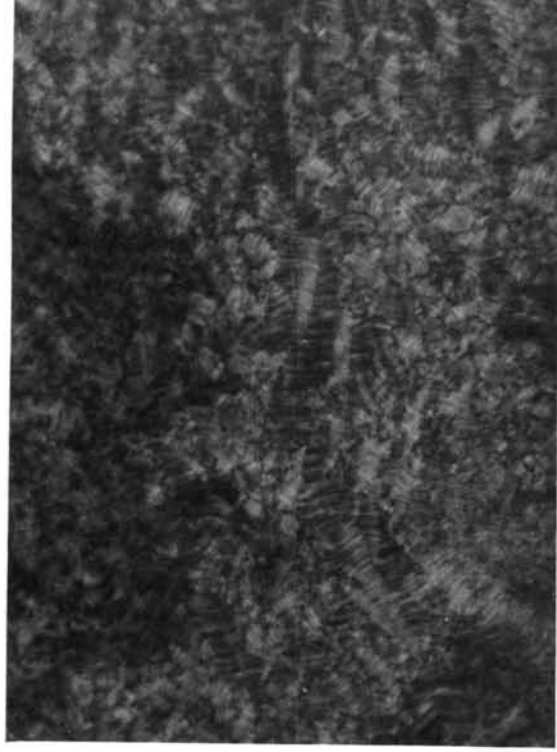




(a)



(b)



(c)

**Fig. 3.2**  
Textures of FLC  
(a) Banded focal conic texture of OBOB  
(b) Petal texture of CE3  
(c) Texture of OBOB under a dc field

kept less than 200 ohms/sq.cm, so that only a very small portion of the applied voltage is dropped across these electrodes. The glass plates are cleaned and evened out in a plasma discharge to get a surface evenness of 1 to 2 microns. To check the presence of ionic contaminants on the glass surface, water break test is conducted. For this the glass plates are immersed in a beaker of deionised water and then it is removed vertically. Only those glass plates which held the film at least for 40 seconds are selected.

The main methods used for alignment of ferroelectric liquid crystal in planar configuration are SiO oblique evaporation [60], epitaxial growth from a spacer edge [61], polyimide, PBT or PVA coating followed by rubbing [62] and application of magnetic or electric fields.

Since the two ferroelectric liquid crystals CE3 and OBOB shows the cholesteric to smectic C\* transition, the method of alignment suggested by Patel [62] is used in our investigations.

For this, the selected glass plates are dried and then dipped in a 1% solution of - (Methacryloxy)- propyl trimethoxy silane in alcohol which acts as an adhesion promoter. It is then dipped in a 1% solution of polyvinyl alcohol in dimethyl formamide. The concentration of the solution and the rate of withdrawal are adjusted to give a

very thin uniform film of PVA.

The glass plates are dried and then rubbed in a single direction. This process involves the movement of the glass plates across a piece of cloth in a straight line.

In some samples, instead of PVA, polybutylene terephthalate (PBT) solution is used, as PVA is found to be susceptible to moisture. Also rubbing the polymer coating before it is dried fully gave better alignment.

The ferroelectric liquid crystal material is drop filled in the isotropic state. Thickness is controlled by means of Mylar spacers and is confirmed by optical methods. The cell is assembled with the rub-directions on the two glass plates parallel to each other.

The sample in the isotropic state is cooled in the presence of an ac electric field of magnitude greater than the unwinding field ( $1.5 \times 10^4$  V/cm) and frequency slow enough to cause molecular orientation.

#### 3.4. EXPERIMENTAL ARRANGEMENTS.

The ferroelectric liquid crystal sample is mounted on a cell holder kept inside a metallic chamber having optical windows. It is electrically insulated from the sample holder and chamber.

A pulse generator/function generator is used to generate pulses. To increase the pulse height, the output from the pulse generator is connected to a switching transistor (BD 115) as shown in Fig.3.3. By varying the supply voltage to the switching transistor, desired pulse height is achieved.

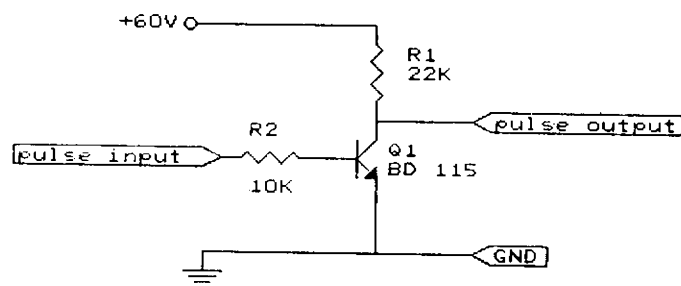


Fig. 3.3 Circuit for increasing the pulse height

### 3.5. TEMPERATURE CONTROLLER.

A microprocessor based temperature controller is developed for the characterisation studies. Functional block diagram of the system is shown in Fig.3.4.

A standard SDK 85 kit along with a power controller and data acquisition system (DAS) (Fig.3.5) is

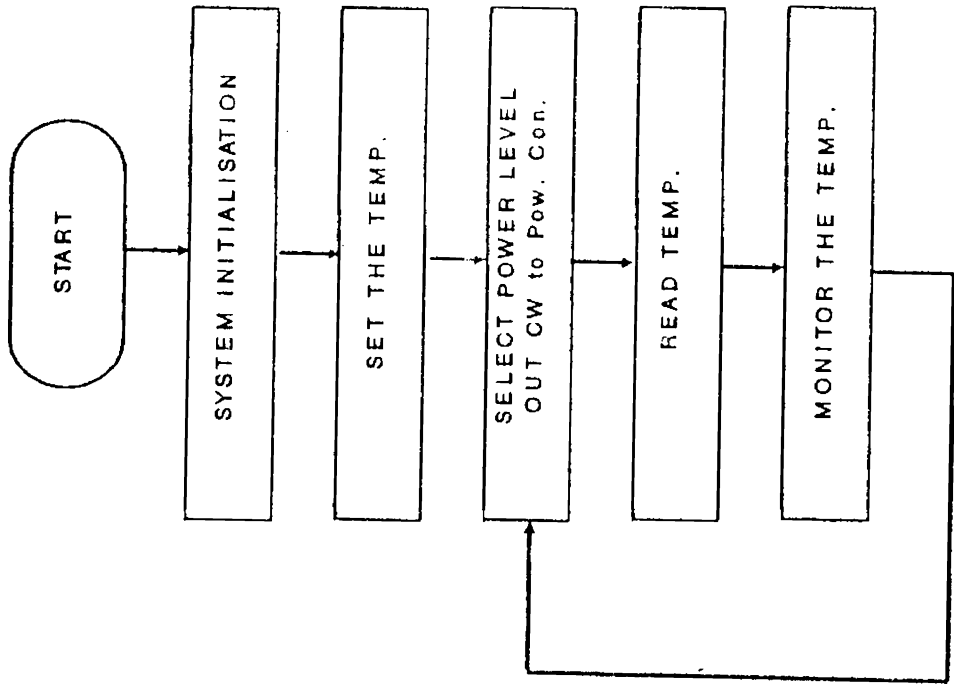


Fig. 3.4 Functional block diagram of temperature controller

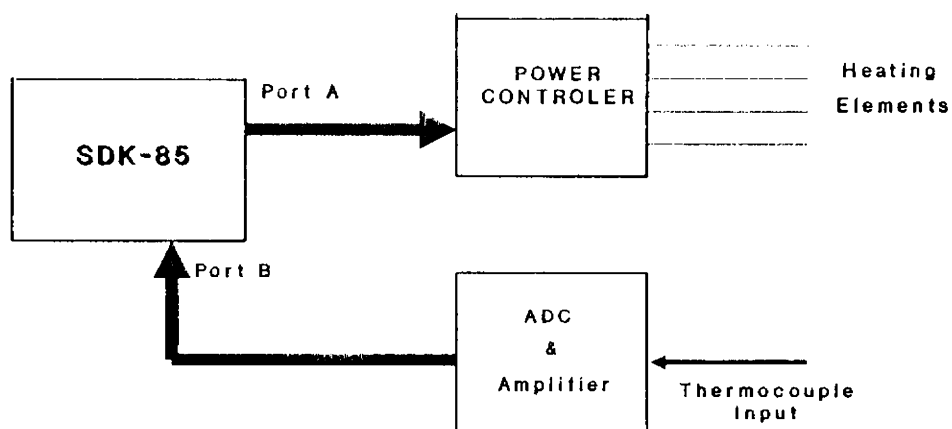


Fig. 3.5 Data acquisition system and power controller using a SDK 85 Kit.

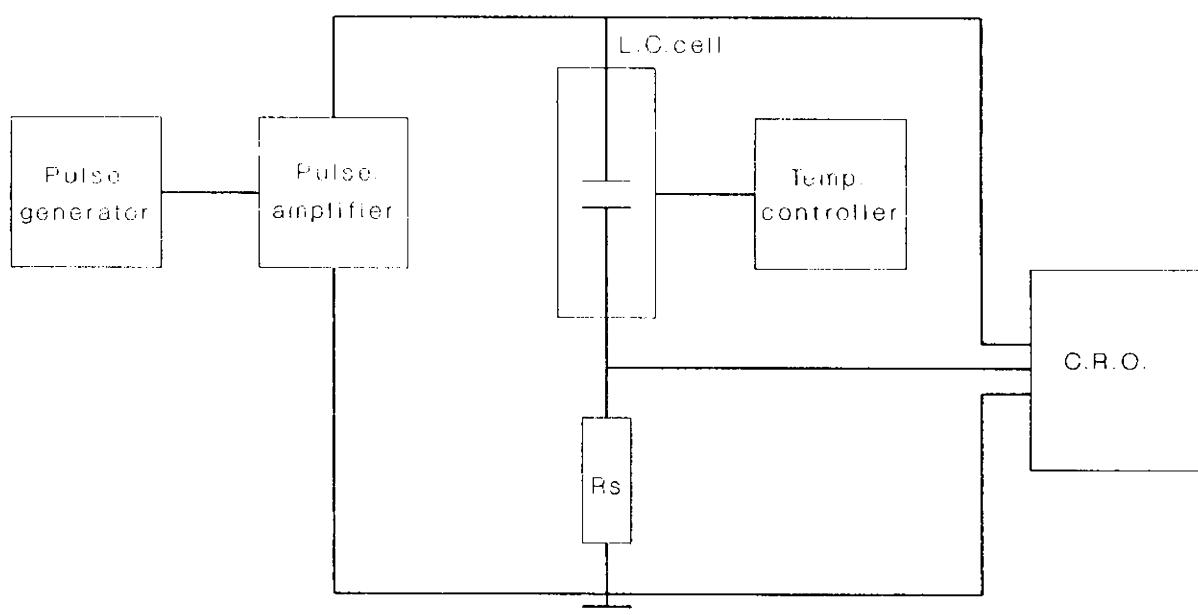


Fig. 3.6 Expt:1 set up for evaluating spontaneous polarisation and Rotational viscosity

used for this purpose. The power controller is a solid state relay controlled by a variable duty cycle pulse generator which is digitally programmable and is connected to one of the output ports of the microprocessor.

Two copper-constantan thermocouples placed on the two sides of the glass plates of the liquid crystal cell function as temperature sensors. The output from the thermocouple is amplified and connected to the DAS based on a 0809 chip. The digital output from the DAS is connected to the input port of the kit. Suitable programs are developed for setting the system at a desired temperature and monitoring the temperature on the processor kit display.

By keeping the specimen in a vacuum ( $10^{-3}$  Torr), an accuracy of  $\pm 1^\circ\text{C}$  can be attained using this controller.

### 3.6. SPONTANEOUS POLARISATION.

The spontaneous polarisation is the most distinct material parameter of a ferroelectric liquid crystal. Its linear coupling with an applied electric field is the basis of all device applications of these compounds. Under such a coupling the electro-optic switch on and switch off processes are very fast since they are brought about just by changing the polarity of the applied field. Thus the

polarisation plays a major role to determine the switching time of the device.

Various techniques have been employed for the measurement of spontaneous polarisation (Ps) [6,7]. At first it has been deduced from the value of the field necessary to unwind the helical structure ( $E_c$ ). Pyroelectric effect, shearflow, capacitance bridge method and light scattering on thin films have also been used for measuring the value of the spontaneous polarisation.

In the present study the method of measuring the transient current developed in the sample due to the polarisation reversal, by changing the polarity of the applied electric field is used.

#### 3.6.1. METHODOLOGY.

Experimental set up is shown in Fig.3.6. The function generator delivers a sine, square or triangular wave which is amplified to 100 volts with a 2 microsecond rise time. The square wave voltage when applied to the sample, causes a reversal of the dipoles in the ferroelectric liquid crystal. The current associated with this process is measured as the voltage drop across a series resistor and the signal (appearing as a bump on the background current) is fed to a memory oscilloscope.



Planar samples of OBOB are prepared by the method explained in section 3.3. Sample thickness is controlled by means of Mylar spacers. The tin oxide conductive coating is etched to obtain an area of about 25 sq.mm active overlapping area.

The main difficulty in extracting the polarisation reversal current is to separate it from the current corresponding to the induced polarisation (charge accumulation in the ferroelectric liquid crystal dielectric) and the ionic movements.

For this, first let us consider a model of the ferroelectric liquid crystal sample between the electrodes in the absence of ferroelectric behaviour [6]. The sample can be represented by a capacitor  $C$  in parallel with a resistance  $R_p$  (Fig.3.7). The resistance  $R_s$  ( $\sim 10\text{ k}$ ) in series with  $C$  and  $R_p$  represents the resistance in the connections and conductive coatings. The current sensor ( $\sim 2\text{k}$ ) is also included in this series resistance.

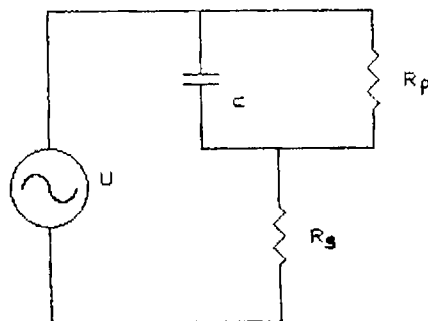


Fig. 3.7 Equivalent circuit of a FLC between two electrodes in the absence of  $P_s$

On applying a pulse of height  $U$ , the equation for the background current  $I$  can be written as

$$C R_s \frac{dI}{dt} + \frac{(R_s + R_p) I}{R_p} = \frac{U}{R_p} + \frac{dU}{dt} \quad [6]$$

The solution of the equation gives the value of  $I$  at any instant  $t$ . Subtracting this from the measured current the spontaneous polarisation current is obtained. It is integrated to give the charge on the plates due to the polarisation reversal. This method is independent of the shape of applied voltage. A separation between the different current components can be obtained by selecting a proper shape of the voltage pulse. Accordingly a square pulse is used to produce a time separation where as a triangular pulse is used to produce a shape separation. A comprehensive result based on current measurements are presented here.

### 3.6.2. RESULTS AND DISCUSSIONS.

#### 3.6.2.1. RECTANGULAR WAVES- TIME SEPARATION.

A rectangular pulse has the advantage that the spontaneous polarisation reversal is very quick. The ionic

currents show a nonlinear behaviour whenever the pulse voltage is increased. This is mainly due to the movement of chemically stable ions under the applied field. At higher voltages this gives a current peak very similar to that due to polarisation reversal. But in most of the observations, the applied voltage could be kept low, as the spontaneous polarisation reversal is extremely quick. Hence the ionic current can be assumed to be constant and low during the polarisation reversal.

The electro-optic switching corresponding to the pulses are also obtained on the cathode ray oscilloscope along with the current peaks. Their time evolution of amplitudes for growth and decay is as shown in the Fig.3.8. The current reaches its maximum value by the time electro-optic response reaches 30% of its peak. This fits well with the theoretical curves obtained by Xue et al. [24]. This confirms that the curves are those due to the spontaneous polarisation reversal currents.

The series resistance  $R_s$  has been kept low to get a considerably shorter time constant for the exponential decay compared to the spontaneous polarisation reversal time. Then the current peak due to spontaneous polarisation reversal is well separated from the capacitative current and also from the conductive current peak coming later.

The numerical computations of the background curve is done by computer (Fig.3.9). The area under the polarisation current peak is given by

$$A = 2 \cdot a \cdot P_s$$

where  $a$  is the area of the sample electrodes.

Experiment is repeated at different temperatures. (Fig.3.10). At higher temperatures the ionic currents increases and the area under the spontaneous polarisation current peak is much reduced.

Variation of polarisation with temperature is plotted in Fig.3.11.

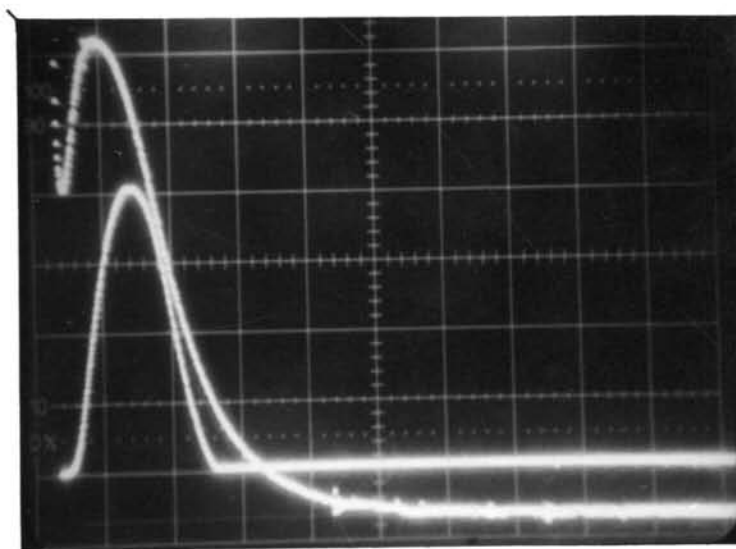


Fig. 3.8 The simultaneous plot of current response and electro-optic response of OBOB for a square pulse

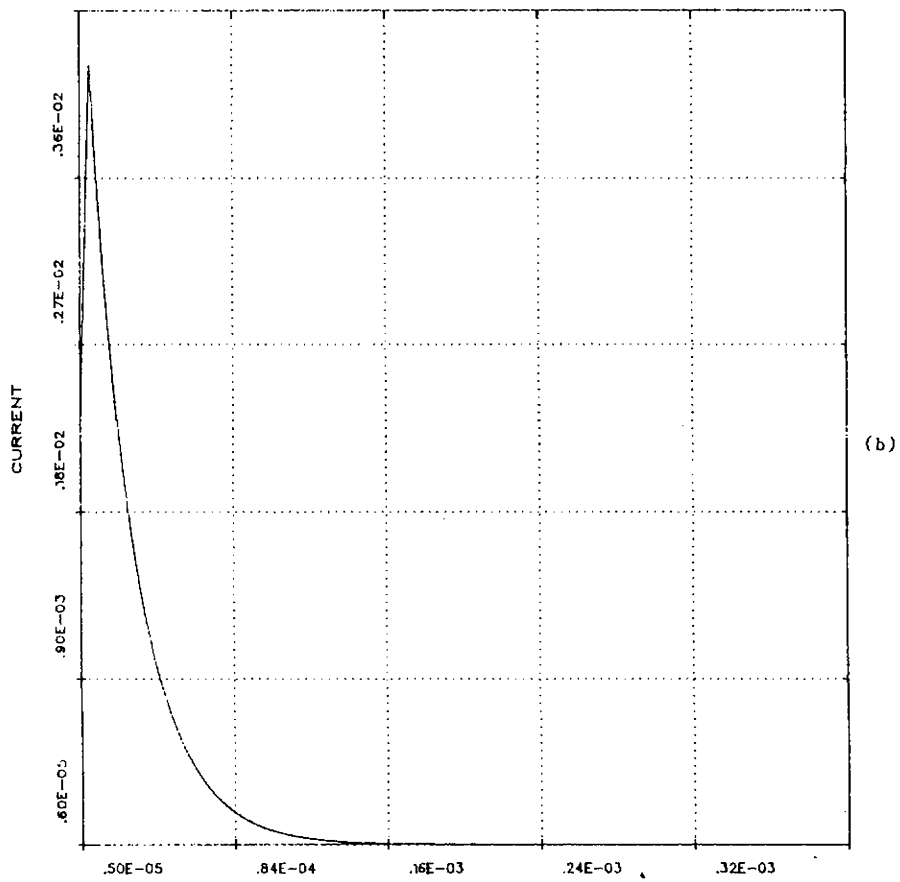
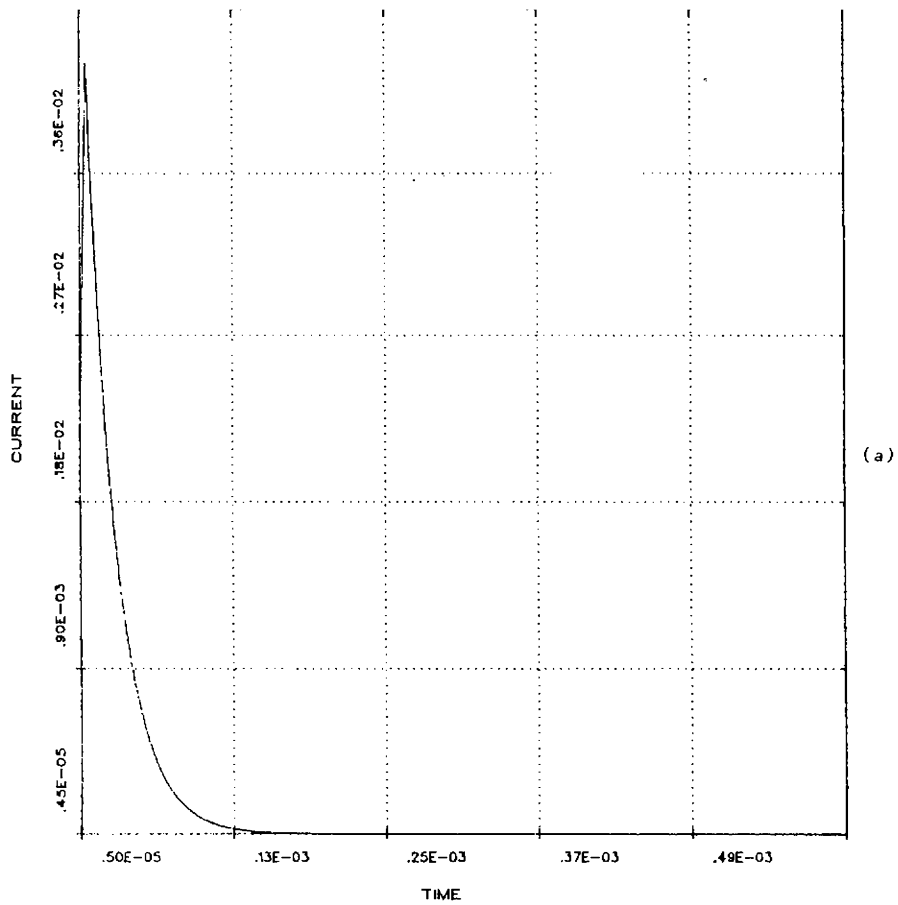


Fig. 3.9 Background curve for OBOB, computed from the equation (a) 67°C (b) 70°C (c) 74°C

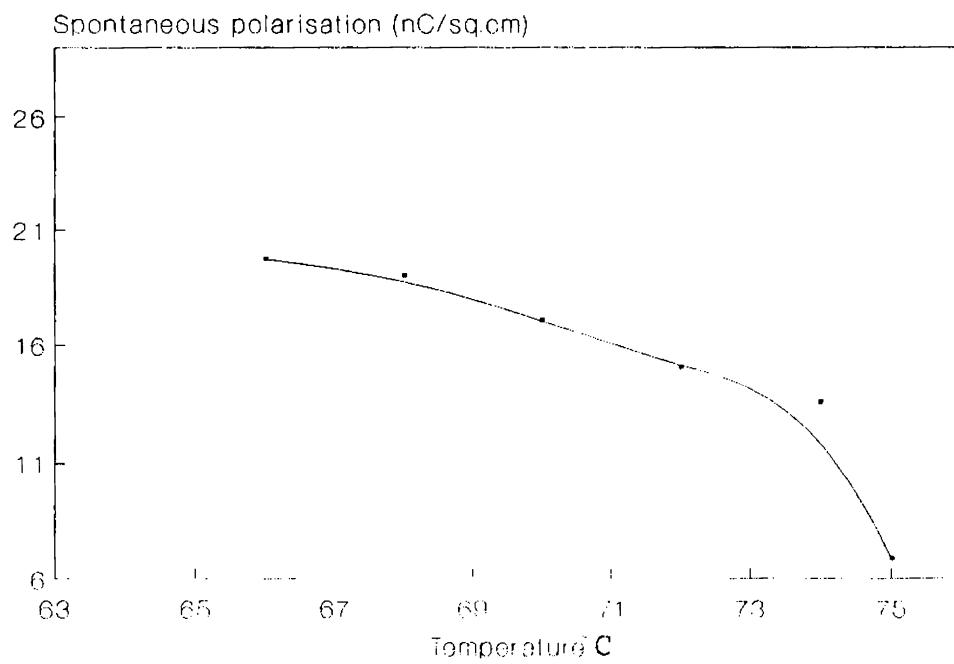
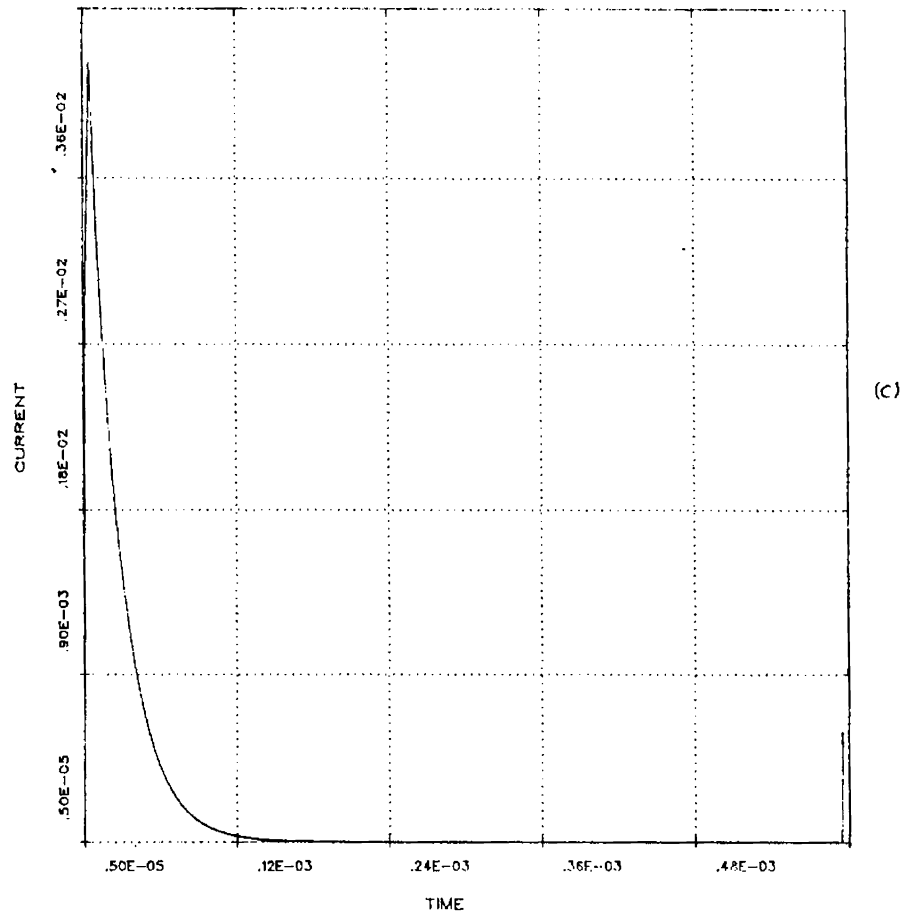
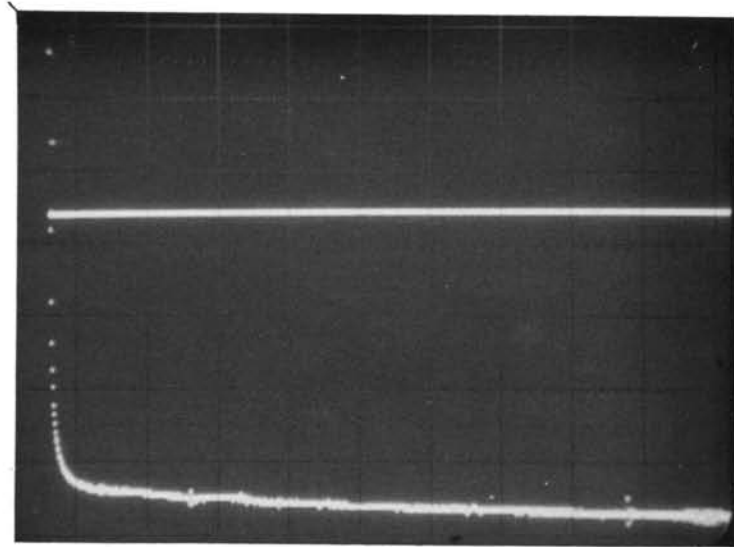
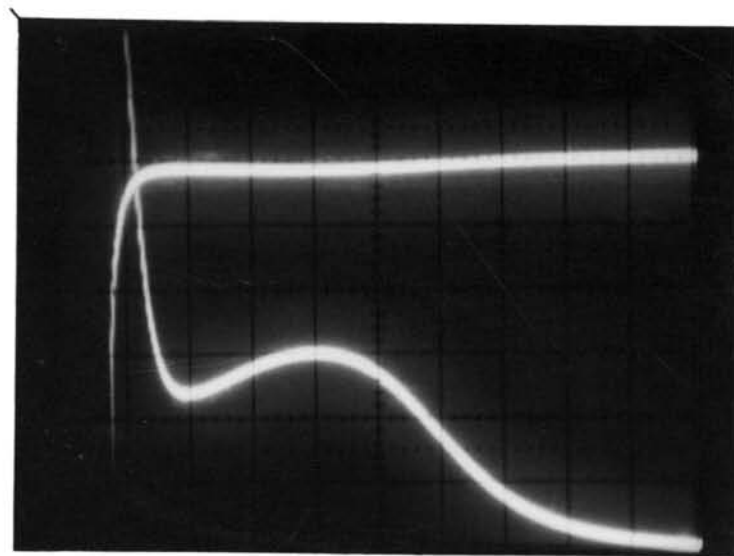


Fig. 3.11 Variation of spontaneous polarisation of OBOB with temperature (square wave method)

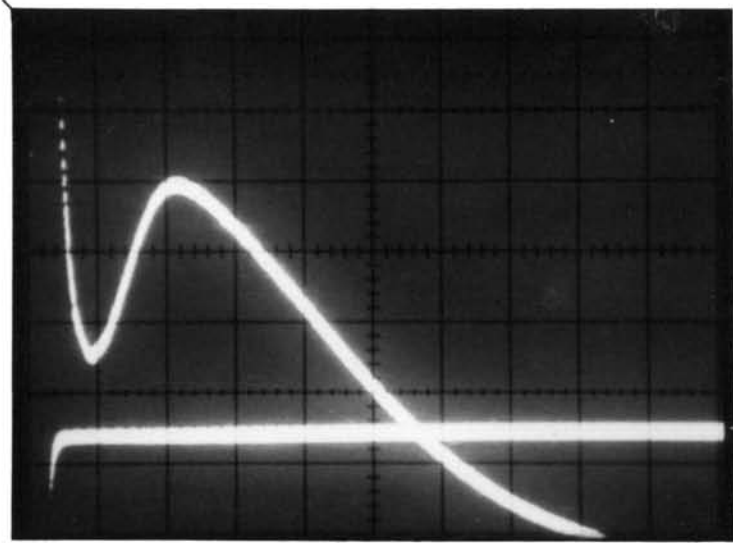


(a)

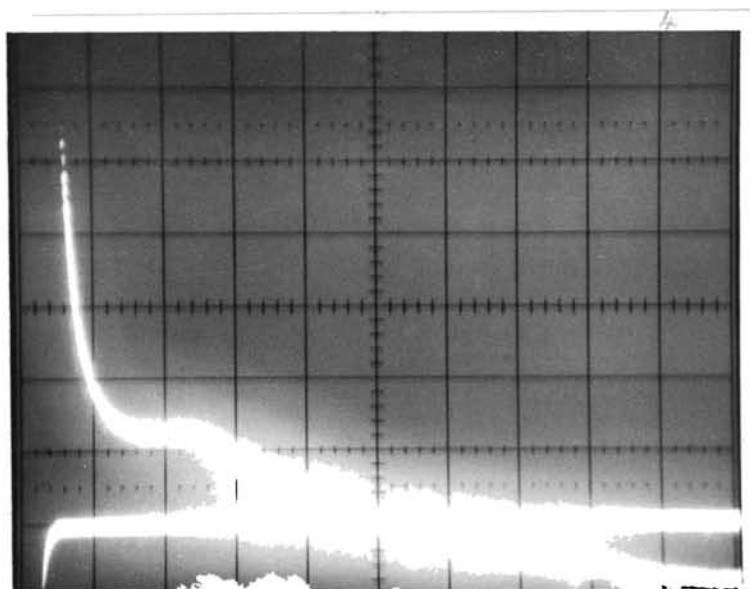


(b)

Fig. 3.10: Current response of GBOB, for a square pulse at different temperatures (a) N<sup>\*</sup> state - 77°C (b) 74°C (c) 71°C (d) 70°C (e) 68°C (f) 66°C

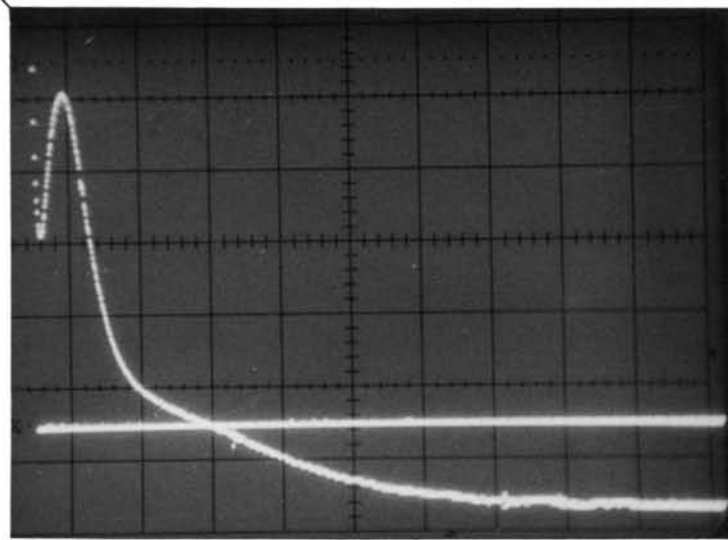


(c)

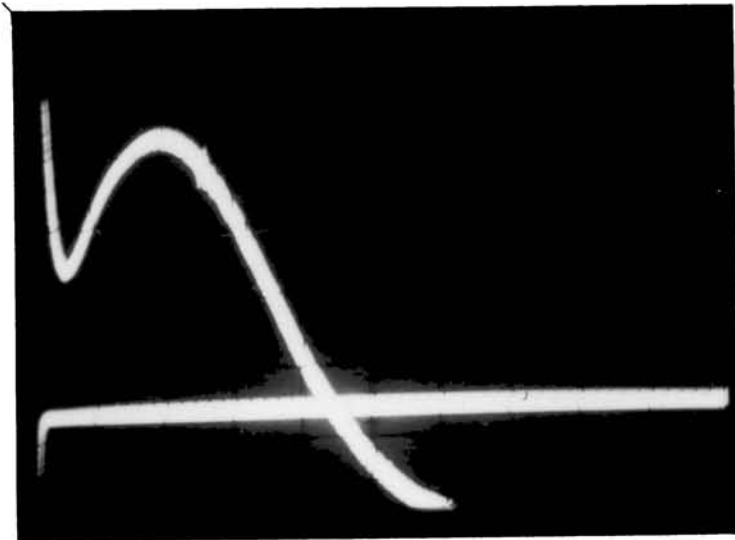


(d)





(e)



(f)

### 3.6.2.2. TRIANGULAR PULSES- SHAPE SEPARATION.

When square pulses are applied to the ferroelectric liquid crystal as already seen, large ionic and capacitive currents are also produced in the sample. The ionic currents are nonlinear in time. Hence eventhough a good separation in time is obtained between these currents and that due to spontaneous polarisation, each time a calculation for the background current is essential.

When a symmetric triangular wave is used, the slow variation in voltage helps to keep a uniform variation of ionic current. ie the  $dU/dt$  term in the above differential equation is very small. Thus a base line corresponding to the background current can be drawn unambiguously (Fig.3.12).

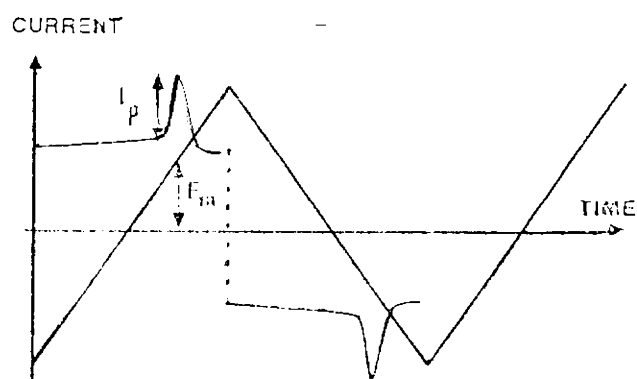


Fig. 3.12 Current response to a triangular pulse showing a straight base line

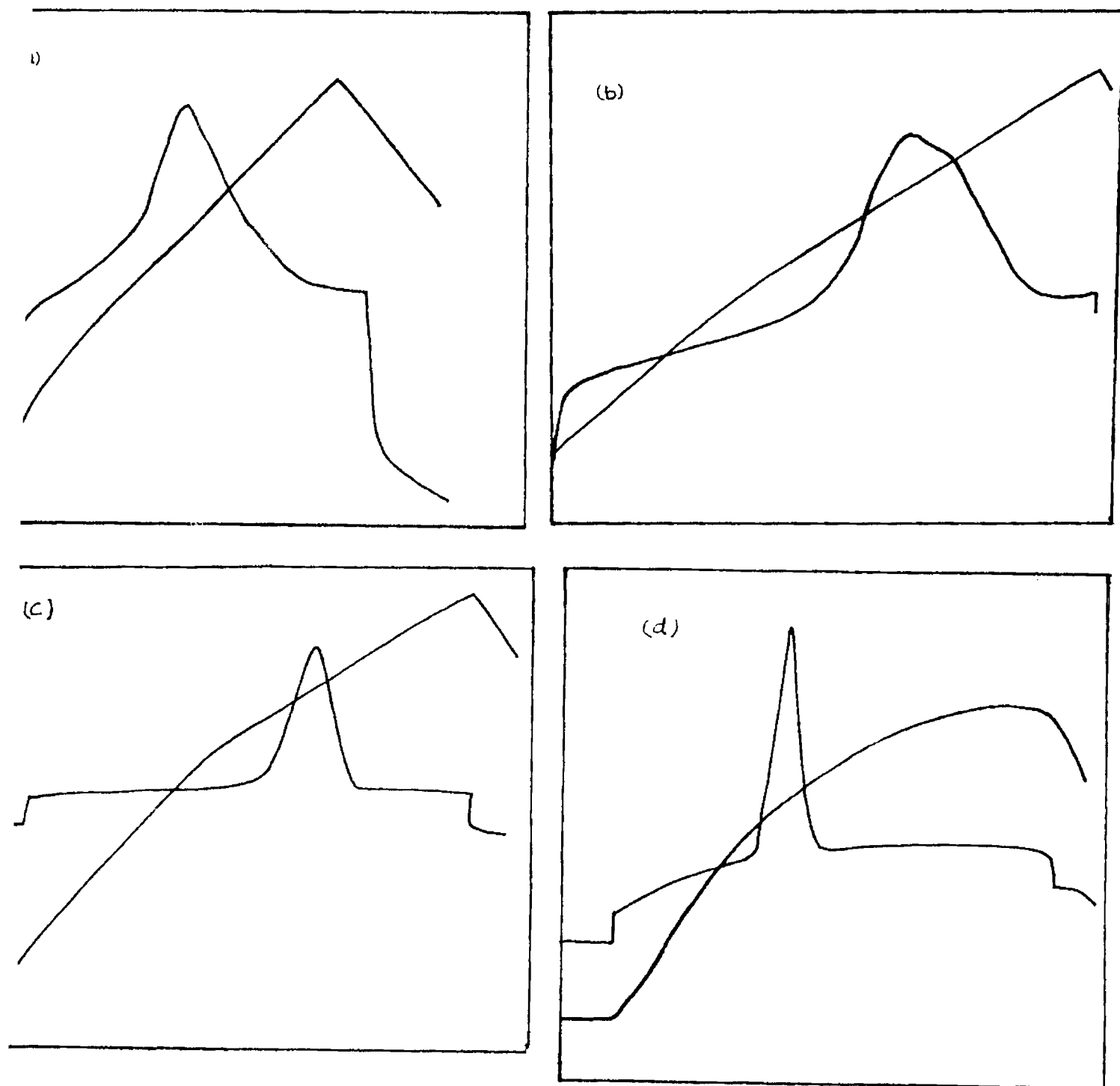
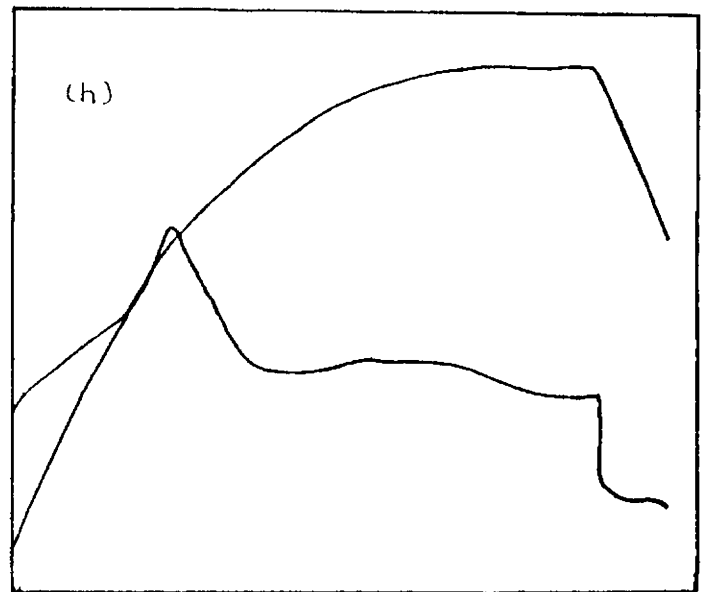
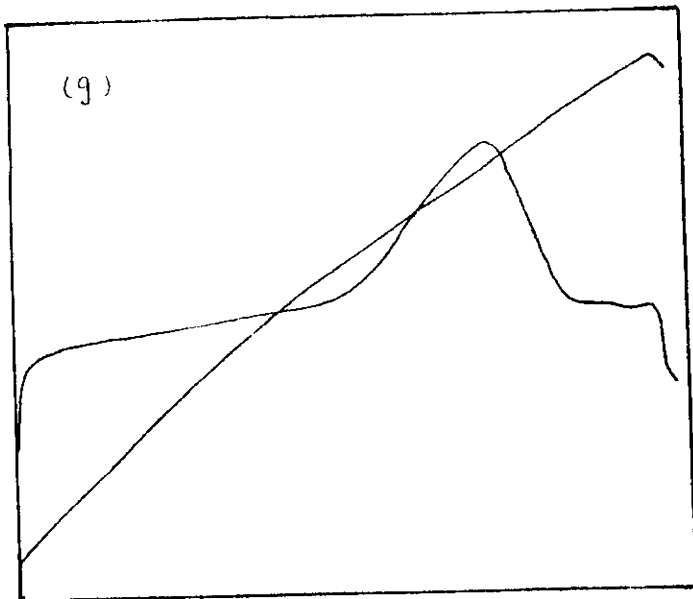
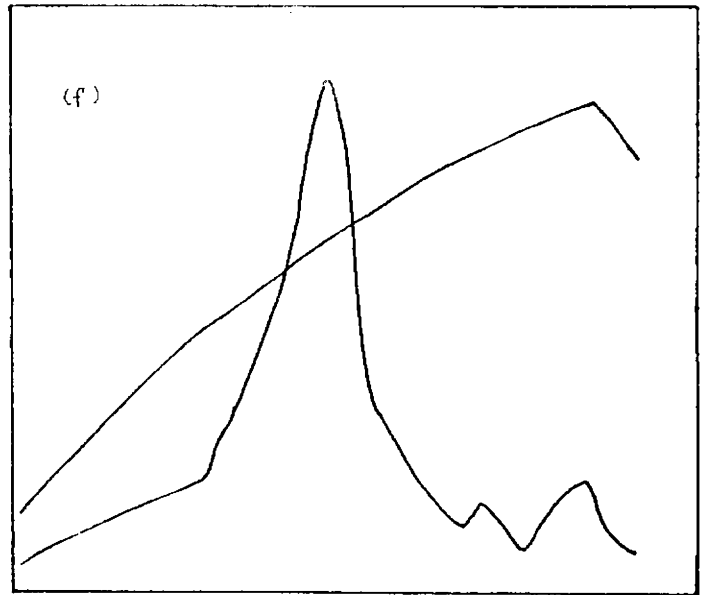
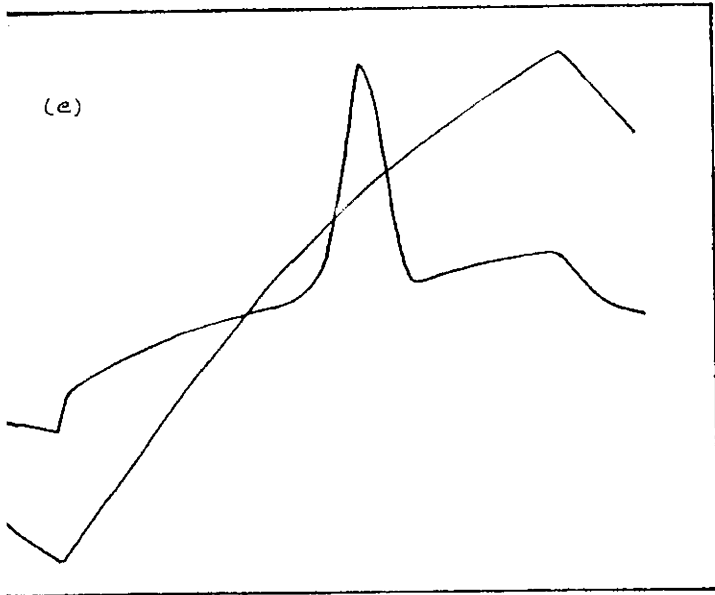


Fig. 3.13 Current response of OBOB for a triangular pulse at different temperatures.  
 (a) 75°C (b) 74°C (d) 71°C (e) 69°C (f) 68°C  
 (g) 67°C (h) 65°C (c) 69°C



The bump due to the polarisation realignment at the sign reversal of the voltage appears on this straight base line. The values of spontaneous polarisation current can be directly obtained by subtracting the background value. Triangular waves of frequency 10 Hz to 100 Hz are used in the present study. Their amplitudes range from 10 V to 150 V. The charts plotted at different temperatures are shown in Fig.3.13. They clearly show that the base line is actually a straight line.

The measurement is done on samples of thickness 20, 50, and 100 microns. At higher thickness higher voltages are required to switch the specimen. Variation of spontaneous polarisation with temperature is shown in Fig.3.14.

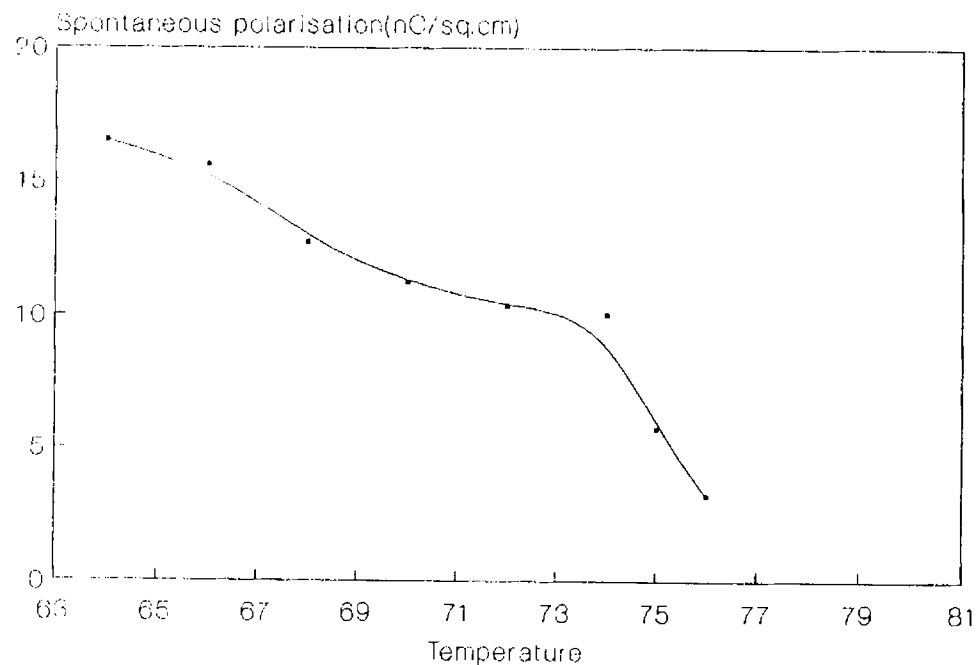


Fig. 3.14 Variation of spontaneous polarisation of OBOB with temperature (triangular method)

When temperatures are low the bump loses its sharpness and it becomes difficult to draw accurate base lines. So the variation of spontaneous polarisation with temperature is not accurate at lower temperatures.

Frequency dependence of spontaneous polarisation is also observed at moderate temperatures. Spontaneous polarisation increases with decreasing frequency and becomes constant below 10 Hz. This may be due to lack of complete response of spontaneous polarisation at higher frequencies due to the high viscosity of the ferroelectric liquid crystal. However at low specimen thickness this variation is negligible as specimen got switched completely even at higher frequencies.

The values of spontaneous polarisation in each case is computed graphically by integrating the current bump. The results agree with those obtained by other methods.

### 3.7. ROTATIONAL VISCOSITY.

Among several parameters entering the macroscopic models for SmC\* phase, viscosity is of obvious importance when studying the dynamical switching phenomena. It controls the switching speed of ferroelectric liquid crystal

devices in all configurations.

When the applied voltages are comparatively low, as in the present study, movement of molecules in the SmC\* phase is mainly confined to the rotation along a cone with a constant tilt angle  $\theta$  (Goldstone mode). Therefore in the present investigation we restrict our attention to the study of rotational viscosity  $\gamma_{\phi}$

Measurement of rotational viscosity has been done by many methods [25, & 63]. They involve the measurement of response times in electro-optic and polarisation reversal switching experiments [64]. Though the switching mechanism in ferroelectric liquid crystal depends on many factors like cell configuration, alignment techniques, the thickness of the specimen compared to the helical pitch and the shape of the applied pulses, a relevant response time that is useful in viscosity calculation can be defined in all these cases.

In this section, rotational viscosity is evaluated by observing the response times of the polarisation reversal current using both square and triangular pulses. The experimental set up is same as in the earlier section.

### 3.7.1. SQUARE WAVE EXPERIMENTS.

Consider the response of the ferroelectric liquid crystal to a square wave applied to it. The most important

parameter of relevance for the rotational viscosity is the half width of current peak,  $T_w$  [25]. For determining rotational viscosity the most appropriate formula is

$$\gamma_{\phi} = 1/1.8.T_w.Ps.E$$

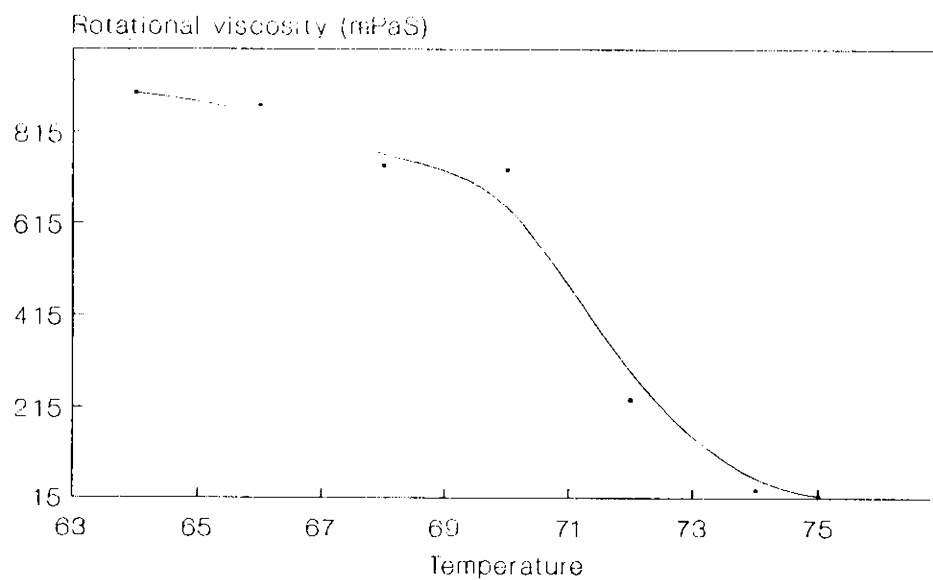


Fig. 3.15 Variation of rotational viscosity of OBOB with temperature. ( square wave method )

The time  $T_w$  is noted for square pulses of different voltages and at different temperatures and  $\gamma_{\phi}$  is calculated in these cases. Fig.3.15 shows the variation of rotational viscosity with temperature.

Errors in measurements can happen due to the effects of smectic layer tilt, elastic boundary effects of smectic layer and dielectric torques [25]. Within these experimental errors the values of viscosity match with those in the literature.



### 3.7.2. TRIANGULAR WAVE EXPERIMENTS.

The current response on a triangular pulse has also been analysed to yield information on rotational viscosity by the method suggested by Geelhar et al.[28].

The evaluation method is shown in Fig.3.16. In the current peak, the maximum height  $I_m$  at the electric field  $E_m$  is noted. Then the viscosity is given by

$$\gamma_{\phi} = A P_s E_m^2 / I_m \quad (A \text{ is the area of the electrodes})$$

Variation of rotational viscosity with temperature is shown in Fig.3.17. Estimated values of viscosity from these measurements are compared with those obtained from square pulse method. They agree within the limit of experimental errors.

### 3.8. DIELECTRIC CONSTANT.

For the applications of ferroelectric liquid crystal in electro-optic devices, it is important to know not only the ferroelectric torque responsible for switching between different states, but also the dielectric torque that may cooperate or counteract the ferroelectric torque during different phases of switching. Thus the stabilization of the molecular axis in its position after

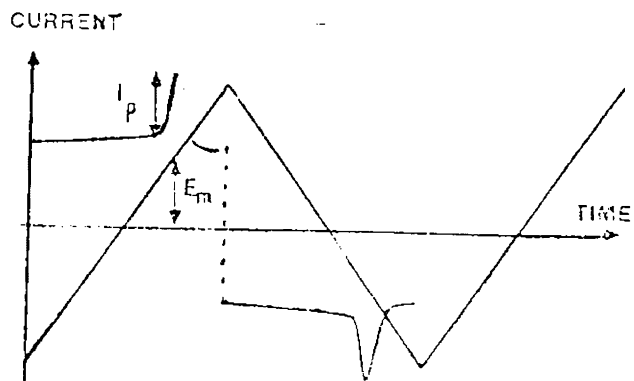


Fig. 3.16 Triangular pulse method of evaluating rotational viscosity of OBOB

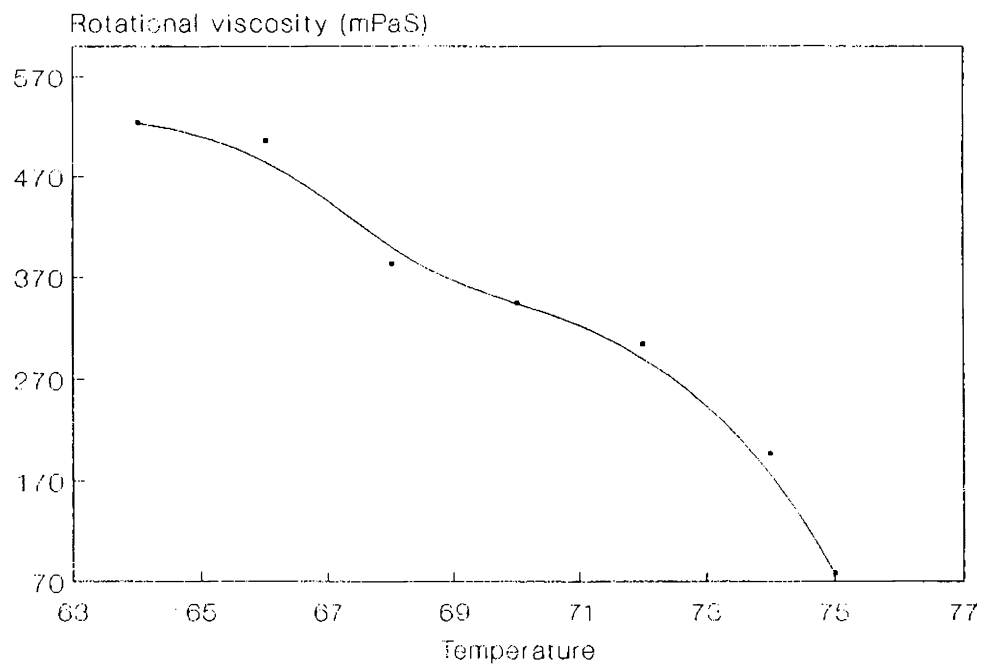


Fig. 3.17 Variation of rotational viscosity with temperature ( Triangular wave method )

switching, depends on the sign of the dielectric torque. Hence the design of appropriate addressing modes and the specific waveforms require a detailed knowledge of dielectric properties of the ferroelectric liquid crystal material used.

In the study of the dynamics of switching behaviour of ferroelectric liquid crystal materials, involving the dielectric torque, the dielectric anisotropy is the most important parameter. It is given by

$$\Delta\epsilon = \epsilon_{\parallel} - \epsilon_{\perp}$$

where  $\epsilon_{\parallel}$  relates to an electric field applied along the molecular axis and  $\epsilon_{\perp}$  represents the electric field applied perpendicular to the molecular axis.

Further this value is to be known for relevant frequency range, which is from about 50 Hz to several hundred KHz. In the non-tilted smectic phases the  $\epsilon_{\parallel}$  and  $\epsilon_{\perp}$  values can be determined by measuring the capacitance of liquid crystal cells aligned in homeotropic and planar orientations respectively.

But in tilted smectic phases, such as SmC\*, both in homeotropically and homogeneously aligned samples, the measuring field makes an angle  $\theta$  (the tilt angle) with the

director. Hoffmann has suggested [36] a method to calculate the actual  $\epsilon_{\parallel}$  &  $\epsilon_{\perp}$  values from the measured values ( $\epsilon_{\parallel m}$  and  $\epsilon_{\perp m}$ ). On the basis of this method the values of  $\epsilon_{\parallel}$  and  $\epsilon_{\perp}$  were determined for the sample of OBOB in the SmC\* phase. The variations of  $\epsilon_{\parallel}$ ,  $\epsilon_{\perp}$  and  $\Delta\epsilon$  with change in frequency is also studied for the low frequency and high frequency regions (30 Hz to 1 MHz).

### 3.8.1. EXPERIMENTAL DETERMINATION

To determine the dielectric constant of the material, the capacitance of empty cell is measured first. Then it is filled with the ferroelectric liquid crystal in vacuum by capillary action upon heating the sample to the isotropic phase. The capacitance is measured again. The capacitance measurements are carried out using the HP 4192.A impedance analyser (5Hz to 13MHz). The thickness is controlled by Mylar spacers and is kept at 12 microns, both for  $\epsilon_{\parallel}$  and  $\epsilon_{\perp}$  measurements.

For  $\epsilon_{\perp}$  measurements, specimen is oriented in planar alignment (Fig.3.18 ) so that measuring field is normal to the helical axis, ie it makes an angle  $\theta$  with the director. This is achieved by slowly cooling the sample between tin oxide electrodes, from the cholesteric phase in a magnetic field of 1.5 Tesla, through the SmC\* phase.

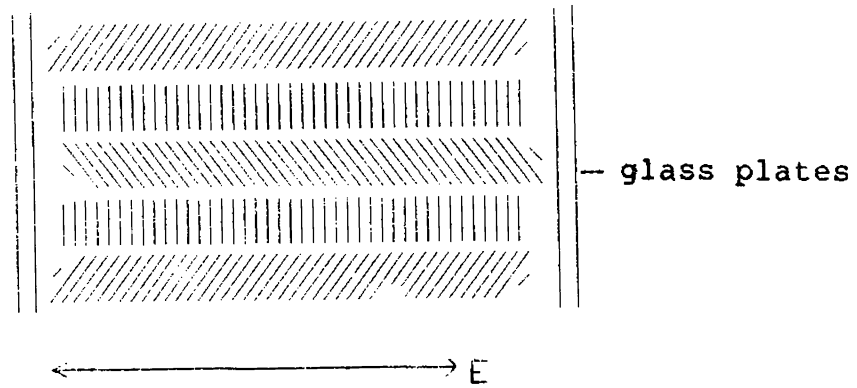


Fig. 3.18 Planar alignment of OBOB for measurement of  $\epsilon_{\perp}$ . Field makes an angle  $\theta$  with Helical axis

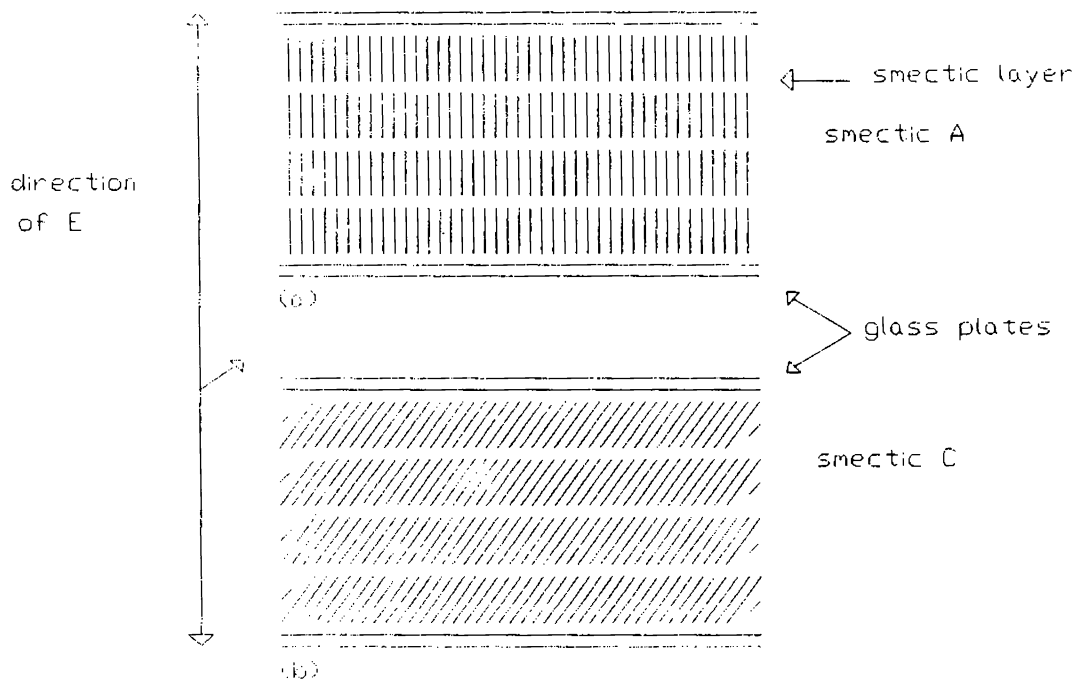


Fig. 3.19 Homeotropic alignment of OBOB for  $\epsilon_{\parallel}$  measurements. Measuring field makes an angle  $\theta$  with the director

For  $\epsilon_{\parallel}$  measurements, the SnO<sub>2</sub> coated glass plates are initially coated with a silane to achieve homeotropic orientation. In the SmC\* phase the measuring ac field is perpendicular to the smectic layers. Hence the field makes an angle  $\theta$  with director as shown in Fig.3.19. The empty cell capacitance ( $C_0$ ) and that of the ferroelectric liquid crystal cell ( $C$ ) is measured for low and high frequencies. Real part of  $\epsilon^*$  is calculated as  $\epsilon = C/C_0$

### 3.8.2. RESULTS AND DISCUSSION

In the SmC\* phase  $\epsilon_{\perp}$  shows a very high value for low frequencies (30 Hz to 1 KHz) (Fig.3.20). A moderate increase is shown up to 10 KHz. From 10 KHz to 1 MHz,  $\epsilon_{\perp}$  is found to be frequency independent (Fig.3.21). The large dielectric constant perpendicular to the helical axis in the SmC\* phase at low frequencies can be interpreted as due to contribution from the Goldstone mode. It originates from the fluctuations of the azimuthal angle of the molecular long axis around the helical axis.

In the SmC\* phase, for low frequencies  $\epsilon_{\parallel}$  shows a slight decrease. But for the frequency range  $10^2$  to  $10^6$  Hz, its value decreases considerably and above  $10^6$ , it remains more or less constant (Fig.3.22). This corresponds

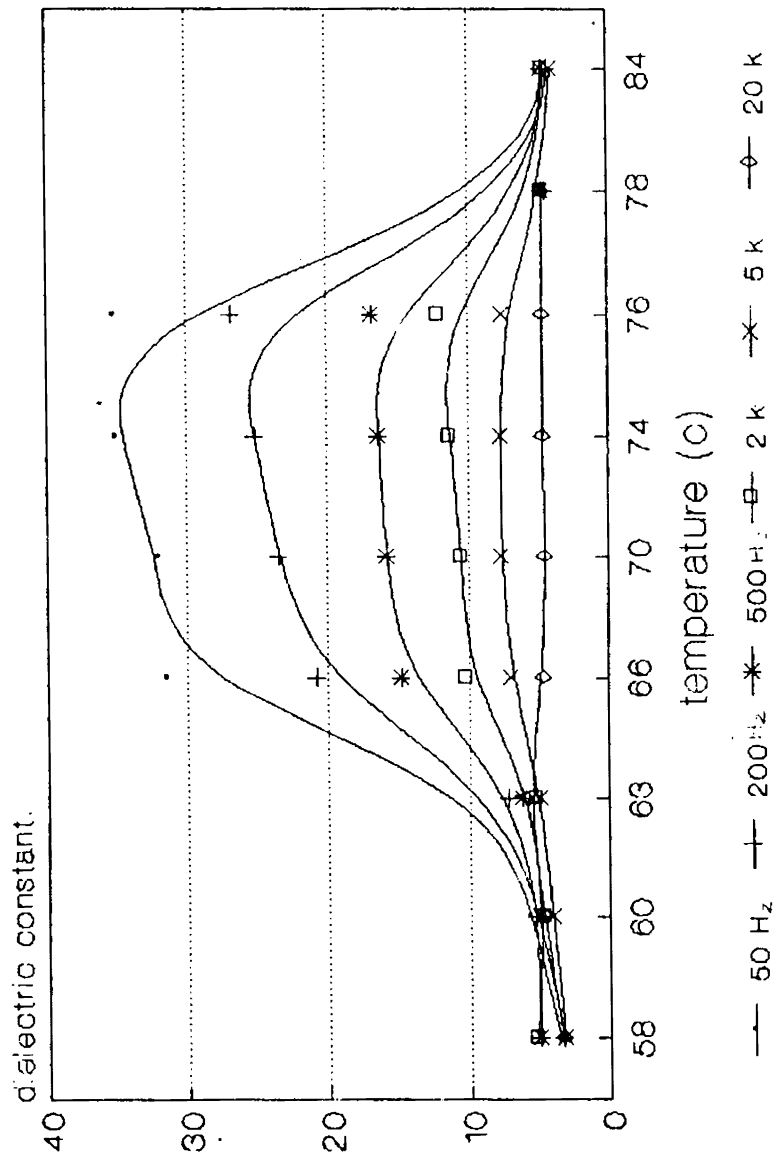


Fig. 3.20 Variation of  $\epsilon_L$  with temperature for frequencies from 30 Hz to 20 KHz

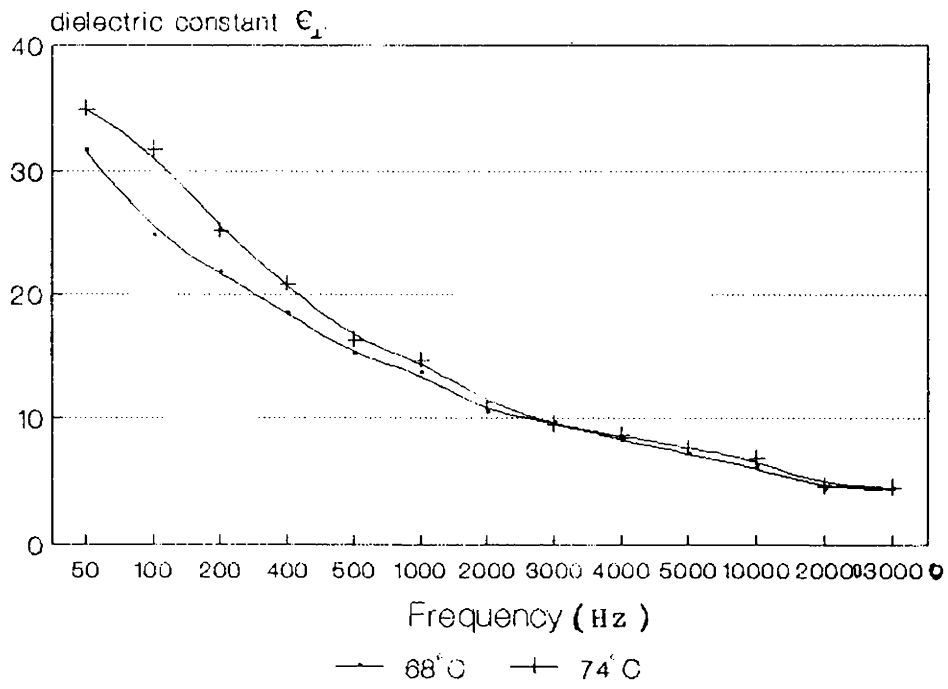


Fig. 3.21 Variation of  $\epsilon_{\perp}$  of OBOB with frequency

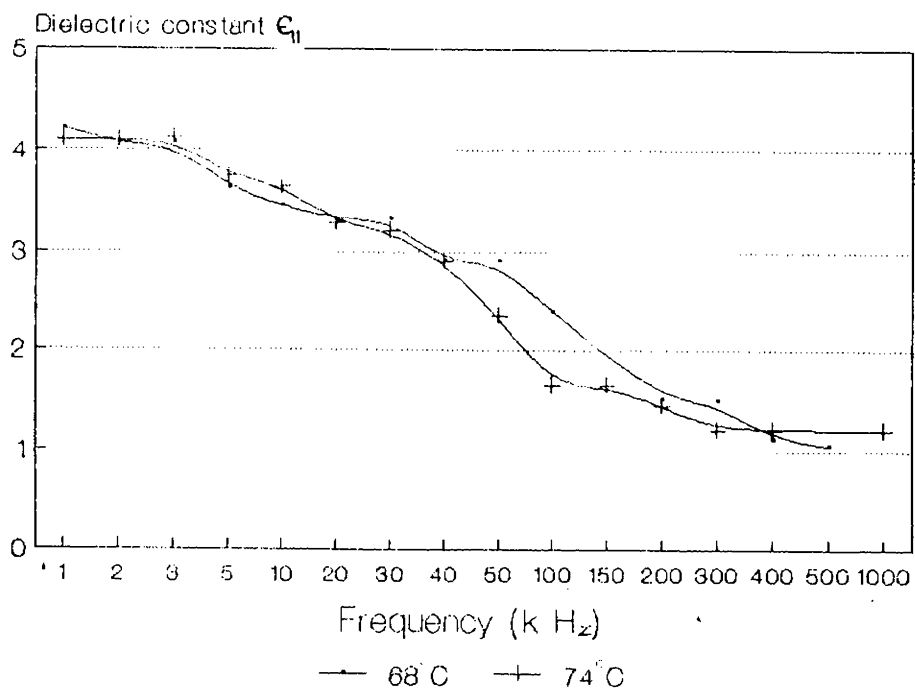


Fig. 3.22 Variation of  $\epsilon_{\parallel}$  of OBOB with frequency



to the molecular rotation around short axis [36].

The dielectric anisotropy of the material is also calculated for the frequency range  $10^2$  to  $10^6$  Hz.

Referring to Hoffmann et al.[36], if the biaxiality in the SmC\* phase is neglected, the measured dielectric constant on a homeotropically aligned sample, denoted by  $\epsilon_{\parallel m}$  is given by

$$\epsilon_{\parallel m} = \epsilon_{\parallel} \cos^2 \theta + \epsilon_{\perp} \sin^2 \theta$$

For planar orientation,

$$\begin{aligned} \epsilon_{\perp m} &= \frac{1}{2} (\epsilon_{\perp} (1 + \cos^2 \theta) + \epsilon_{\parallel} \sin^2 \theta) \\ \Delta \epsilon_m &= (\epsilon_{\parallel} - \epsilon_{\perp}) - \frac{3}{2} (\epsilon_{\parallel} - \epsilon_{\perp}) \sin^2 \theta \\ \Delta \epsilon_m &= \Delta \epsilon - \frac{3}{2} \Delta \epsilon \sin^2 \theta \end{aligned}$$

For OBOB,  $\theta = 42^\circ$ ,

$$\Delta \epsilon = \frac{\Delta \epsilon_m}{1 - \frac{3}{2} \sin^2 \theta}$$

The variation with frequency in the range of  $10^2$  to  $10^6$  Hz is shown in Fig.3.23. It is seen that  $\Delta \epsilon$  of OBOB is negative for these frequencies, thus promoting a stabilising action for the error pulses in a multiplexed drive.

Thickness (microns)	Applied dc field. Volt	Angle of rotation of the stage ( $2\theta$ )	Tilt ( $\theta$ )
15	20	$80^\circ$	$40^\circ$
15	50	$84^\circ$	$42^\circ$
100	50	$82^\circ$	$41^\circ$
100	100	$84^\circ$	$42^\circ$

Table 3.2: Measurement of tilt angle of OBOB

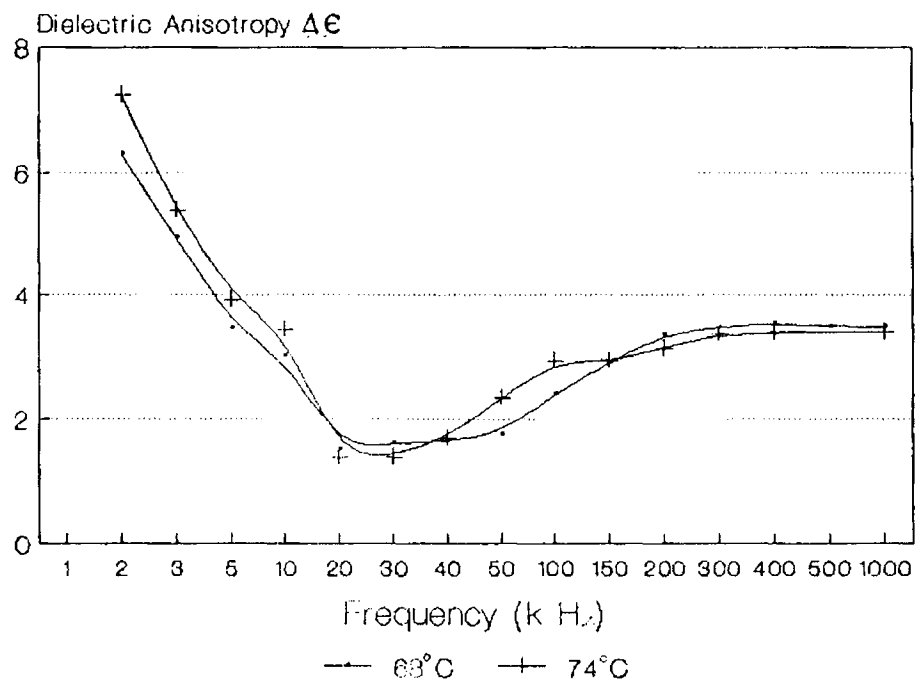


Fig. 3.23 Variation of dielectric anisotropy of OBOB with frequency

### 3.9. TILT ANGLE.

The tilt angle is the order parameter of the SmC\* state since the spontaneous polarisation itself is proportional to  $\theta$ . Hence its measurement is important in electro-optic studies.

The measurement of the tilt angle of OBOB is performed using an optical method. In optical measurements one actually measures the tilt angle of the main axis of the optical dielectric tensor. In principle this is possible by observing the helicoidal texture of a the SmC\* material normally to its axis [38]. But practically it is more accurate to measure the tilt after helix unwinding.

The sample cell is prepared in the planar geometry. A strong electric field is applied to unwind the helix. Then the uniform texture obtained is one of an ordinary C phase which can be approximated to be optically uniaxial. The molecules are parallel to each other and parrallel to the glass plates. They are tilted across the normal to the layer by the tilt angle  $\theta$ . The neutral lines of the sample slab gives the two optical axis of the optical tensor. The tilt  $\theta$  is the angle between the largest axis and the rubbing direction.

The sample is placed on a rotating stage between

two crossed polarisers. Then a dc field across it is applied, whose magnitude is above the unwinding field. Let the molecules be tilted from the layer normal by an angle  $\theta$ . The stage is rotated and its position for complete extinction of light is determined. Then the polarity of applied field is reversed. In this case the molecules are tilted by an angle  $-\theta$ . The stage is rotated to regain the position of complete extinction. The difference between the two readings gives twice the tilt angle. The uniformity in extinction depends on the uniformity of the sample. Areas of slightly different alignment remain transparent even after rotating through  $2\theta$ . The tilt values are quite reproducible for 100 micron samples (Table 3.2).

In the smectic C phase (unwound SmC\*) there will be a transition layer close to the plates where the mean molecular orientation turns to adjust the bulk tilted orientation. In the above experiment we assume that the thickness of this layer is small enough so that the optical properties of the sample are that of the uniform bulk texture.

The experiment is repeated by applying fields which are many times larger than the critical unwinding

observed. Hence we conclude that tilt angle is the same in the helicoidal and unwound texture and that the effect due to the transitional layer can be neglected.

## Chapter 4. STUDIES ON ELECTRO-OPTIC SWITCHING

- 4.1. Introduction
- 4.2. Experimental setup
- 4.3. Method, Results and Discussion
  - 4.3.1 Nature of response
  - 4.3.2 Grey scale
  - 4.3.3 Bistability
  - 4.3.4 Switching - dependence on field parameters
  - 4.3.5 Decay of switched state
  - 4.3.6 Multiple pulses
  - 4.3.7 Rotational viscosity
- 4.4 Conclusions

## STUDIES ON ELECTRO-OPTIC SWITCHING

### 4.1 INTRODUCTION

An essential requirement of liquid crystals, which find applications in electro-optic devices such as spatial light modulators and displays, is a fast response to an applied signal. Further in multiplexed and large area matrix addressed displays the pixels should retain their switched state till next addressing. This implies that a memory effect or a bistable operation is also a necessary characteristic of these materials.

The stability of the states depends on its decay time after switching process. A critical analysis of the switching characteristics can reveal the process involved in switching. Hence a study of these dynamic characteristics is important from the scientific as well as application points of view.

The definition of the timings involved in the electro-optic switching (optical response) are usually derived from a plot as shown in Fig.4.1.

The electro-optic effect observed is not instantaneous with the application/removal of electric field. The time delay associated with this is termed as

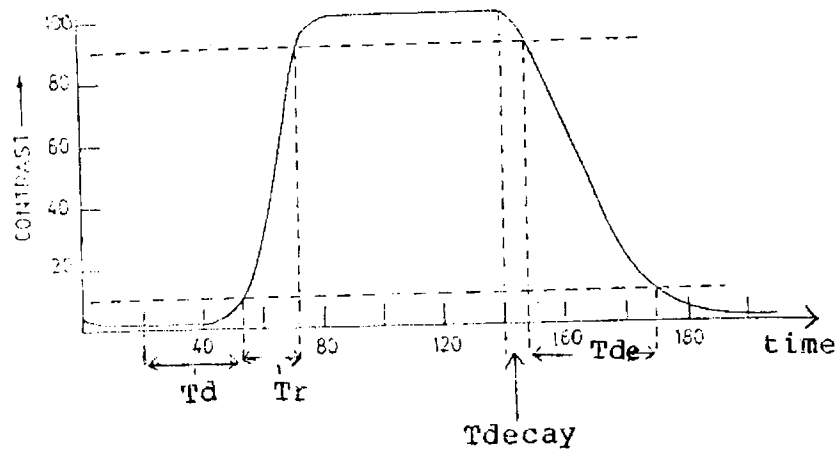


Fig. 4.1 The electro-optic switching times of a FLC

delay time ( $T_d$ ). It is the time required for a 10% change in transmission (from 0% to 10% during rise or from 100% to 90% during decay). Rise time ( $T_r$ ) is defined as the time during which the device gets 90% transmission (absorption) from the 10% level and decay time ( $T_{de}$ ) is the time in which the contrast falls from 90% level to 10% level.

In actual device operations the rise and decay times include the delay time also. Usually the delay time during decay is very small, while it is significant during



rise. Hence actual ON time and OFF time of electro-optic devices are

$$T_{on} = T_r + T_{do}$$

$$T_{off} = T_{de} + T_{dl}$$

where  $T_{do}$  and  $T_{dl}$  are the delay times during rise and decay respectively.

In conventional liquid crystal devices using nematic and cholesteric materials (DSM and TN modes), response times are limited to the order of milliseconds. In these cases the driving force for molecular reorientation is derived from the interaction of the applied field with anisotropy of the dielectric tensor.

In ferroelectric liquid crystals, due to the permanent dipoles associated with their molecules, an applied field can couple with the spontaneous polarisation. This polarisation torque added to the dielectric torque enhances the response time of the device.

The electro-optic response time of a ferroelectric liquid crystal (FLC) device depends on the cell configuration, temperature, strength of spontaneous polarisation and other material constants like tilt ( $\theta$ ), apart from the parameters of the applied field.

Ferroelectric liquid crystals are characterised by an intrinsic helix of the director orientation, with its

axis perpendicular to the smectic layers. In thin samples where thickness is very much less than the helical pitch ( $d \ll p$ ), this helix can be suppressed by means of interaction between the liquid crystal and closely spaced bounding glass plates as in the case of surface stabilised ferroelectric liquid crystals (SSFLC) [45 & 65]. In such configurations high switching speed (submicroseconds) and bistability have been obtained by many workers.

For relatively thicker samples ( $d \gg p$ ), optical switching is usually explained on the basis of the unwinding of the helix of the ferroelectric liquid crystals [66]. Devices based on this phenomena make use of the two switched states corresponding to the fully unwound and fully wound conditions. OBOB, the ferroelectric liquid crystals used in the present study, has a comparatively high rotational viscosity and a low value of pitch. Hence a large energy is required to unwind the helix of this material. For electric fields above the critical unwinding value, the area of ferroelectric domains that get switched depends on the amount of energy transferred to molecules. For low voltages, the helix of the ferroelectric liquid crystals is partially unwound. Hence for a given pulse width, the extent of unwinding and hence the light transmitted through the ferroelectric liquid crystals cell

should be proportional to the voltage of the pulse. This suggests the possibility of voltage controlled optical intensity levels (grey levels) in the material. Under suitable conditions of temperature and sample thickness, for a range of field values, these optical transmission levels can be sustained for a reasonably long duration. The work presented in this chapter is an attempt in this direction with excellent results.

Studies have also been conducted on the rise time, the delay time, the decay time and bistable switching characteristics of the ferroelectric liquid crystals in planar configuration. Applications are suggested in spatial light modulators and electro-optic displays. Experiments are repeated with two commercially available ferroelectric liquid crystals CE3 and CE8 (BDH, UK) and the dynamic characteristics are compared with that of OBOB.

#### 4.2 EXPERIMENTAL SETUP

Experimental setup is shown in Fig.4.2. The sample is mounted on a cell holder kept inside a metallic chamber with optical windows. The cell holder can be tilted on a horizontal and vertical axis perpendicular to the path of the incident beam of light. The cell is illuminated by a 0.95 milli watt unpolarised He-Ne laser of wavelength 632.8 nm through a light attenuator and a polariser. The cell is

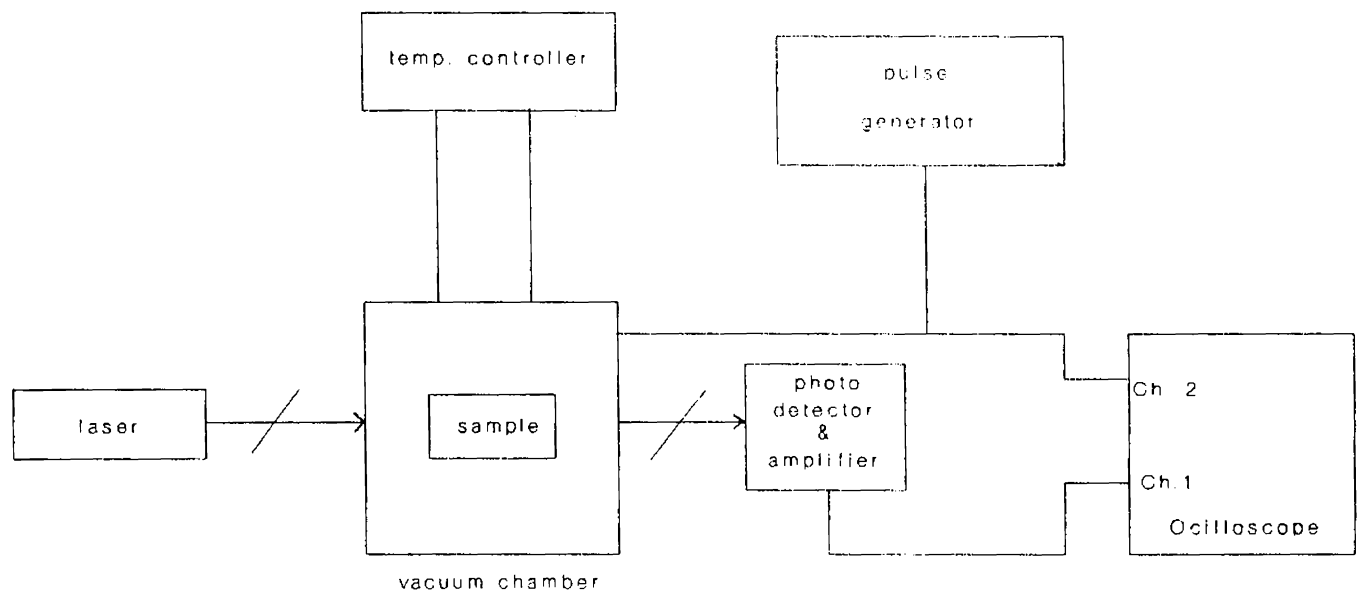


Fig. 4.2 Expt:1 setup for studying the electro-optic switching of OBOB

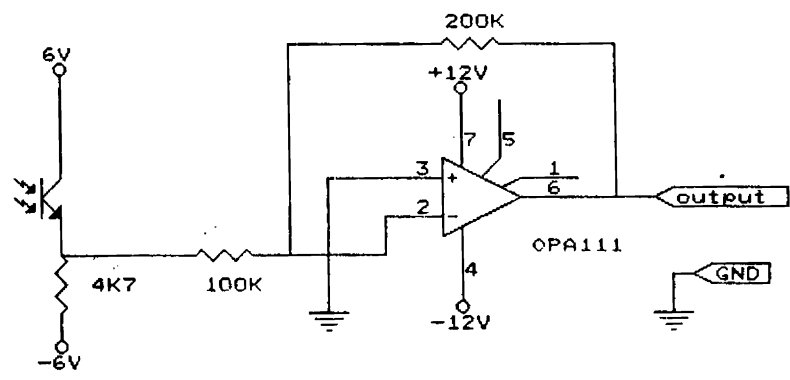


Fig. 4.3 Optical detection unit

mounted so that the laser beam can pass from normal incidence into the preferred viewing quadrant.

The detection unit consists of a photo diode having a uniform response for the light source (Fig.4.3). The current through the series resistance 4.7 K is proportional to the intensity of light falling on the photo transistor. The resulting voltage drop across the resistance is fed to an inverting amplifier constructed around OPA 111 (a low noise DIFET op.amp.). The output of the amplifier is fed to the cathode ray oscillograph.

The pulse generation and amplification unit as well as the microprocessor controlled temperature controller are same as those described in chapter 3. The applied signal and output of the detector are displayed on a digital storage oscilloscope.

The sample of ferroelectric liquid crystals is sandwiched between two conducting glass plates whose resistivity is less than 200 ohms/sq.cm. The glass plates are cleaned and evened out in a plasma discharge and pre-treated with silane and polyvinyl alcohol as suggested by Patel et al.[62]. Alignment of the sample obtained by unidirectional rubbing is improved by applying a slowly varying electric field.

### 4.3 METHOD, RESULTS AND DISCUSSION.

Experiments are conducted mainly using samples of OBOB with a thickness of 15 microns. Electro-optical effects are observed in the  $SmC^*$  phase of the sample for various temperatures, pulse widths and for different voltages. The transmitted intensities of the light are recorded by applying preset pulses preceded by probe pulse in order to avoid voltage- transmission hysteresis. While measuring time constants, care was taken to keep the length of the cable to a minimum so as to avoid the stray capacitance.

#### 4.3.1 Nature of response

Experiments on dynamic characteristics and bistability are conducted with samples kept in open circuit and short circuit conditions after applying a pulse voltage. The samples of OBOB showed ferroelectric behaviour in the  $SmC^*$  state ( $72^\circ C$  to  $65^\circ C$ ) during cooling cycle. The response of the ferroelectric liquid crystals depends both on time duration (pulse width) and magnitude (pulse height) of the applied electric pulse. However there is a threshold voltage  $U_{th}$  for each pulse width, below which there is no electro-optic effect. The electro-optic response for a

square wave has a general shape as shown in Fig.4.4. This shows two different stages. As the pulse height or width is increased it switches faster and the point of inflection disappears. At higher temperatures, for pulses of even lower height and duration faster and more linear switching takes place.

Here the electro-optic effects take place in two stages. In the first stage molecules well inside the sample undergo a reorientation without the motion of the molecules

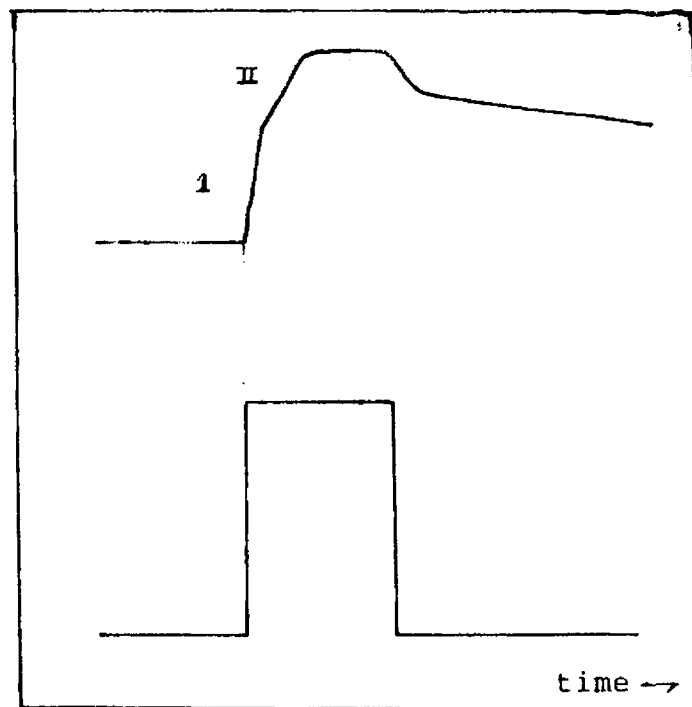


Fig. 4.4 General shape of response curve for a square pulse applied to OBOB

at the surfaces and hence the domain walls do not move. This is due to the strong interaction of the molecules with the rubbed glass electrodes. In the second stage the molecules at the surface also reorient producing switching. This explains the appearance of the point of inflection. At higher fields these two processes take place simultaneously with the disappearance of the step.

#### 4.3.2 Grey scale capability

In this section the main aim is to investigate the existence of well defined intermediate transmission levels for various pulse width-voltage combinations of the applied voltage as well as to examine the possibilities of bistability in the material.

At the higher temperature region ( $72^{\circ}\text{C}$ ,  $74^{\circ}\text{C}$ ) of the  $\text{SmC}^*$  phase, for pulses of moderate pulse widths and voltages, permanent switching is obtained. For voltages below the threshold value no switching is observed. Thus only these two states are possible at these temperatures.

In the super cooled low temperature region ( $65^{\circ}\text{C}$  to  $70^{\circ}\text{C}$ ), for pulses of 100 ms, 80 ms and 30 ms duration and for high amplitudes ( $U > 40 \text{ V}$ ), the sample switches to the maximum transmission state ( $L_{\text{max}}$ ). The material retains the switched state for a long time (for seconds) even after



- G 5354 -

the field is removed. When amplitude of the pulse is reduced the duration for which the material retains the switched state ( $L_{max}$ ) gradually decreases. On further reduction of pulse-height the switching curve shown in Fig.4.5 is obtained. Here, after initially getting switched to 100% transmission state a relaxation follows and a lower level ( $L_r$ ) is reached. (The value of light transmission, 750 ms after the applied voltage across the cell is reduced to zero, is taken as  $L_r$ ). This switched level depends on the height and width of the applied pulse and remains in the

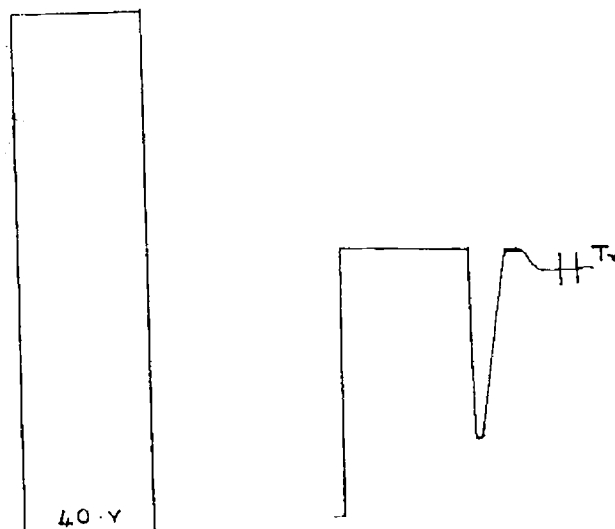


Fig. 4.5 Relaxation of fully switched state of OBOB to intermediate transmission level for comparatively low pulse heights.

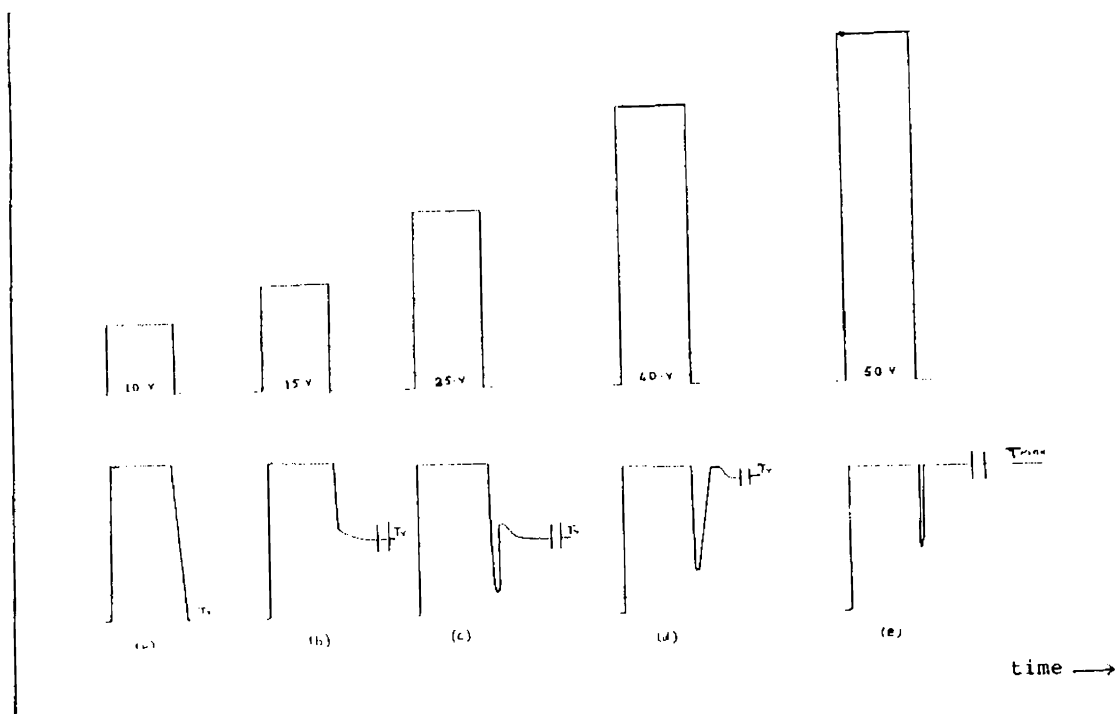


Fig. 4.6 A. Transmission levels for different voltages (pulse width 30 m.s) a: Threshold voltage-b,c,d and e above  $U_{th}$ .

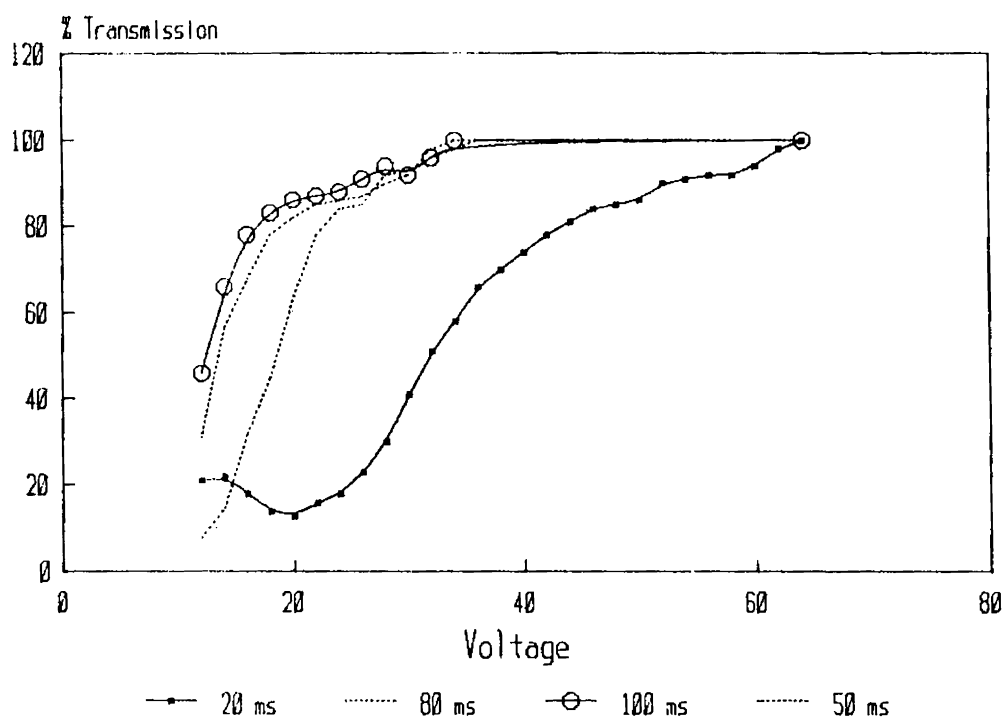


FIGURE 4.6.B-Voltage Vs Transmission Curve, for different pulse widths

state for a long time after the pulse is removed. The response curves for lower voltages are shown in Fig.4.6.(A & B) The voltage range for this partial switching region is very small and is close to the voltage required for full switching.

Now, using pulses of comparatively smaller pulse widths ( 20 ms, 10 ms, 5 ms and 3 ms ) starting from a threshold voltage for switching, a linear variation of transmitted light intensity ( $L_r$ ) with pulse amplitude is obtained (Fig.4.7). In Fig.4.8, the applied voltage has been normalised with respect to the voltage  $U_0$  required to switch the sample to 50% transmission. The shape of the graph remains fairly universal for different pulse widths. This linear dynamic range can be used for obtaining various grey levels.

#### 4.3.3. Bistability.

Below a certain voltage  $U_{th}$ , for a chosen pulse width there is no permanent switching. However a small transient electro-optic effect is observed.

Another interesting result in all these cases is that when the sample in its switched state is subjected to a pulse whose amplitude is just below the threshold  $U_{th}$ , the stable state (  $L_{max}$  and  $L_r$  ) is switched back to the opaque

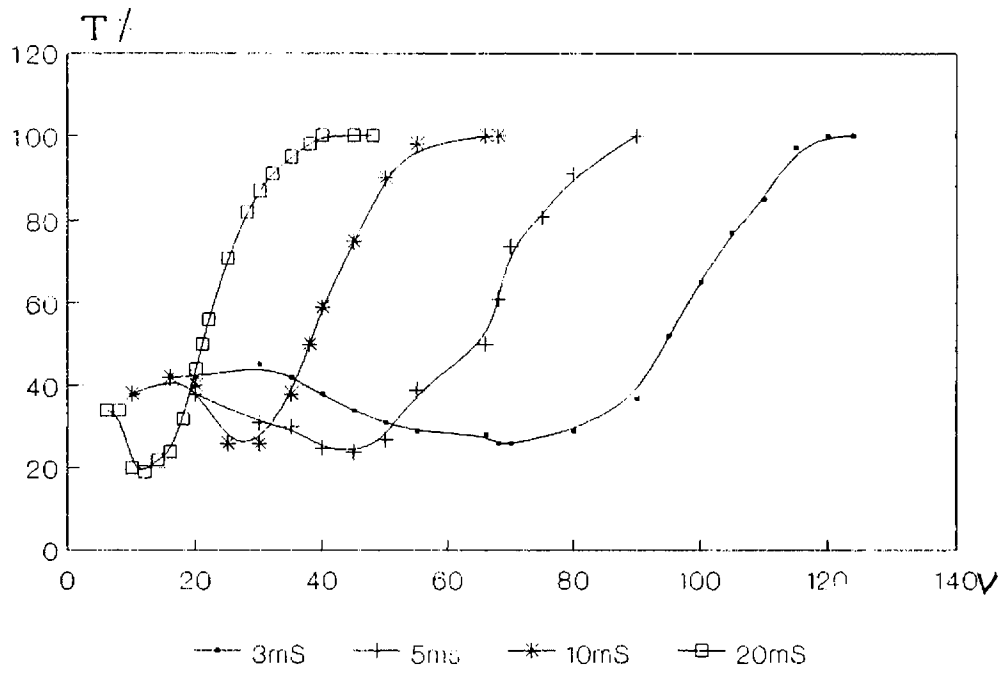


Fig. 4.7 Voltage - Transmission curves for lower pulse widths

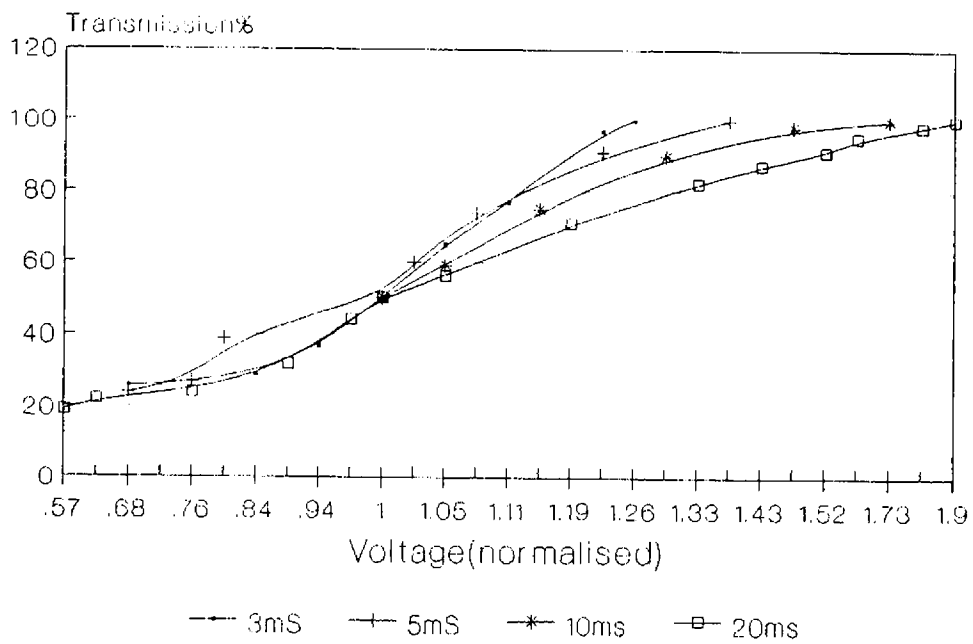


Fig. 4.8 Normalised voltage - Transmission curves for lower pulse widths

state. Hence these pulses can be used as reset pulses. Depending on the pulse width, pulses of 10 to 12 V were used in the present case for resetting the switched state. Thus the ferroelectric liquid crystals can be switched from opaque to high transmission state by a pulse of high amplitude ( $U > U_{th}$ ) and from high transmission state to opaque state by a reset pulse ( $U < U_{th}$ ). Thus bistability is achieved in the material.

In all transmission values observed, the probe pulse is preceded by a reset pulse. The time duration between the pulses is 500 ms. This avoids the hysteresis in voltage-transmission characteristics. A typical reset and probe pulse is as shown in Fig.4.9.

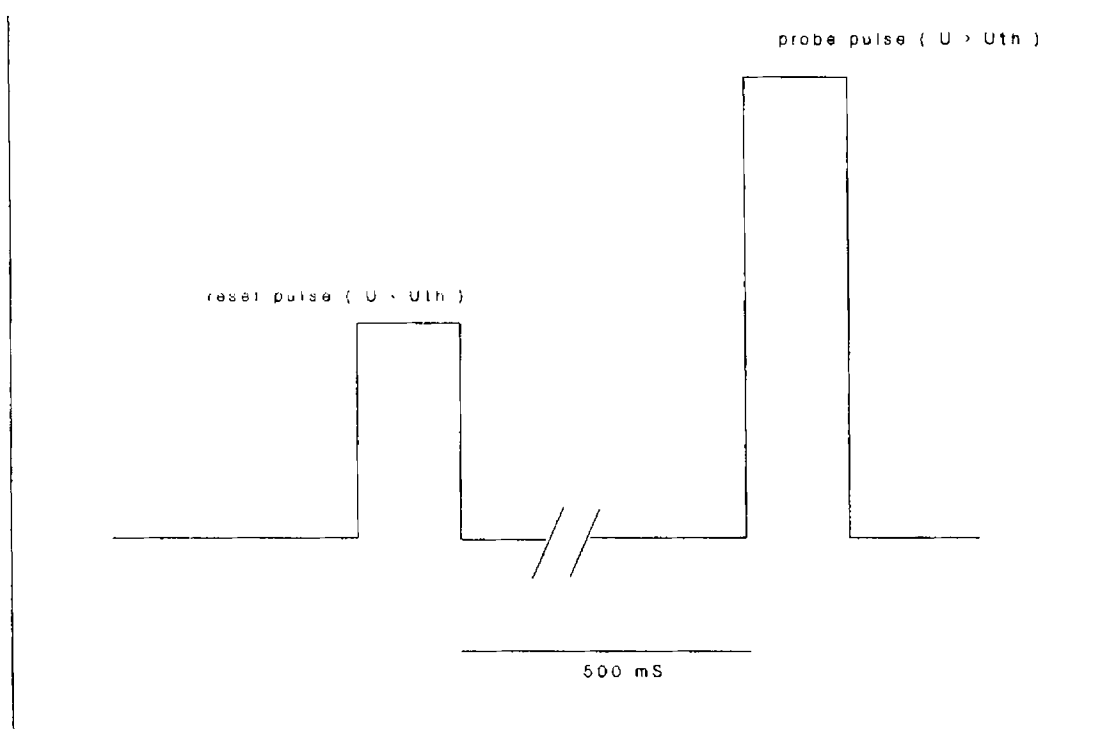


Fig. 4.9 A reset and probe pulse

#### 4.3.4. Pulsewidth - Voltage Relations in Switching.

The relationship between pulse width and voltage is obtained by considering their values corresponding to a particular transmission level. Then the experiment is repeated for different transmission levels. When the reciprocal of pulse width is plotted as a function of the corresponding voltages a linear relationship is observed as seen from Fig.4.10. This suggests that the product of pulse

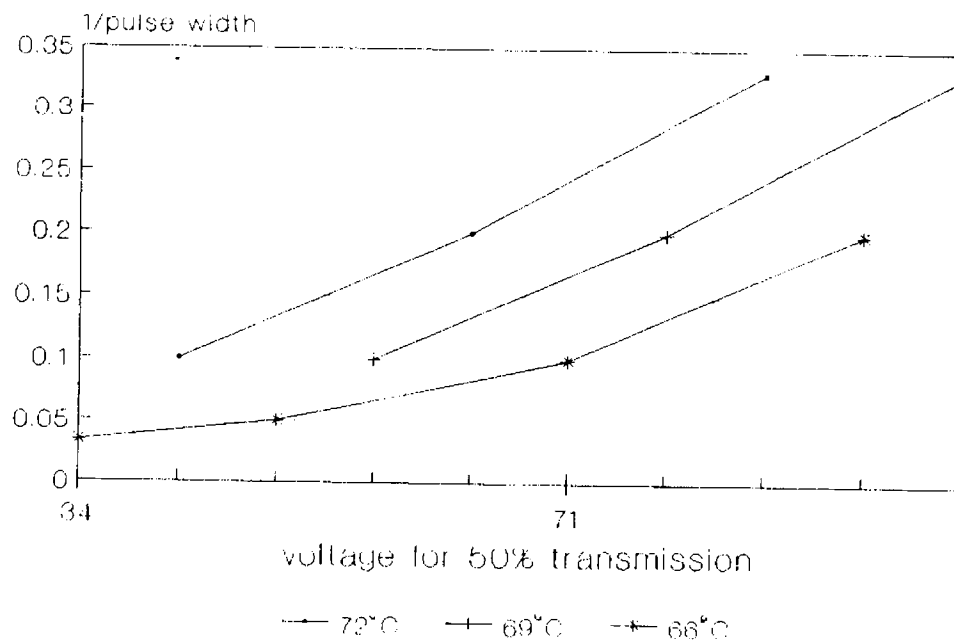


Fig. 4.10 Voltage Vs Pulse width for a given transmission level

width and voltage decides the extent of unwinding induced in the helical structure. However the line does not pass through the origin indicating that such an area law is valid only above a certain voltage.

The threshold voltage required for switching as well as voltage necessary for getting the specimen switched to any particular transmission level decreases with increase in pulse width. This is due to the fact that by increasing the pulse width more energy is transferred to molecules.

On increasing the temperature the voltage required for any given transmission level decreases considerably. At these temperatures for higher pulse widths ( $>10$  ms) the linear region reduces further and shifts to small pulse amplitudes ( $U < 20$  V). For pulses of smaller width and moderate pulse heights, good linear region was obtained. This is due to the lower resistance offered to the dipole moments at higher temperatures as the viscous forces are less at these temperatures.

The mechanism behind the creation and stabilisation of the levels can be explained as follows. During switching the permanent dipoles of the liquid crystal molecules are rotated through a definite angle. During this process a certain amount of charge is transported across the cell thickness. For a certain voltage  $U$ , the cell of

capacitance  $C$  is loaded with a charge  $CU$  within the pulse time. When the cell responds this charge is transported to other side of the electrodes and thus gets compensated. For higher voltages, larger amount of charge will have to be compensated. This makes the molecules rotate through larger angles which results in a higher transmission level.

In addition to the spontaneous polarisation charges, ionic charges also cause switching of the domains. But this effect dies down quickly leaving the spontaneous polarisation effects only. This is why transmission level first goes to maximum and then relaxes to certain definite  $T_r$  values. This ionic switching can be avoided at lower voltages which is possible in thin samples.

#### 4.3.5. Decay of switched states.

Since bistable switching depends on the life time of the switched state, decay times were studied by keeping the sample under open and short circuit conditions, just after application of the pulse. The  $L_{max}$  state (refer section 4.3.2) reached under pulses of higher amplitudes and of higher pulse widths is retained for very long duration in all cases. But the decay time of the intermediate levels, the dynamic range ( $L_r$ ) depend on the circuit conditions. The light transmission decreases and comes to a lower level



(20-30%) in 1 to 2 seconds, when the circuit is short circuited. But in open circuit condition (immediately after applying a pulse) the transparent state is retained for a very long time, as shown in Fig.4.11. Similar phenomena is observed by terminating the circuit with a high impedance. The persistence of transparent state even after opening the circuit may be due to the charges stored in the capacitance of the ferroelectric liquid crystals itself. Due to the

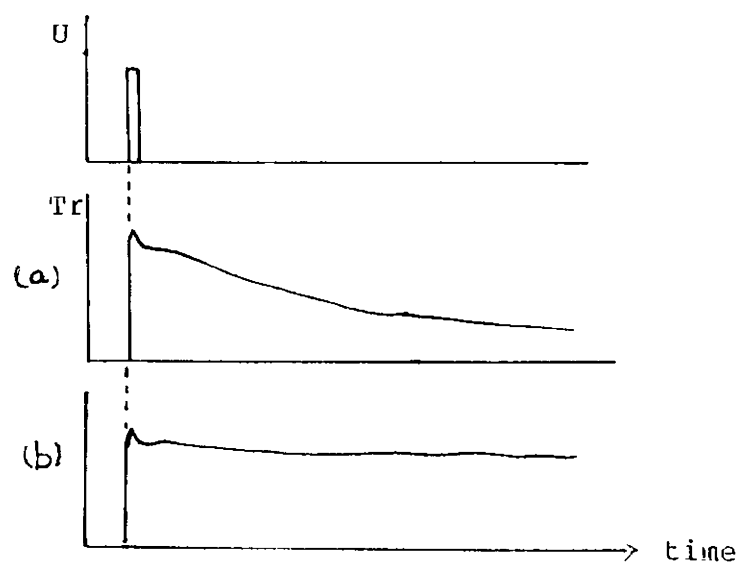


Fig. 4.11 Decay of switched state under (a) short circuited condition (b) open circuited condition

extremely large dielectric constant, the capacitance of the ferroelectric liquid crystals is large compared with the conventional liquid crystals. This results in a long decay time of the state when the circuit is opened or terminated with a large resistance.

#### 4.3.6. Multiple pulses.

A pixel in a matrix addressed display will be subjected to a series of pulses of different voltages and pulse widths in a small interval of time. The main aim of studying the effect of multiple pulses is to examine the presence of cumulative switching under such conditions. In the present case, for voltages higher than the threshold voltage ( $U_{th}$ ), the resulting state will depend on the previous state. Hence a blanking or reset pulse should be applied before giving the information signals. As explained in the previous section a pulse of voltage almost equal to the threshold value can be used for this purpose. Under this condition an addressing scheme employing an active device like a thin film transistor (TFT) or metal insulator metal (MIM) is highly suitable. As the TFT can open circuit the pixel after application of pulses, the intermediate

level  $L_r$  remains stable for a long time.

#### 4.3.7. Rotational viscosity.

The effective ON and OFF times of electro-optic devices are  $T_{on} = T_r + T_d$  and  $T_{off} = T_{decay} + T_{delay}$  in decay. The rotational viscosity of the ferroelectric liquid crystal can be calculated by measuring  $T_r$  separately under increasing pulse voltages.

Such measurements are carried out for the samples of OBOB and the results are plotted in figure 4.12.

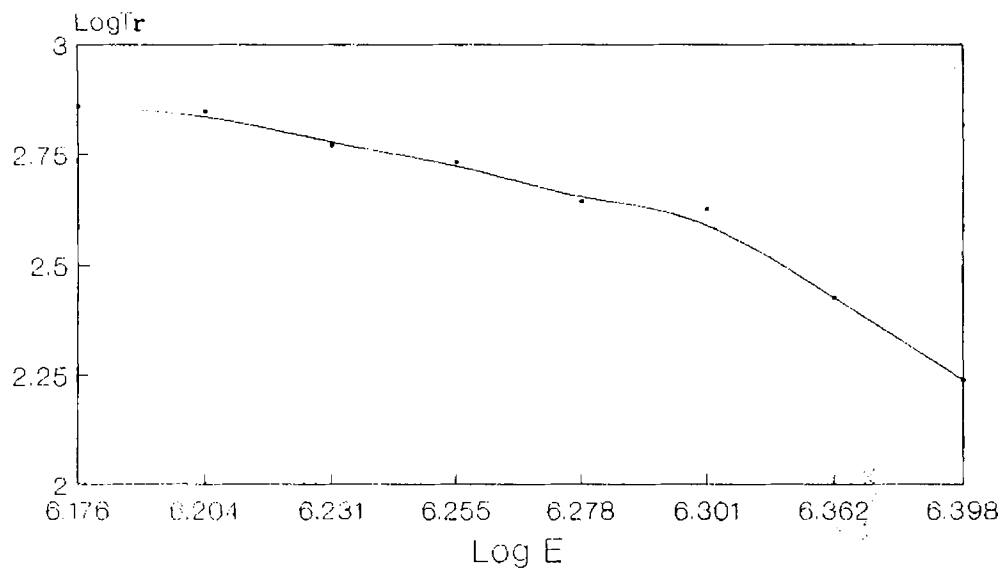


Fig. 4.12 Variation of rise time with voltage of the applied pulse

When pulses of magnitude  $U > U_{th}$  are applied, initially both rise time  $T_r$  and decay time  $T_d$  decrease with increasing pulse voltage (for a given pulse width).  $T_r$  shows a  $1/E$  dependence for a good range of field. But when the field is further increased  $T_r$  does not change appreciably with voltage. Fastest response time ( $T_d+T_r$ ) of 400 microseconds are observed at 50 Volt pulses and at 100 millisecond pulse width [4.13] with a sample thickness of 15 micrometer. Such speeds are observed at decreased pulse widths also; but for higher voltages.

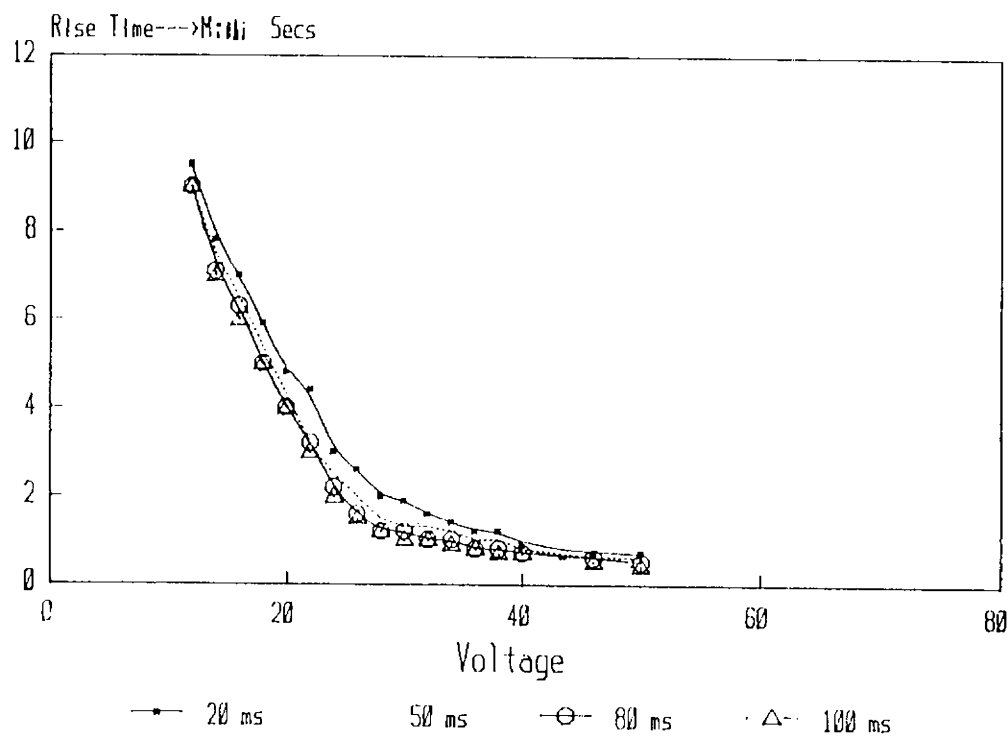


Fig. 4.13 Variation of response time ( $T_d+T_r$ ) with voltage for pulses of different durations

The electro-optical properties of CE3 and CE8 are also investigated using the same arrangement. For CE3, even pulses of 120 volts do not produce any switching in the SmC\* state. Though switching is obtained for CE 8, the response time is 4 to 5 times higher than that for OBOB under similar conditions of cell thickness and applied field.

In chapter 3, section 3.7, the importance of coefficient of rotational viscosity has been established. Its value is calculated from the current curves corresponding to the spontaneous polarisation switching under the reversal of electric field. Coefficient of viscosity can be calculated from the electro-optic characteristics also [64]. It is given by the equation

$$\gamma_{\phi} = 1/1.8 \cdot \text{Ps} \cdot E \cdot T_r$$

Here  $T_r$  is the rise time for those field values where it decreases as  $1/E$ .

The value of rotational viscosity calculated using this equation is of the same order as those calculated from field reversal experiments.

#### 4.4 CONCLUSIONS.

The results of electro-optic switching studies of ferroelectric liquid crystals OBOB show that by aligning the

material in the planar geometry, stable grey levels can be achieved even in thick samples ( $d > P_0$ ) under suitable conditions of temperature and field parameters. The presence of a threshold switching voltage enables this material to be used as pixels in a multiplexed display. Though it requires higher switching voltages and has lower switching speed, (400 microseconds) it can find applications in active matrix displays and light valves.

## CHAPTER 5. MODULATION STUDIES.

5.1. Introduction.

5.2. Experimental set up, Methodology and Results.

5.3. Discussion.

5.4. Conclusions.

## MODULATION STUDIES

### 5.1. INTRODUCTION

Coverision of an electrical signal into an identical optical waveform is an integral part of all electro-optic devices. This electro-optical modulation can be obtained either by direct switching of the light source or by using an external modulator whose refractive index can be changed in the presence of an applied electric field. Here the light beam is the carrier whose phase or intensity is modified according to the modulating signal.

Liquid crystals offer a good choice of material for passive optical modulation due to their characteristic electro-optic properties. Polarised light passing through a liquid crystal undergoes a phase shift and intensity change due to the anisotropic index of refraction that depends on the deformation profile of the liquid crystal. Further the deformation profile can be controlled by an applied voltage across the liquid crystal cell. Thus a voltage dependent phase shift and intensity variation can be imposed on a light beam passing through a liquid crystal medium. Liquid crystal cells as optical intensity modulation devices for projection purposes have been



developed in the last few years [67]. They are rather small and inexpensive compared to the conventional type employing electrically deformable oil films for image generation in large screen projectors.

The performance of these liquid crystal electro-optic modulators depends on the structure and properties of the liquid crystal material. Ferroelectric liquid crystals, due to their inherent helical structure and fast response offer a better material for electro-optic modulators than the nematic liquid crystal.

This chapter gives an account of the attempts to make use of the deformed helical structure of the ferroelectric liquid crystals, OBOB for designing an electro-optical intensity modulator. The results show that under specific dc biasing, the light passing through the OBOB in the ferroelectric liquid crystal phase can be modulated corresponding to a train of pulses. The modulating frequencies range from a few hertz to those in the audio frequency (2k to 5k Hz) region. The effects of changing the frequency and amplitude of the pulses on the modulation depth are also studied.

## 5.2. EXPERIMENTAL SETUP, METHODOLOGY AND RESULTS

The experimental setup is as shown in Fig.5.1. A

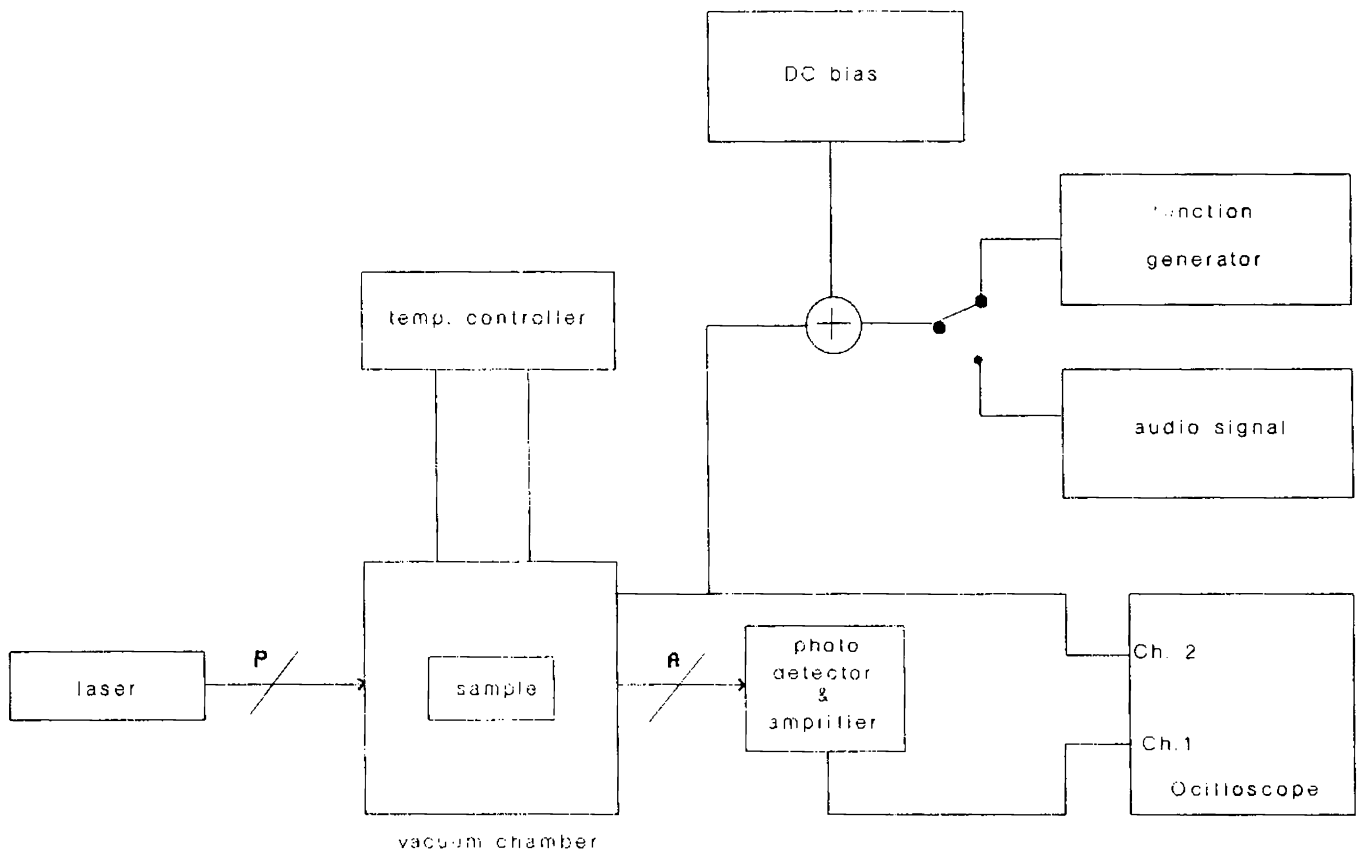


Fig. 5.1 Expt:1 setup for modulation studies

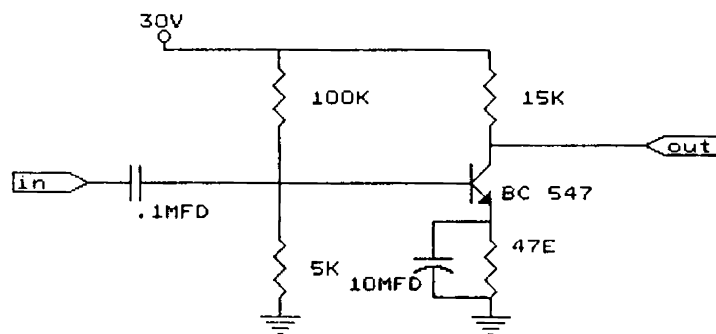


Fig. 5.2 Circuit for biasing the signals with a constant dc

Helium-Neon laser is used as the light source. A dc bias can be given to the signals applied to the specimen by using the circuit shown in Fig.5.2. The modulating signal and modulated output are displayed on the memory scope. P is a polariser and A an analyser. They are placed with their polarisation directions making an angle  $\alpha$  ( $\alpha < \theta$ , the tilt angle.) with the helical axis, which in this case is along the direction of rubbing.

Two types of cells are prepared in planar configuration. In the first type alignment is done by coating a film of polyvinyl alcohol and rubbing as explained in the previous chapter. In these samples the thickness is controlled by Mylar spacers and is of the order of 10 to 15 microns.

Samples of OBOB are also prepared by using vacuum evaporated silicon monoxide films ( $\sim 2$ microns) as spacers. The ferroelectric liquid crystal is sandwiched between two tin oxide coated glass plates whose surfaces are obliquely coated with silicon monoxide film ( $\sim 500 \text{ \AA}$ ). SiO is evaporated at a rate of  $5 \text{ \AA}$  per second and at a pressure below  $10^{-5}$  Torr. The deposition angle, defined as the angle between the direction of the evaporation beam and the normal to the glass plate, is  $83.2^\circ$  (Fig.5.3). The glass plates are assembled to form antiparallel cells (Fig.5.4).

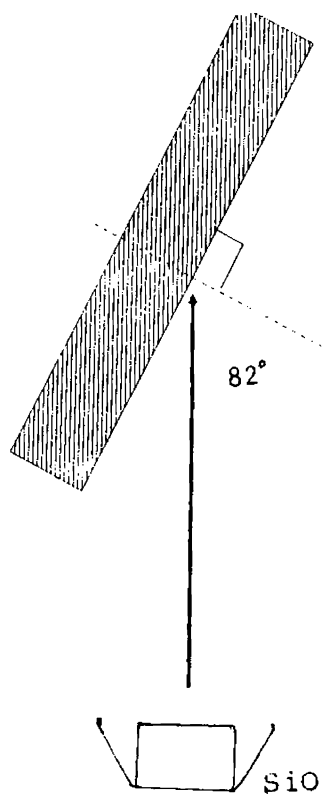


Fig. 5.3 Oblique evaporation of SiO<sub>2</sub> aligning layer under vacuum

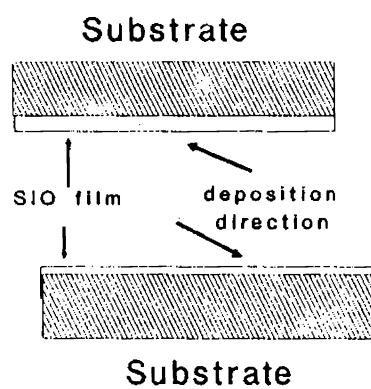


Fig. 5.4 OBOB molecules in antiparallel configuration (~2 micron thickness)

In order to investigate the modulation of light by time varying electrical signals, a systematic study is carried out by applying the following signals and recording their responses.

1. A pure sine wave with zero average dc :

On applying this unbiased sine wave, without using polarisers, the frequency of the modulated signal becomes twice the frequency of the modulating signal.(Fig.5.5). In polarised light the response is as shown in fig.5.6. The pattern remained unchanged with a change in frequency or amplitude of the applied signal.

2. A sine wave of constant frequency with an average dc of 12 V

In this case the response follows the sine wave variations, but with a constant phase lag (Fig.5.7). The amplitude of the response decreases at high frequencies. When the amplitude of the sine wave is increased above the dc bias, clipping appears in the response curve during negative cycle.

3. A dc biased sweeping sine wave with varying sweep time and frequency range.

The response to the sweeping sine wave is as shown in Fig.5.8. The variation in amplitude of the response with

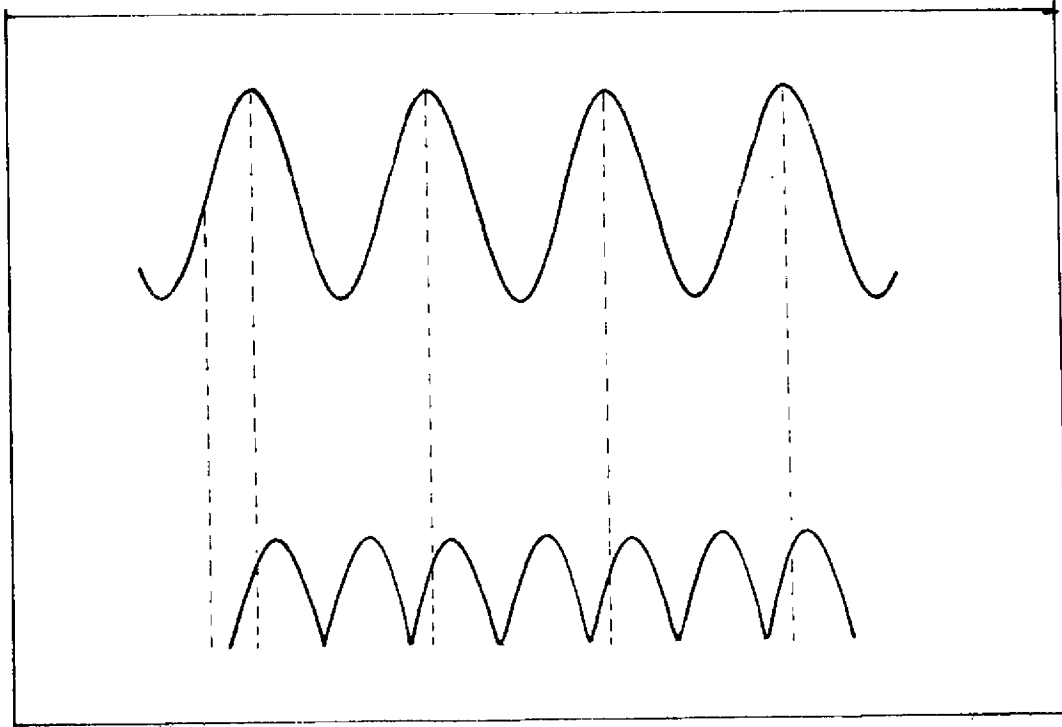


Fig. 5.5 Optical response of OBOB corresponding to a sine wave of zero average dc- (using a polariser and analyser)

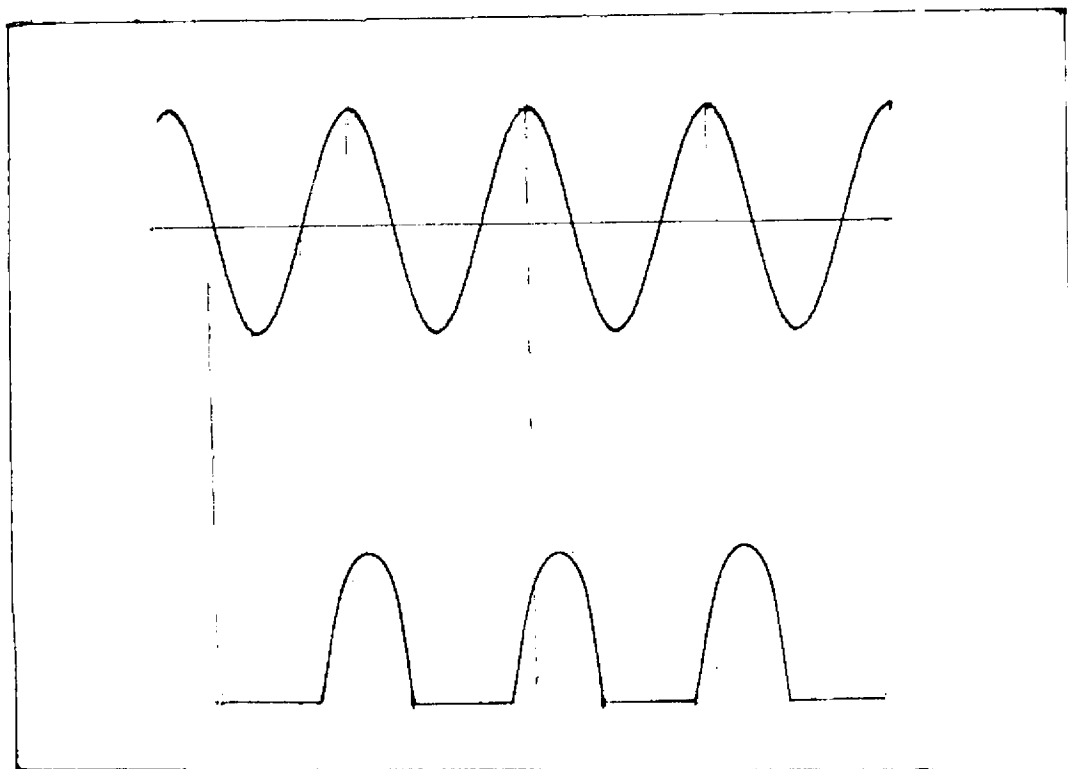


Fig. 5.6 Optical response of OBOB corresponding to a sine wave of zero average dc- (without polariser and analyser)

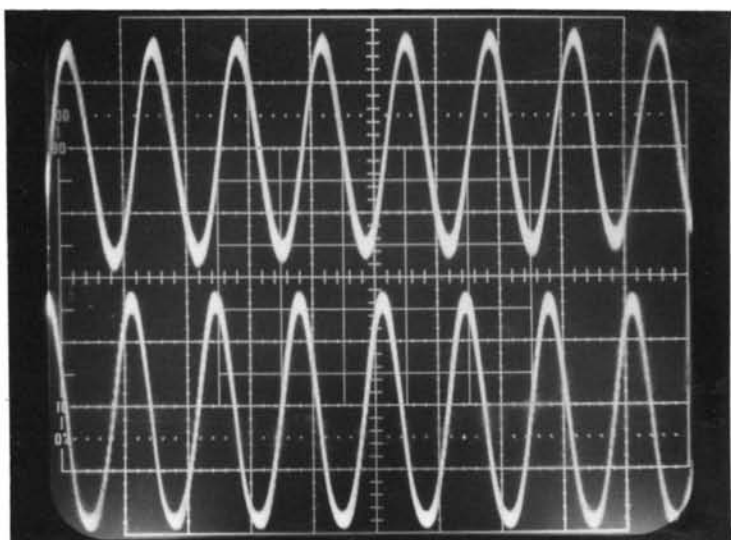


Fig. 5.7 Optical response for a sine wave with an average dc of 12 V

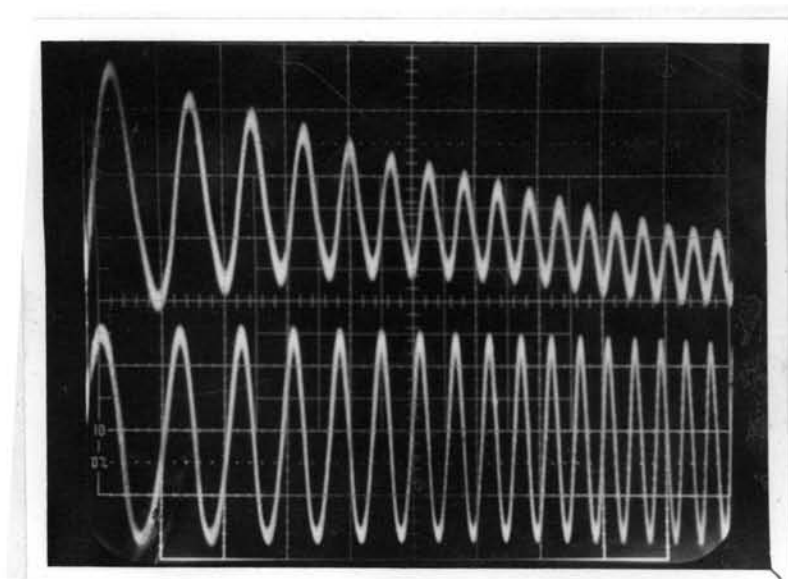


Fig. 5.8 Optical response corresponding to a dc biased sweeping sine wave

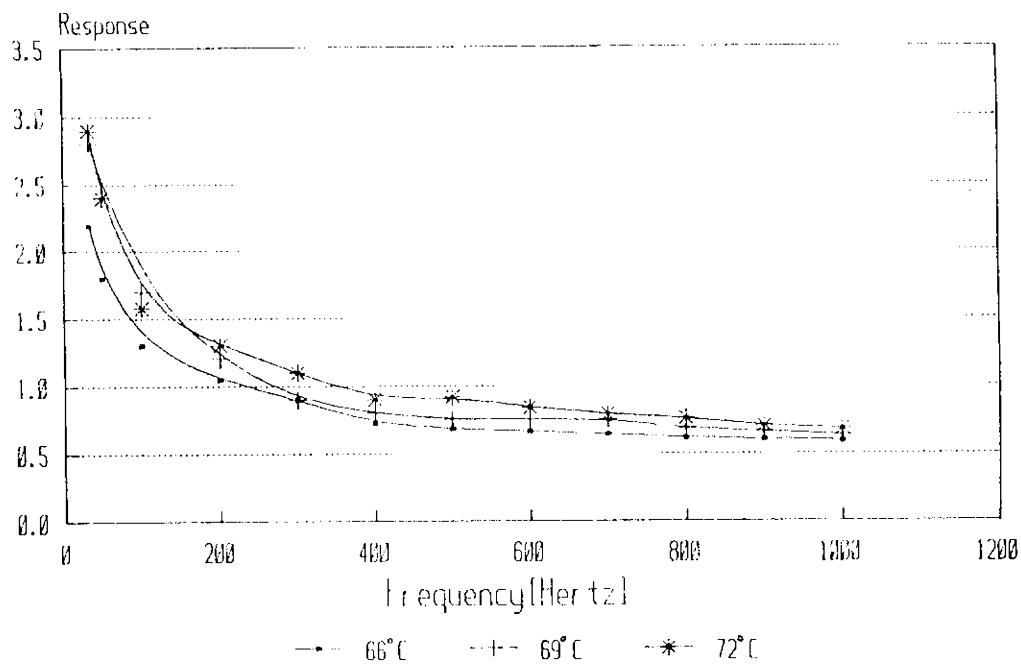


Fig. 5.9 Variation of optical response with frequency of sine wave

frequency is as shown in Fig.5.9. The experiment is repeated for various sweep times and different frequency ranges (Fig.5.10). The phase lag of the response with the applied signal varies from 0.2 ms to 0.05 ms for a change in frequency from 300 Hz to 5 kHz.

4. Properly amplified, dc biased Speech signals from an audio tape head.

Speech signals from an audio tape head is applied to the ferroelectric liquid crystals and the response is fed



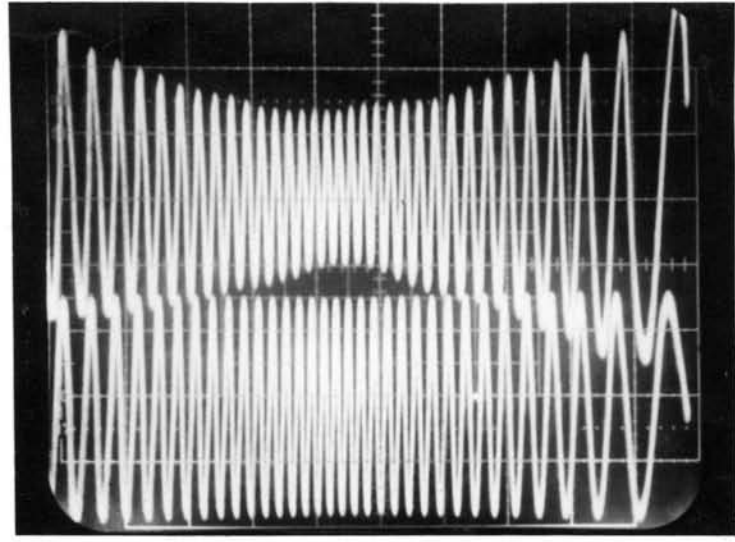


Fig. 5.10 . Optical response under different sweep times and frequencies

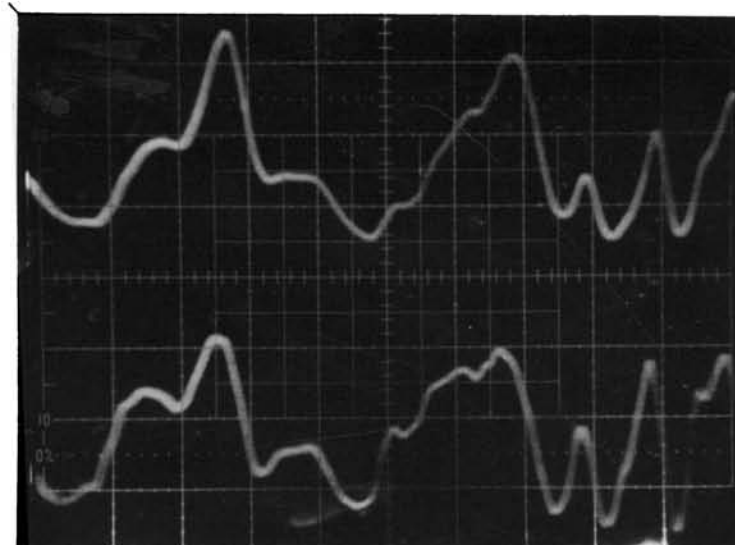


Fig. 5.12 Audio signals and the corresponding optical response of OBOB

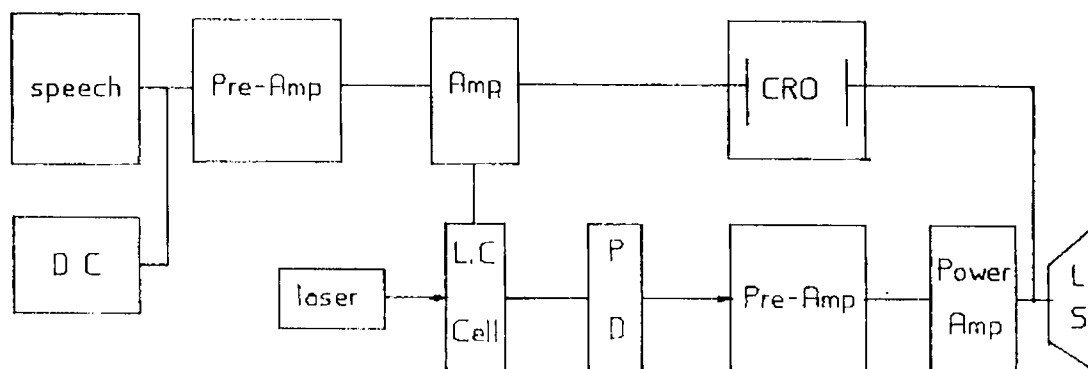


Fig. 5.11 Circuit for applying amplified audio signals to OBOB

to a speaker as shown in Fig.5.11. The quality of the sound reproduced is good. Fig.5.12. shows the music and corresponding response signals in the storage oscilloscope.

### 5.3. DISCUSSION

The above results can be explained on the basis of modifications in the average refractive index of the sample due to the winding and unwinding of the helix of the molecular arrangement of ferroelectric liquid crystals under an applied electric field. These processes take place under the combined effect of dielectric, elastic and ferroelectric forces as suggested by Gouda, Lagerwall et al.[37].

When there is no electric field across the transparent electrodes, the ferroelectric liquid crystal is in the fully wound state. In this condition though the director  $\bar{n}$  rotates on translation along the helical axis, on the macroscopic scale (for a light spot of diameter  $D \gg P_0$ , the pitch) the optical axis coincides with the helical axis  $Z$ , parallel to the rubbing direction. Due to the high amount of scattering in this state the ferroelectric liquid crystal transmits only a very small amount of light.

When a pure sine wave is applied, the molecules are rotated along both directions about the helical axis for positive and negative cycles, causing continuous winding and unwinding of the helix. Maximum unwinding occurs at the peak voltages. This results in a continuous change in the azimuthal angle  $\psi$  which defines the projection of the director on the smectic layer plane. A qualitative picture of this helix distortion and the field behaviour of the average optical index is shown in Fig.5.13. [43]. For a given value of the electric field let the deviation of the average optic axis be  $\langle \theta \rangle$  on the plane of the cell. Then a small portion of the light incident on ferroelectric liquid crystal gets transmitted. Maximum transmission is obtained at the maximum unwound position i.e. at the peak voltages. At the sign reversal i.e. the zero crossing region of the sine

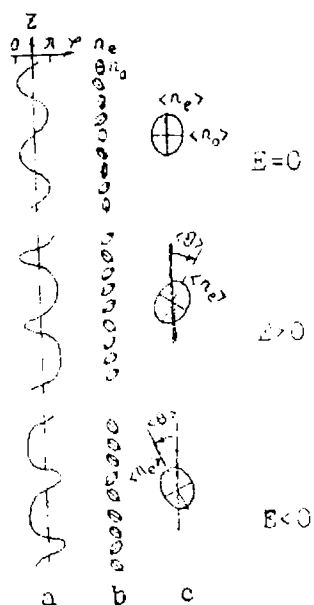


Fig. 5.13 (a) Azimuthal angle ( $\alpha$ ), (b) local optical indicatrix and (c) averaged over space optical indicatrix for a helical FLC under an applied field

wave, reorientation from one switched state to the other causes violent molecular motions. This produces intense light scattering resulting in a low transmission state. Thus without polarisers, in a cycle of sine wave two high transmission states are obtained with a low transmission state in between.

When a polariser is placed as shown in fig.5.1, a response curve shown in Fig.5.6. is obtained. Here for one peak of the sine wave the molecules are aligned at an angle  $+\langle\theta\rangle$  (tilt of the ferroelectric liquid crystal) parallel to the polariser for which a maximum transmission state is

obtained. But for the next peak molecules are aligned on the other side ( $-\langle\theta\rangle$ ) causing very small transmission.

In the second case the dc bias initially unwinds the helix partially (Fig.5.14). OBOB is a material having positive spontaneous polarisation. Hence when a dc field is applied into the plane of the paper a large number of molecules rotate so as to have their  $\bar{c}$  directors in the quadrant 2. ie tending to align parallel to the direction of the polariser. This causes an increase in transmission. When a sinewave is applied along with the dc bias, the specimen is subjected to a varying direct voltage having a non-zero minimum value. Hence the movements of the molecules are rather confined mainly in the quadrant two. When the voltage rises from A to B more molecules align parallel to the polariser causing a further increase in transmission. From B to C just the reverse rotations takes place and a corresponding decrease in transmission is obtained. At D the voltage value is minimum and the helix is just unwound. The average  $\bar{c}$  director makes a small angle with Y axis and hence the transmission is minimum. Thus the optical output varies according to the variations in the electric field. Here at the maximum switched position of the molecule there can be a hysteresis effect due to ferroelectricity. It is avoided by keeping the maximum field (at B) always less than the

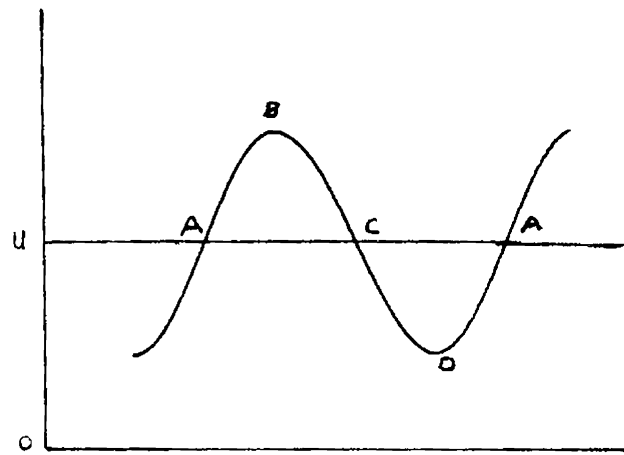
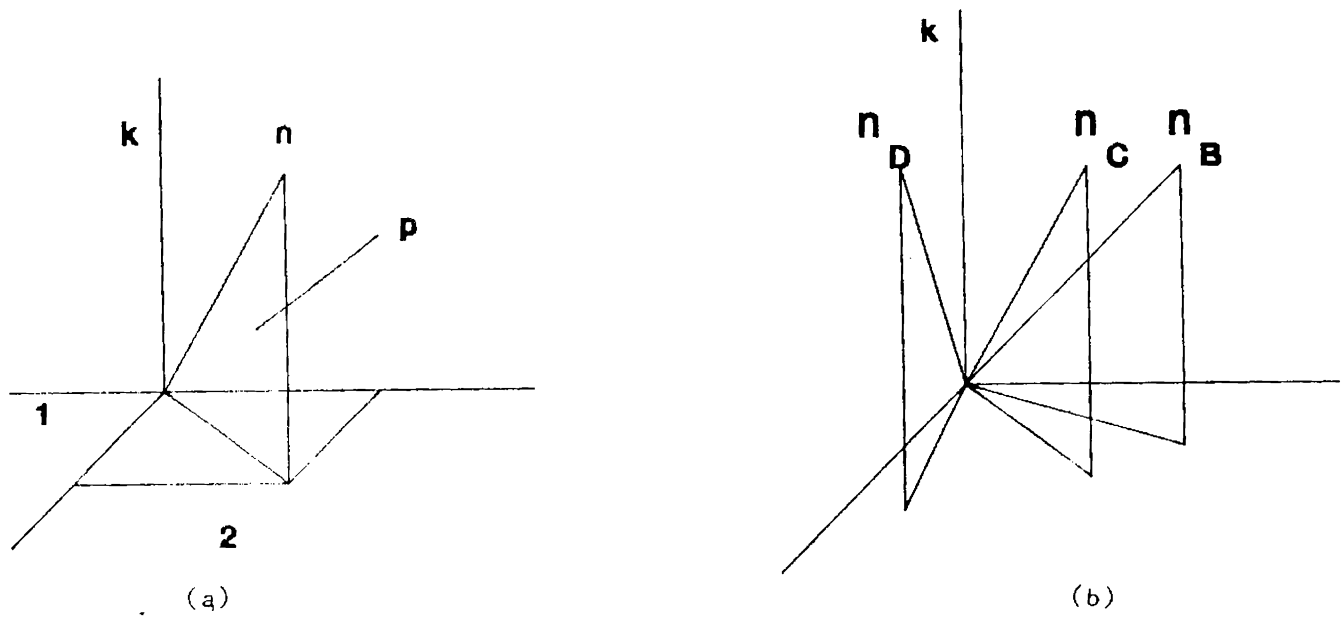


Fig. 5.14 The orientation of C director for (a) a dc. field (b) a sine-wave biased with a dc

critical unwinding field ( $E_c$ ). Thus a linear response is obtained.

However there is a constant phase lag between the applied field and the optical output. This lag corresponds to the response time of the ferroelectric liquid crystals. When the amplitude of the sine wave is increased the response also increases, as more and more molecules get aligned, until it reaches the critical unwinding field ( $E_c$ ). At this point the helix unwinds fully causing saturation/ clipping of the response curve during positive half cycle also. On increasing the sine frequency the amplitude of the response decreases. This indicates that the wave frequencies are now around the relaxation frequency of the material corresponding to the Goldstone mode.

The sweeping sine wave is applied to study systematically the variations in response with a continuously varying frequency. A decrease in amplitude of the response is obtained at higher frequencies. This results in a reduction of the modulation depth as shown in figs: 5.8 and 5.10. Hence in order to get a uniform response a boosting of high frequency components is required.

Such a selective amplification is carried out for speech signals as shown in figure 5.11 and results are represented in fig:5.12. It is seen that the response is a

replica of the speech signal. Thus the ferroelectric liquid crystals is effectively used as a modulator for audio signal.

When the temperature of the ferroelectric liquid crystal is increased, higher modulation depth is obtained. The ferroelectric liquid crystal gets switched even for small voltages and saturation is produced in the output profile for slight increase in the modulating signal amplitude. Also at higher temperatures the lag between modulating signal and response is decreased. Now rotational viscosity decreases with increase in temperature. Hence the resistance to the orienting forces is less at higher temperatures. As a result response of ferroelectric liquid crystal increases which explains the above observations. Studies conducted in samples of thickness  $\sim 2$  microns show similar behaviour, but for less applied voltages. It is to be noted that even for these samples, thickness is very much higher than the helical pitch ( $\sim 0.3$  microns)

#### 5.4. CONCLUSIONS

Under dc biased conditions the amount of light transmitted through partially wound helical structure of the ferroelectric liquid crystal OBOB varies linearly with the applied field. For relatively lower voltages modulating



signals upto 5 kHz can be used. Hence such materials with small helical pitch and high spontaneous polarisation can find application as low-voltage light modulators and image converters. Since the modulating properties are retained at lower thicknesses (~2 microns), these materials can find application in integrated light modulating devices.

CHAPTER 6

C O N C L U S I O N S

## CHAPTER 6 CONCLUSIONS

In this thesis the electro-optic properties of a comparatively thick cell of a ferroelectric liquid crystal, whose helical structure has been deformed by an electric field are investigated. Though relatively higher switching voltages are required in this case, the cell thickness and quality of alignment are not that critical, as in the case of thin film configurations, in deciding the electro-optic properties of the cell. Further it reveals some novel electro-optic effects.

A new ferroelectric material OBOB is studied in this work. The phase transition sequence is studied by differential scanning calorimetry and texture observations. It shows that on heating, from the ferroelectric SmC\* state the material passes to cholesteric state instead of the usual SmA phase observed for most of the ferroelectric liquid crystals. Further OBOB has a high degree of twist (pitch of the order of tenths of microns) and a comparatively high value of spontaneous polarisation which is a characteristic feature of materials with this phase transition sequence. This gives rise to a critical unwinding field of very high value and hence to a range of partially unwound states corresponding to different applied fields.

From DSC studies and texture observations the temperature range, in which OBOB is ferroelectric is confirmed as 65°C to 74°C. All the material parameters of the ferroelectric liquid crystal such as spontaneous polarisation, rotational viscosity and dielectric constant are evaluated in this temperature range. The variation of these properties with temperature also has been studied by various methods. Results show that OBOB has a fairly large value of spontaneous polarisation (25 nC/sq.cm) and rotational viscosity (900 m.Pa.S). A high value of spontaneous polarisation reduces the response time where as that of rotational viscosity increases it. But a moderately high value of rotational viscosity is necessary for stabilising the switched state. The fact that OBOB exhibits fast response and a latched state shows that the compromise between these two material constants is ideal in this material. The dielectric anisotropy of the material is determined for various frequency ranges and is found to be negative. This shows that ac field stabilisation methods can also be used to align the material in specific configurations.

Response times of the order of hundreds of microseconds are obtained for cell thickness of 15 to 20 microns. After switching, the ferroelectric liquid crystal

retains the optical transmission levels for a long time. Further the extent of switching is found to depend both on height and duration of the square pulse.

Below a certain value of pulse height there is no electro-optic switching, irrespective of the width of the pulse. Thus the switching shows a threshold behaviour which is a prerequisite for multiplexing. Hence when this ferroelectric liquid crystal is used as pixels for such multiplexed displays cross talk will be minimum.

Another interesting result is that a pulse whose height/ width combination is near to but lower than that of the threshold value, can bring the high transmission state back to opaque state. Hence these pulses can be used as reset pulses. To avoid cumulative switching in pixels such pulses can be applied in between two information signals.

The presence of an optical threshold voltage, a memory state and a one to one correspondence of optical transmission level to a pulse width/ height combination shows that this ferroelectric liquid crystal can be used as pixels for multiplexed dynamic displays.

A ferroelectric liquid crystal material used as an electro-optic modulator or light valve will be subjected to signals of continuously varying frequency and amplitude. A detailed study is conducted to evaluate the performance of

OBOB under such conditions.

When samples of OBOB, prepared in planar orientation is subjected to sine wave signals, the light passing through the material is not properly modulated. But on applying the signal along with a dc bias, excellent modulation of light is obtained. Experiments done with continuously varying signals and audio signals showed that up to 5kHz good modulation depth is obtained in this material. Experiments done with thin samples (still  $d > p$ ) showed similar results.

A qualitative analysis based on the change in direction of the average optical axis under an applied field explains these results. At moderate voltages, due to the extremely high value of the critical unwinding field of OBOB, the helix is only partially unwound. When a low voltage, time varying signal is applied to such a deformed helix, small perturbations are produced to the molecular orientations. Then the variations in the space averaged value of the projection of the phase angle on the cell plane ( $\langle \theta \rangle$ ) will be linear to the applied field. This explains the variations in light intensity with the signal. This property makes the material suitable for applications in electro-optic modulators.

This modulating property of the ferroelectric liquid crystal can find applications in the field of optical communication and optical information processing such as pattern recognition and optical computing. One of the important problems that remains in this field is the development of a high contrast, high resolution spatial light modulator capable of performing functions such as incoherent to coherent image conversion, light amplification and spatial information storage. Presently nematic liquid crystals are used as light modulators along with some photoconductors. Instead, if ferroelectric liquid crystals in the deformed helix configuration are used as modulators, considerable improvement in response time, contrast ratio and resolution will be attained.

From these investigations and discussions it is evident that the electro-optic effects in the SmC\* state of OBOB have many advantages over other known liquid crystal effects. Most important is the director orientation under the influence of electric fields of different signs. Here one can achieve a high rate of switching from one optical state to another. The experiments showed the possibility of obtaining 100% modulation of light beam for frequencies upto 5 kHz. As the condition  $d > p$  can be maintained for OBOB even at one or two micron thickness, such materials can be very usefull in fabricating integrated devices. With ferroelectric liquid crystals of higher spontaneous polarisation and lower rotational viscosities higher

switching speeds and modulation corresponding to higher frequencies can be realized.



#### REFERENCES

1. F.Reinitzer. *Montash Chem.* Vol.9. P.421. 1888.
2. O.Lehmann. *Z.Krist.* Vol. 18. P.464. 1890.
3. U.Efron, S.T.Wu et al. *Ferroelectrics.* Vol.73. P.315. 1987.
4. J.G.Grabmaier, W.F.Greubel and H.H.Kruger. Third international conference. Berlin. August. 24-28, 1971.
5. R.B.Meyer, L.Liebert, L.Strzelecki and P,Keller. *J.Phys.Lett.* Vol.30. P.69. 1975.
6. K.Skarp, I.Dhal, S.T.Lagerwall and B.Stabler. *Mol.Cryst.Liq. Cryst.* Vol.114. P.283. 1984.
7. K.Miyasato, S.Abe, H.Takezoe, A.Fukuda and E.Kuze. *Jpn.J. Appl.Phys.* Vol.22. L.661. 1983.
8. J.L.Alabart, M.Marcos, E.Melendez and J.L.Serrano. *Ferroelectrics.* Vol.58, P.37. 1984.
9. M.Imasaki, S.Kai, Y.Narnshige and T.Fujimoto. *Ferroelectrics.* Vol. 58. P.47. 1984.
10. D.Gunther, W.Hemmerling, G.Illian, I.Muller and R.Winger. *Ferroelectrics.* Vol. 114. P. 241. 1991.
11. J.W.Goodby and T.M.Leslie. *Mol.Cryst.Liq.Cryst.* Vol.110. P.175.1984.
12. T.Uemoto, K.Yoshino and Y.Inuishi. *Jpn.J.Appl.Phys.* Vol.18. No.7. P.261. 1979.
13. T.Sakurai, K.Sakamoto and K.Yoshino. et.al. *Ferroelectrics* Vol.58. P.21. 1984.

14. K.Yoshino et.al. Jpn.J.Appl.Phys. Vol.25. No.5. P.295.1986.
15. R.J.Twieg, K.Betterton, W.Hinsberg, P.Wong, W.Tary and H.T. Nguyen. Ferroelectrics. Vol.114. P.295. 1991.
16. C.Tschierske, D.Jouchimi, D.Demus et.al. Ferroelectrics. Vol.114. P.289. 1991.
17. L.J.Yu, C.S.Lee, C.S.Bak and M.M.Labes. Phys.Rev.Letters. Vol.36. L.69. 1976.
18. L.M.Blinov, L.A.Bersenev et.al. J.Physique, Vol.40. C3-269. 1979.
19. Ph.Martinot Lagarde. J.de.Physique. Letters. Page L.17. 1977.
20. Y. Ouchi, T.Uemura, H.Takazoe and A.Fukuda. Jpn. J. Appl. Phys. Vol.24. L.235. 1985.
21. P.G. de. Gennes. The Physics of Liquid Crystals. P.163.
22. Carlson and B.Zeks. Liq. Cryst. Vol.5. P.359. 1989.
23. P.Pieranski, E.Guyon and P.Keller. J.Physique. Vol.36. P.1146. 1975.
24. Xue.J.Z, Handschy.M.A and Clark.N.A. Ferroelectrics. Vol.73. P.305. 1987.
25. K.Skarp, K.Flatischler and S.T.Lagerwall. Ferroelectrics. Vol.84. P.183. 1988.
26. S.Kimura, S.Nishiyama, Y.Ouchi, H.Takzoe and A. Fukuda. Jpn.J.Appl.Phys. Vol.26, L.255. 1987.

27. C.Escher, T.Geelhar and E.Bohm. Liq.Cryst. Vol.3. P.469. 1988.
28. T.Geelhar, C.Escher and E.Bohm. Vol.17. Freiburger Arbeitstagung Flussigkristalle. 1987.
29. A.Levstik, Z.Kutnjak.et.al. Ferroelectrics. Vol.113. P.207. 1991.
30. K.Yoshino, M.Ozaki. et al. Ferroelectrics. Vol. 58. P.283. 1984.
31. Glogarova. et al. Ferroelectrics. Vol. 58. P.161. 1984.
32. N.Maruyama. Ferroelectrics. Vol.58. P.184. 1984.
33. C.H.Bahr, G.Heppke. and N.K.Sharma. Ferroelectrics. Vol.76. P.151. 1987.
34. J.Pavel and M.Glogarova. Ferroelectrics. Vol.84. P.241. 1988.
35. C.Legrand. et al. Ferroelectrics. Vol.84. P.249. 1988.
36. J.Hoffmann.et al. Ferroelectrics. Vol.76. P.61. 1987.
37. F.Gouda et al. J.Appl.Phys. Vol.67 (1). P.180. 1990.
38. Ph.Martinot-Lagarde, R.Duke and G.Durand. Mol.Cryst.Liq. Cryst. Vol.75. P.249.
39. H.Takezoe et al. Ferroelectrics. Vol.58. P.55. 1984.
40. K.Yoshino, K.G.Balakrishnan, T.Uemoto. Jpn.J.Appl.Phys. Vol.17. P.597. 1978.
41. K. Yoshino and M. Ozaki. Jpn. J.Appl. Phys.Vol.23. No.6. L.385. 1984.

42. B.I.Ostrovski and V.G.Chigrinov. Kristallographiya. Vol.25. No.3. P.560. 1980.
43. L.A.Bersenev, L.M.Blinov and D.I.Dergachev. Ferroelectrics. Vol. 85. P.173. 1988.
44. J. Funfschilling and M. Schadt. J.Appl.Phys. Vol.66 (8) P. 3877. 1989.
45. N.A.Clark and S.T.Lagerwall. Appl.Phys.Letter.36. P.899. 1980.
46. J.S.Patel. Appl.Phys.Letters. Vol.47. P 1277. 1985.
47. J.S.Patel and J.W.Goodby. J.Appl.Phys. Vol.63(1).P.80. 1988.
48. J.P.Le Pesant, B.Mourey, M.Hareng, G.Deobert, J.C.Dubois. Fourth International Display Research Conference, Paris, P.217. 1984.
49. P. Schiller, G. Pelzl and D. Demus. Liq. Cryst. Vol.2. P.21. 1987.
50. T.Nagata, T.Umeda, T.Iguwa, Y.Hor and A.Mukoh. IEEE. Trans. on El. devices. Vol.36.(9), P. 1892. 1989.
51. W.J.A.M. Hartmann.IEEE Trans.on electron devices. Vol.36. 9, P.1895. 1989.
52. S.Garoff and R.B.Meyer. Phy. Rev. Lett. Vol. 38. P.848. 1977.
53. G.Anderson, I.Dhal, L.Komitov, S.T.Lgerwall, K.Skarp and B.Stebler. J.Appl.Phys. Vol.66 (10). P.4983. 1989.

54. Y.Panarin, E.Pozhidev and V.Chigrinov. *Ferroelectrics*.  
Vol.114. P.181. 1991.
55. D.Armitage, J.I.Thackara and W.D.Eades. *Ferroelectrics*.  
Vol.85. P.291. 1988.
56. S.Yamamoto, T.Ebihara, N.Kato and H.Hoshi. *Ferroelectrics*.  
Vol.114. P.81. 1991.
57. C.C.Mao, K.M.Johnson and G.Moddel. *Ferroelectrics*.  
Vol.114. P.45. 1991.
58. A. Karppinen, S.Lottholz, R.Myllyla, G.Anderson et.al.  
*Ferroelectrics*. Vol.114. P.93. 1991.
59. G.Anderson, I.Dahl, L.Komitov, M.Matuszczyk et.al.  
*Ferroelectrics*. Vol.114. P.137. 1991.
60. Y.Ouchi, Ji Lee et al. *Jpn. J. Appl. Phys.* Vpl.27.No.11.  
P.L 1993. November 1988.
61. K.Ishikawa, K. Hashimoto. et al. *Jpn.J.Appl.Phys.* Vol.23  
NO. 4. P. L 211. 1984.
62. J.S.Patel, and J.W.Goodby. *J.Appl. Phys.* Vol. 59. No.7.  
P. 2355. April 1986.
63. H.Dubal, C.Escher. et al. *Ferroelectrics*. Vol. 84.  
P.143.1988.
64. K.Skarp. *Ferroelectrics*. Vol.84. P.119. 1988.
65. N.A.Clark, M.A.Handschy and S.T.Laggerwall. *Mol.Cryst.*  
*Liq.Cryst.* Vol.94. P.213. 1983.
66. K.Yoshino and M.Ozaki. *Ferroelectrics*.Vol.59. P.145. 1984.
67. M.Fritsch, H.Wohler, G.Hass and D.A.Mlynski. *IEEE Trans-*  
*actions on electron devices.* Vol.36. No.9.P.1882. 1984.

- G 5354 -

LIST OF PUBLICATIONS OF THE AUTHOR

1. Optical intensity modulation using Ferroelectric Liquid Crystals. SPIE. Vol.1337. Nonlinear Optical properties of Organic Materials. 111. (1990). P.381.
2. Dynamical Characteristics and Transmission Studies of the FLC OBOB. Ferroelectrics. Vol.113. P.395. 1991.
3. Mechanism of Optical Modulation using Ferroelectric Liquid Crystals. Smart. Mater.Struct. Vol.1. P. 168. 1992.
4. Ferroelectric Liquid Crystals for a better dynamic display. National Conference on ELECTRONIC CIRCUITS & SYSTEMS, Nov.2-4,1989, Roorkee.
5. Ferroelectric Liquid Crystals light valve for Optical Modulation. National Symposium on Instrumentation, Nov. 17-20, 1992, Gauhati.
6. Optical Modulation using Ferroelectric Liquid Crystals. National symposium on Antennas & Propagation, Dec. 29-31, 1992, Cochin.